

THE INFLUENCE OF DOPANTS
ON THE SURFACE PROPERTIES OF ZIRCONIA.

MATTHEW KEENAN

A thesis submitted in partial fulfilment of the requirements of
The Nottingham Trent University for the degree of Doctor of Philosophy

1997

ProQuest Number: 10290278

All rights reserved

INFORMATION TO ALL USERS

The quality of this reproduction is dependent upon the quality of the copy submitted.

In the unlikely event that the author did not send a complete manuscript and there are missing pages, these will be noted. Also, if material had to be removed, a note will indicate the deletion.



ProQuest 10290278

Published by ProQuest LLC (2017). Copyright of the Dissertation is held by the Author.

All rights reserved.

This work is protected against unauthorized copying under Title 17, United States Code
Microform Edition © ProQuest LLC.

ProQuest LLC.
789 East Eisenhower Parkway
P.O. Box 1346
Ann Arbor, MI 48106 – 1346

REF.

PH.D/CP/97

KEE

Abstract

The surface area of zirconia is known to decrease dramatically upon heating. The addition of dopants to zirconia has been found to stabilise the surface area of zirconia against sintering. The dopants investigated were silica, lanthana and ceria, over the calcination temperature range 400 to 1050°C. The surface area of pure zirconia decreases from 109 m²g⁻¹ at 400°C to 15 m²g⁻¹ at 900°C (it has a surface area < 3 m²g⁻¹ at 1050°C), whereas, 3.5wt% SiO₂/ZrO₂ has a surface area of 170 m²g⁻¹ at 400°C and 13 m²g⁻¹ at 1050°C. The addition of 3mole% lanthana stabilised the surface area to a similar amount as silica but the addition of ceria did not stabilise the surface area against sintering.

Varying the nature of the preparation of the mixed oxides determined the phase of the sample. Coprecipitation preparation stabilised the tetragonal phase of zirconia up to 1050°C whereas, impregnation preparation stabilised the monoclinic phase of zirconia up to 900°C. The phase composition was identified using powder x-ray diffraction.

The catalyst surface was characterised using x-ray photoelectron spectroscopy. Enrichment of the surface with the dopant was observed with increasing calcination temperature.

From the catalytic decomposition of propan-2-ol test reaction, the addition of dopants altered the surface properties of pure zirconia. Zirconia produced the acid product in the reaction whereas, silica doped zirconia showed enhanced acidity, lanthana doped zirconia showed basic activity and the addition of ceria suppressed the catalytic activity. From the decomposition reaction, the enhanced acidity of silica doped zirconia was investigated using combined Fourier transform infrared spectroscopy and pyridine adsorption. The results showed that the catalytic activity was taking place at Lewis acid sites.

Acknowledgments

I would like to thank Richard Joyner and the members of the Catalysis Research Centre for their guidance over the past few years. The help of the University of Twente and J. Lercher is appreciated for the infrared work. The financial support and scientific input from MEL Chemicals is most appreciated. Finally, I would like to acknowledge the encouragement from my family and friends, both in Nottingham and Liverpool.

Contents

1. Introduction

1.1 Scope of thesis.....	1
1.2 Crystallography.....	1
1.2.1 Monoclinic Zirconia. (ZrO_2).....	1
1.2.2 Tetragonal Zirconia.....	2
1.2.3 Cubic Zirconia	3
1.2.4 Orthorhombic Zirconia	3
1.2.5 Zirconia in solution.....	4
1.3 Metastable Tetragonal Zirconia	4
1.3.1 PRECIPITATION FROM SOLUTION	5
1.3.2 THERMAL DECOMPOSITION	6
1.3.3 ADDITION OF DOPANTS.	6
1.4 Tetragonal to Monoclinic phase transformation.....	12
1.4.1 The Effect of Dopants on the Tetragonal to Monoclinic Transformation.....	16
1.5 Zirconia as a catalyst and catalyst support.....	18
1.5.1 Automotive Exhaust Catalyst	18
1.5.2 Natural Gas	19
1.5.3 Pollution Control	21
1.5.4 Sulfated Zirconia-Superacidic Catalysis.....	21

2. Experimental

2.1 Surface Area Determination	27
2.2 X - Ray Photoelectron Spectroscopy	28
2.3 Fourier transform infrared spectroscopy (FTIR)	31
2.4 Powder X-ray Diffraction	33
2.4.1 Determination of phase composition	34
2.4.2 Determination of strain and crystallite size	35
2.5 Microreactor studies	37
2.5.1 Reactor Design.....	38
2.6 Gravimetric analysis	39

3. Zirconia and Lanthana Doped Zirconia

3.1 Preparation of zirconium oxide.....	42
3.2 Preparation of lanthana doped zirconia.....	43
3.3 Surface Area Results.....	44
3.4 Powder X-Ray Diffraction (XRD) results	47
3.5 X-ray Photoelectron Spectroscopy (XPS)	54
3.6 Discussion.....	57
3.7 Characterisation Conclusions	62

4. Silica doped zirconia

4.1 Preparation of silica doped zirconia.....	65
4.2 Surface Area Results.....	66
4.3 Powder x-ray diffraction results.....	68

4.4 X-ray photoelectron spectroscopy results.....	74
4.5 Discussion of Characterisation	78
4.6 Infrared spectroscopy combined with pyridine adsorption to investigate the acidic nature of the surface.....	83
4.6.1 Semiquantification of acid sites on the surface.....	98
4.7 Conclusions	104
5. Ceria Doped Zirconia	
5.1 Preparation of ceria doped zirconia	107
5.2 5.2 Surface area results.....	108
5.3 Powder XRD results.....	110
5.4 XPS results.....	114
5.5 Discussion	115
5.6 Conclusions	117
6 Reactor Studies	
6.1 Mechanisms for Decomposition	118
6.2 Binary Metal Oxide Acidity.....	123
6.3 Reactor Studies Results	127
6.3.1 Zirconia results.....	127
6.3.2 Silica Zirconia Coprecipitated Results	128
6.3.3 Silica Impregnated Results.....	132
6.3.4 Ceria doped Zirconia Results.....	135
6.3.5 Impregnated Ceria - Zirconia Results.....	139
6.3.6 Lanthana	140
6.4 Silica Zirconia Acidity.....	141
6.5 Conclusions	142
7. Discussion of Characterisation and Reactor Studies	144
8 Summary	
8.1 Coprecipitated doped zirconia.....	150
8.2 Impregnated, doped zirconia.....	152
8.3 Catalytic Studies	153
8.4 Conclusions	154

1. Introduction

1.1 Scope of thesis.

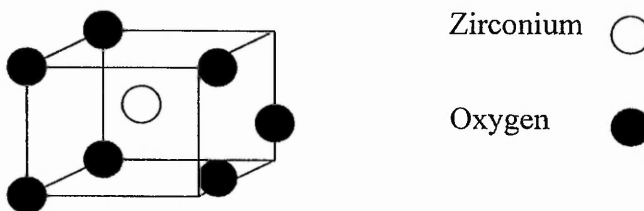
The use of zirconium dioxide is well established in the ceramics industry. However, its importance in catalysis is being more widely investigated. Zirconia can act as a catalyst support or as an active catalyst. It possesses redox properties along with acidic and basic character, proving it to be a system worthy of investigation.

The addition of dopants to stabilise the surface area of zirconia is the initial aim of this work. The surface area of pure zirconia decreases significantly with increasing calcination temperature. The dopants investigated are lanthana, silica and ceria. Each dopant alters the physical and chemical properties of the system under investigation in a specific way.

1.2 Crystallography

1.2.1 Monoclinic Zirconia. (ZrO_2)

Monoclinic zirconia is the naturally occurring form of zirconium oxide (baddeleyite). This phase is stable up to a temperature of $1170^{\circ}C$. The central zirconium atom is coordinated to seven oxygen atoms. Baddeleyite was first isolated from zircon ($ZrSiO_4$) in 1789 by Klaproth¹.

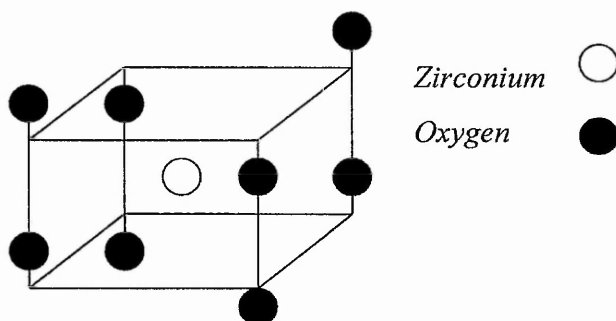


The crystallographic structure shows seven differing zirconium oxygen bond lengths within the repeat unit, and six differing zirconium/zirconium distances² within the system.

Neighbour	Distance /Å						
Zr-O	2.051	2.057	2.151	2.163	2.189	2.222	2.285
Zr-Zr	1x3.341	2x3.433	2x3.461	1x3.463	1x3.588	2x 3.923	

1.2.2 Tetragonal Zirconia

From 1170°C to 2370°C the tetragonal phase is stable and its structure is that of a distorted fluorite (CaF₂). The central zirconium atom is coordinated to eight oxygens.



The crystallographic data shows that the tetragonal structure is an elongated tetrahedron³.

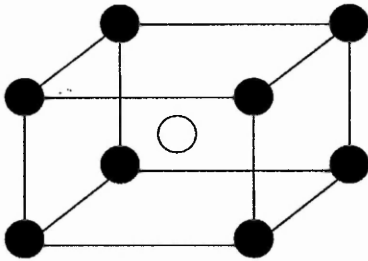
Neighbour	Distance /Å	
Zr-O	4x2.065	4x2.455
Zr-Zr	4x3.64	4x3.68

1.2.3 Cubic Zirconia

Above 2370°C the cubic form of zirconia is stable with a fluorite structure.⁴

Zirconium ○

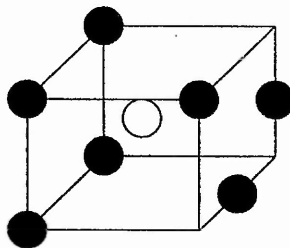
Oxygen ●



Neighbour	Distance /Å
Zr-O	8x2.28
Zr-Zr	8x3.72

1.2.4 Orthorhombic Zirconia

The structure is similar to that of monoclinic zirconia, with different neighbour distances.⁵



Oxygen ●



Zirconium ○



Neighbour	Distance /Å						
Zr-O	2.063	2.110	2.152	2.187	2.198	2.200	2.208
Zr-Zr	2x3.418	3.428	3.515	2x3.517	2x3.734	2x3.776	

The orthorhombic phase occurs from a stress induced tetragonal to orthorhombic transformation. The phase was first reported by Scholoeilein and Heuer ⁶. It was found that tetragonal zirconia precipitates would transform to orthorhombic symmetry during examination by transmission electron microscopy. The orthorhombic phase can be distinguished from both tetragonal and monoclinic phases by the reciprocal lattice geometry. The stress induced tetragonal to monoclinic transformation may involve an orthorhombic phase as an intermediate.

1.2.5 Zirconia in solution

ZrO₂ is virtually insoluble in excess base. In solution there is no evidence of Zr⁴⁺ or ZrO²⁺ under any conditions. There is evidence for the ion [Zr(OH)₈(H₂O)₁₆]⁸⁺, which crystallises out in dilute hydrochloric acid to give zirconium oxychloride ⁷. In solution the zirconium atoms lie in a distorted square, linked by pairs of hydroxo bridges and also bound to four water molecules, so that the zirconium atom is coordinated by eight oxygen atoms in a distorted dodecahedral arrangement.

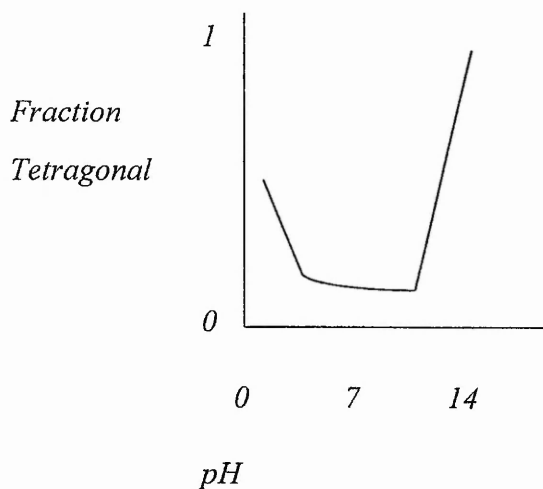
1.3 Metastable Tetragonal Zirconia

The high temperature tetragonal phase cannot be retained upon rapid cooling to room temperature, however, the phase can be obtained in a metastable condition at lower temperatures if the zirconia is prepared by precipitation from solution or by thermal decomposition of zirconium salts, and by the addition of dopants ⁸.

1.3.1 PRECIPITATION FROM SOLUTION

Garvie⁸ describes precipitation of zirconium hydroxide from hot zirconyl nitrate using a sodium hydroxide solution. The samples were calcined, for 24 hours, over a range of temperatures up to 1000°C. The tetragonal form of the oxide was stable up to 650°C, with a mixed phase of monoclinic and tetragonal up to 800°C, and purely monoclinic above this temperature. However, Garvie makes no mention to the pH of the precipitation.

The effect of pH on the phase of zirconia precipitated from solution was investigated by Davis⁹. The zirconia gel was precipitated from a zirconyl nitrate solution using a range of bases, with a variation in the pH of precipitation. The samples were calcined at 600°C. The bases used, ammonium hydroxide, sodium hydroxide and potassium hydroxide, all gave similar results. In the pH range 4 to 6.5, between 40 and 60 % tetragonal phase was obtained. The range 6.5 to 10.5 showed less than 10% tetragonal, and the range 10.5 to 14 had the greatest amount of tetragonal phase with almost 100% tetragonal at pH = 14, using sodium hydroxide as the base.



A similar investigation by Crucean¹⁰ showed that samples precipitated at pH 4 and 6 and calcined below 800°C consisted of a mixture of tetragonal and monoclinic phases. Jada et al.¹¹ investigated the pH of the precursor solution starting from

zirconyl acetate. The pH range investigated was 3.2 to 6.6 and the samples were calcined at 850°C and 1100°C. In all the samples calcined at 1100°C, the phase was monoclinic. However, at the lower temperature, between 30 and 40 % tetragonal zirconia was obtained.

1.3.2 THERMAL DECOMPOSITION

Garvie⁸ prepared zirconia from thermal decomposition of anhydrous zirconium nitrate, which was calcined at 400°C for four hours. The tetragonal phase was stable up to 500°C, with a mixed phase of monoclinic and tetragonal up to 800°C, and purely monoclinic above this temperature.

1.3.3 ADDITION OF DOPANTS.

The addition of dopants to stabilise the tetragonal phase of zirconia has been very widely investigated. The structures of the tetragonal and cubic phases of zirconia can be kinetically stabilised at room temperature by the addition of many different metal oxides, such as, MgO, CaO, Sc₂O₃, Y₂O₃, La₂O₃, Er₂O₃, SiO₂ and CeO₂, to form solid solutions¹². The amount required for the stabilisation of either polymorph depends on the nature of the dopant and the method of preparation.

1.3.3.1 Lanthana

Lanthana, La₂O₃ has an oxidation state of +3 whereas zirconia, ZrO₂ has an oxidation state of +4. Therefore, when lanthana is used as a dopant, oxygen vacancies are formed to preserve the lattice neutrality. Observations by Ozawa¹³ show that the metastable phase can be synthesised from the coprecipitate by

heating the hydrate precursor. The initial characterisation of the phase using DTA gave a crystallisation peak shift to higher temperatures, increasing with lanthana content, with respect to pure zirconia. Crystallisation was retarded by the dopant. From the powder x-ray diffraction studies, it was stated that the dopant stabilised the tetragonal phase in the ranges of 2.5 to 5 mole %. Trace amounts of the monoclinic phase were observed in this region. However, for 10 mol% lanthana, the cubic phase was observed at lower calcination temperatures but transformed to the tetragonal phase at higher temperatures. The 10 mol% lanthana stabilised the surface area from $52 \text{ m}^2\text{g}^{-1}$ at 800°C to $24 \text{ m}^2\text{g}^{-1}$ at 1000°C , in contrast with $10 \text{ m}^2\text{g}^{-1}$ at 800°C to $2 \text{ m}^2\text{g}^{-1}$ at 1000°C for pure zirconia.

Franklin¹⁴ records surface areas for 4 and 8 mol% lanthana calcined at 700°C as 58 and $74 \text{ m}^2\text{g}^{-1}$ respectively, and $29 \text{ m}^2\text{g}^{-1}$ for pure zirconia. Again, from powder XRD, the phase of the system was identified as tetragonal.

Bastide¹⁵ prepared a range of lanthana doped systems and found that the tetragonal phase could be stabilised from 2 to 8 mol% lanthana up to 1200°C . However, at the higher temperatures the pyrochlore ($\text{Zr}_2\text{La}_2\text{O}_7$) phase occurred. In the studies discussed so far, structures have been determined by XRD. However, Loong¹⁶ did show, using a neutron scattering study that 10 mole % lanthana stabilised the tetragonal and cubic symmetry up to 1000°C .

In contrast to the tetragonal phase stabilisation, Singh¹⁷, used a liquid melt technique which stabilised the cubic phase at 800°C . From 4 to 24 mole % lanthana the system had cubic symmetry. The samples were identified using XRD and infrared spectroscopy.

Mercera's¹⁸ extensive investigation of lanthana doped zirconia systems consolidated the use of lanthana as an effective dopant in stabilising the surface area and tetragonal phase of zirconia. A series of conclusions were reached in which the incorporation of 2.8 mol% lanthana in zirconia to form a solid solution was found to yield a single phase of tetragonal zirconium oxide up to 900°C . As with Ozawa¹³, the addition of the dopant retarded the crystallisation of zirconia,

and upon crystallisation the samples had a high specific surface area of $87 \text{ m}^2 \text{ g}^{-1}$ at 600°C and $58 \text{ m}^2 \text{ g}^{-1}$ at 900°C .

1.3.3.2 Silica

Dzis'ko ¹⁹ was the first to investigate silica zirconia systems for catalytic properties. Up to 90% silica was used, and from the XRD results, Dzis'ko quotes that the phase was a solid solution with no mention of either the tetragonal or monoclinic phase. However, above 1000°C the phase was identified as zircon. He concludes that the catalysts show properties of a strong acid, changing the colour of an indicator with $\text{pK} = -8.2$, with the original substances being only weakly acidic $\text{pH} = +4$. More recent investigations into silica zirconia systems give more information on the phase and surface area stabilisation.

Using 50 to 95% silica, Rao ²⁰ investigated the stabilisation of the tetragonal phase up to high temperatures. However, all the samples were amorphous up to 1000°C , above which the samples were a mixture of tetragonal and cubic. The use of a high percentage of dopant to stabilise the amorphous phase was also investigated by Soled ²¹ and Bosman ²². From Soled's work only 15 mol.% silica was required to produce the amorphous phase using a sol gel preparation. Using 1 mol% silica calcined at 500°C , the monoclinic phase was observed with a surface area of $48 \text{ m}^2 \text{ g}^{-1}$ as opposed to $19 \text{ m}^2 \text{ g}^{-1}$ for pure monoclinic zirconia. Soled was able to stabilise tetragonal phase using 5 mol% silica which had a surface area, at 500°C , of $66 \text{ m}^2 \text{ g}^{-1}$. During this study, further samples were prepared using an impregnation technique. The results obtained show that the tetragonal phase can be stabilised from 5 to 25 mol% silica at 500°C , with surface areas of 85 and $166 \text{ m}^2 \text{ g}^{-1}$ respectively.

Miller ²³ conducted a similar series of experiments to those of Soled, and states improved results in the stabilisation of the surface area of zirconia. Again, the samples were prepared using a sol gel synthesis. The tetragonal phase was stabilised using only 1 mol% silica calcined at 500°C and had a surface area of $120 \text{ m}^2 \text{ g}^{-1}$. These results differ from those obtained by Soled. At 5 mol% silica the

system was amorphous with a surface area of $145 \text{ m}^2\text{g}^{-1}$. At 900°C , 5 mol% silica had tetragonal symmetry with the lower dopant percentages showing a mixture of monoclinic and tetragonal phases. All of the samples were monoclinic at 1100°C . Miller explained the difference in the two sets of results by stating that supercritical drying yields an oxide network which is resistant to sintering and crystallisation upon thermal treatment.

Silica doped zirconia has now been used as a source of stabilised tetragonal zirconia^{24, 25} in infrared spectroscopy, temperature programmed reduction and temperature programmed desorption. 3.5wt% silica zirconia has been used as a source of tetragonal zirconia with specific surface area of $130 \text{ m}^2\text{g}^{-1}$ at 600°C and $98 \text{ m}^2\text{g}^{-1}$ at 800°C .

1.3.3.3 Ceria

The use of ceria as a dopant for the stabilisation of zirconia has become more common as a result of the increased interest in ceria in the three way automotive catalyst^{26, 27, 28}. Settu,²⁹ using a sol gel preparation, compared pure zirconia and ceria zirconia samples. It was observed that the pure zirconia was tetragonal up to 600°C , a mixture of monoclinic and tetragonal at 700°C and totally monoclinic at 850°C . However, for a 10 mol% ceria zirconia sample, the tetragonal phase was stable from 425°C to 850°C . In contrast to other dopants used the ceria did not stabilise the surface area of the zirconia. (See table below)

Calcination Temperature $^\circ\text{C}$	$\text{ZrO}_2 \text{ m}^2\text{g}^{-1}$	10 mol% $\text{CeO}_2/\text{ZrO}_2 \text{ m}^2\text{g}^{-1}$
385	90	16
600	18	7
850	4	2

From coprecipitation methods of preparation of ceria zirconia systems, varying phases and surface areas can be obtained. Urabe³⁰ produced 20% CeO₂/ZrO₂ in the tetragonal form, by calcination at 900°C, whereas Postula³¹ used 7wt% CeO₂/ZrO₂ to produce a cubic phase calcined at 450°C with a surface area of 103 m²g⁻¹. Using an impregnation technique, Ozawa³² prepared a range of ceria loadings from 60 to 90 % . The samples were all calcined at 1000°C and gave a cubic solid solution, with surface areas in the range 9 to 13 m²g⁻¹ for 90 to 70 % ceria respectively. Most of the above produced only high loadings of ceria or single specific samples for their particular application. A more detailed set of experiments was carried out by Franklin,³³ who prepared the samples by coprecipitation and calcined the products at 950°C.

Mole % CeO ₂	Surface Area m ² g ⁻¹	% Tetragonal Phase
1	16	28
2	17	85
3	21	85

From these results it can be seen that only 2 % ceria is required to stabilise the tetragonal phase.

Detailed investigation by Rao^{34,35,36} gave important information on the tetragonal phase of ceria- zirconia catalysts. By firing mixtures of the oxides at 1600°C, solid solutions of ceria/zirconia were produced over a 5 to 90% ceria content. The surface areas of all the samples were 1 to 2 m²g⁻¹. Above 60% ceria, the samples were cubic in structure . During ceramic synthesis, a solid solution was generated and the metastable tetragonal form was produced. A non-stoichiometric cooling rate produces two phases of tetragonal symmetry TZ⁰ and TZ'. These phases exist in their pure form in the compositional range 5-20% CeO₂ and 40-60% CeO₂ respectively. However, at CeO₂ content 20-40%, a mixture of TZ⁰ and TZ' exist. The former phase was characterised by a larger orthogonality (c/a = 1.018)

compared to the TZ' phase ($c/a = 1.010$). Varying the preparation method and calcination temperature of the ceria zirconia system can produce the desired phase.

1.3.3.4 Other Dopants

Many other dopants have been studied for the stabilisation of tetragonal zirconia. However, a brief summary of those studied by Mercera³⁷ will follow. Mercera studied magnesium oxide, yttrium oxide and calcium oxide along with his extensive study of lanthanum oxide. The oxides were selected according to the following two criteria ; (1) the effective cationic radius of the dopant must be similar to, or larger than that of the zirconium ion to minimize the chance of solid solution formation with monoclinic zirconia, and to influence the mass transport mechanism involved in the sintering of the material; (2) the valency of the cation must be invariant to avoid secondary effects arising from oxidation or reduction of the dopant. In concluding, Mercera found that the thermal stability of monoclinic zirconia was considerably improved by the addition of CaO and Y₂O₃ over the temperature range 400 to 900°C. The addition of MgO resulted in an improvement in the thermal stability only up to 800°C.

1.3.3.5 Theoretical observations

Theoretical studies to predict the crystal structure of zirconia have been undertaken³⁸. The objective of the studies was to calculate the free energy of each polymorph as a function of temperature and therefore, obtain transformation temperatures. The author modeled the cubic structure for pure zirconia and upon displacing the oxygen in the cubic simulation, the final relaxed structure turned out to be exactly that of equilibrated tetragonal symmetry. Therefore, it was concluded that the transformation took place due to the instability of the cubic

fluorite structure. Displacing the oxygens in the original tetragonal structure gave a final relaxed state which was an equilibrated monoclinic structure. This transformation was similar to the one from cubic to tetragonal. For the dopant study, one zirconium atom was replaced by a calcium atom, thus decreasing the overall charge. This decrease in charge was found to stabilise the cubic phase. However, when the amount of dopant was reduced to 6.25%, the cubic phase could not be stabilised, however the tetragonal phase was stabilised. These results compare with the above experimental results, that small amounts of dopant will stabilise the lower symmetry tetragonal structure but may not be sufficient to stabilise the higher symmetry phase at the same temperature.

1.4 Tetragonal to Monoclinic phase transformation

In 1929, Ruff and Ebert ³⁹ first prepared the metastable tetragonal phase by igniting zirconium salts. This finding was initially explained by Cypres et al. ⁴⁰. The authors studied the problem using differential thermal analysis, thermogravimetry and x-ray diffraction. They concluded that small amounts of bound OH groups in solid solution stabilised the tetragonal form at room temperature. When the solid was heated in the region 600°C to 900°C, the OH groups were given off as water, and the simultaneous formation of the monoclinic phase was noted. This idea was discredited by Clearfield, ⁴¹ who prepared an amorphous precipitate of hydrous zirconia which was heated under reflux in water. The amorphous → tetragonal and tetragonal → monoclinic phase transformations were observed. He therefore concluded that the OH groups did not play a role in the formation of the metastable tetragonal phase. From closer analysis of Cypres' results, it was noted that the samples were ground in butan-2-ol in preparation for infra red spectroscopy. This may account for the presence of OH groups in the system.

Garvie ⁴² investigated the monoclinic to tetragonal phase transformation using powder x-ray diffraction, and related the mean crystallite size to the identified phase. The surface area of the samples was measured by nitrogen adsorption, and

compared to the theoretical surface area calculated from the mean crystallite size. There was a small discrepancy in the experimental and theoretical surface area results due to an internal surface inaccessible for nitrogen. The theoretical and experimental values for the excess energy of the system were calculated. From the above experiments, Garvie surmised that tetragonal zirconia at room temperature appears in active powders of zirconia characterised by small mean crystallite size, large specific surface area and appreciable excess energy. However, when the powders are heated, the crystallites grow so that the specific surface area and excess energy decrease, and a simultaneous phase transformation to the monoclinic structure occurs. At this stage Garvie concluded that if monoclinic and tetragonal phases were in equilibrium at 300°C when the crystallite size was approximately 300Å, then their free energies must be equal.

$$G_m + \gamma_m A_m = G_t + \gamma_t A_t$$

where G = molar free energy of ZrO_2 (kJmol^{-1})

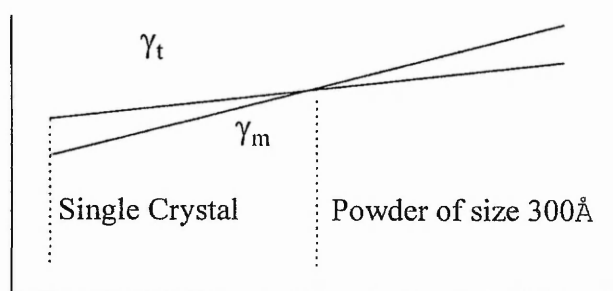
γ = surface energy (kJcm^{-2})

A = molar surface area ($\text{cm}^2\text{mol}^{-1}$)

The subscripts m and t refer to the monoclinic and tetragonal phases respectively.

When the molar free energies were equal, the tetragonal phase was formed, as shown in the graph below.

Free Energy / (Jmol^{-1})



Molar Surface ($\text{cm}^2\text{mol}^{-1}$)

Schematic free energy diagram of monoclinic and tetragonal ZrO_2

This explanation was not fully accepted by Mitsuhashi⁴³, who believed that the domain structure and grain defects required investigation. The first results show that tetragonal zirconia was transformed mechanically to monoclinic zirconia upon grinding in an agate mortar, and also when the samples were treated in alcohol using an ultrasonic vibrator. The strain of the samples was determined by applying Hall's⁴⁴ equation to the x-ray diffraction results. The particle size and domain size were calculated from electron microscopy.

From thermodynamics, Mitsuhashi states that the following relationship must be established at the monoclinic tetragonal transformation temperature.

$$(G_t - G_m) + (A_t \gamma_t - A_m \gamma_m) + (V_t - V_m) = 0$$

In addition to the terms previously explained, the symbol V denotes the strain energy of either the tetragonal or monoclinic phase.

Mitsuhashi stated that the stabilisation of the tetragonal phase must be attributed to a negative surface energy or strain energy, since the first term in the equation is positive at room temperature. It was shown that the strain energy did not contribute to the stabilisation of the metastable phase, since strain free metastable tetragonal particles were observed. The surface energy theory based on Garvie's equation was questioned due to the existence of tetragonal particles $> 1000\text{\AA}$ in diameter and stable monoclinic particles $< 100\text{\AA}$ at room temperature. Mitsuhashi claimed that the stability of metastable phase could not be explained adequately by the surface energy theory. In conclusion he stated that a single domain tetragonal crystal may be transformed to one single domain monoclinic crystal, and the transformation may be diffusionless and rapid. Polydomain metastable particles were found to be more difficult to transform to single domain particles, however, in a polycrystalline particle, domains of monoclinic and tetragonal coexist and therefore, it was suggested that the domain boundaries suppressed the transformation.

In reply to the above work, it was found that upon milling monoclinic zirconia and studying the results with x-ray diffraction, that the monoclinic (1,1,1) and (1,1,-1) lines broadened and decreased, with the eventual emergence of the tetragonal (1,1,1) line. The line increased in intensity with milling time ⁴⁵. This was in agreement with a postulate by Filipovich ⁴⁶, which stated that prolonged and intensive subdivision of the crystals may result in a polymorphic transition to a structure giving a lower surface free energy than the structure of the original crystals. The milling of monoclinic zirconia caused a phase change to tetragonal zirconia due to the subdividing of the crystallites followed by a lowering of the surface energy.

The above results led Garvie ⁴⁷ once again to conclude that the existence of tetragonal zirconia in microcrystals at a temperature well below the normal transformation temperature can be explained by a crystallite size effect. The critical size of tetragonal precipitates in the bulk is governed by the requirement that the transformation must be nucleated.

The effect of water vapour in crystallite growth and the tetragonal to monoclinic phase transformation of zirconia has been investigated by Murase et al. ⁴⁸. Samples of tetragonal and monoclinic zirconia were prepared, calcined at 1000°C and treated with water vapour at various temperatures. It was found that the crystallite growth of monoclinic samples depended on whether the furnace atmosphere was dry or wet. Water vapour increased the crystallite growth in comparison with the samples calcined in dry atmospheres. However, for the tetragonal samples it was seen that the crystallites did not grow over a certain critical size, in accordance with Garvie. The transformation of tetragonal to monoclinic symmetry in the wet atmosphere took place at a lower temperature and at a higher rate than in the dry atmosphere. Therefore, the crystallite growth in the wet atmosphere was accelerated so that the critical size of the transformation could be attained at a lower temperature. However, the critical size was lower in the dry atmosphere than in the wet atmosphere. This shows that Garvie's idea of intrinsic difference between the surface energies of the two phases is not

necessarily correct, and that the difference in the surface free energies is not intrinsic, but is decreased by the water vapour, perhaps by adsorption.

Davis⁴⁹ investigated the role of pH of precipitation in the tetragonal to monoclinic phase transformation. Tetragonal samples were prepared at pH 2.95, 10.4 and 13.5. The sample precipitated at 13.5 was completely tetragonal, and during heating at 500°C for 200 hours did not transform to the monoclinic form. For the sample precipitated at pH 10.4, 20% of the phase was tetragonal after 15 hours at 500°C, decreasing to 18% tetragonal after 200 hours. The tetragonal crystallites precipitated at 13.5 were larger than the tetragonal and monoclinic crystallites from the preparation at pH 10.4. The two phases at pH 10.4 had similar crystallite sizes. However, the sample prepared at pH 2.95 and calcined at 500°C for 15 hours was 73% tetragonal phase, decreasing to 14% after 200 hours. From the crystallographic data obtained for the sample at pH 2.95, the tetragonal crystallites transformed to monoclinic crystallites of approximately half the size. The tetragonal crystallite sizes of the sample prepared at pH 2.95 were smaller than those of the sample precipitated at pH 13.5. Therefore, tetragonal crystallites from pH 2.95 of smaller size were transforming to the monoclinic phase, whereas larger tetragonal crystallites, prepared at pH 13.5, were remaining tetragonal. The stabilisation of the tetragonal phase of zirconia does not occur with all zirconias. The pH of precipitation was shown to be a factor in the stabilisation process.

1.4.1 The Effect of Dopants on the Tetragonal to Monoclinic Transformation

There was very little information about the influence of crystallite size of the tetragonal and monoclinic phases of doped zirconias. However, work by Mercera¹⁸ and Franklin gives information about the particle size of the tetragonal doped zirconia systems.

Franklin¹⁴, in the study of ceria and lanthana doped zirconias gave evidence for Garvie's crystallite size theory for stabilising the tetragonal phase. The crystallite

sizes for tetragonal doped zirconia were all below the 30 nm critical crystallite size both for lanthana (Table 1) and ceria (Table 2).

Table 1 4 mol% Lanthana doped zirconia.

Calcination Temperature/ °C	% Tetragonal Phase	Crystallite Size / nm
400	27	18
500	100	21
600	100	16
700	98	20

Table 2 Ceria doped zirconia calcined at 950°C.

Mole % Ceria	% Tetragonal Phase	Crystallite Size / nm
1	28	22
2	85	21
4	85	21

Mercera's ¹⁸ results again tied in with Garvie's critical crystallite size theory. Lanthana doped zirconia catalysts at 2.8 mol% were prepared and calcined over the temperature range 500°C to 900°C. The crystallite size for the tetragonal phase did not exceed approximately 20 nm, whereas the monoclinic phase crystallite size increased above 30 nm.

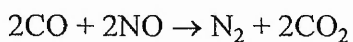
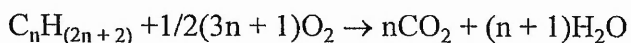
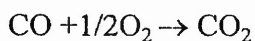
1.5 Zirconia as a catalyst and catalyst support.

Zirconia is the only single metal oxide which may possess acidity or basicity as well as reducing or oxidising ability⁵⁰. Tanabe demonstrated these results through a series of experiments. The acidity of precipitated zirconia has been recorded to be $H_0 = +1.5$ for a calcination temperature of 500°C. Where H_0 is the Hammett acidity function. The acid amounts were 0.06 and 0.280 mmolg⁻¹ at $H_0 = +1.5$ and $H_0 = +4.0$, respectively⁵¹. Zirconia, a weakly acidic oxide demonstrates primarily Lewis acidity, together with partial Brønsted acidity⁵². The basic strength of zirconia evacuated at 500°C was $H_0 = 18.4$ ⁵³, although when calcined in air at 500°C the sample showed no basic property⁵⁴. The oxidising properties of zirconia were investigated using the adsorption of triphenylamine and the addition of oxygen. An ESR signal was observed and assigned to the triphenylamine cation radical, showing the oxidising ability of the zirconia surface⁵⁵. Nitrobenzene was used as a probe molecule to study the reducing property of the sample. A concentration of nitrobenzene radicals was observed to show the reducing ability of zirconia.

These properties of zirconia have led to the use of zirconia in the following catalytic applications. However, due to loss of surface area with increasing temperature, the application of zirconia in catalysis is limited.

1.5.1 Automotive Exhaust Catalyst

An automotive exhaust catalyst must perform the three following reactions.

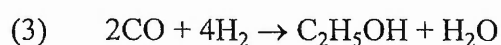
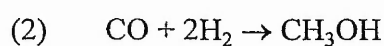
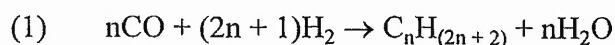


Conventional catalysts comprise platinum, rhodium and palladium on alumina. Recent developments have seen zirconia being incorporated into the exhaust catalyst. At full working power of the engine, the catalyst may exceed temperatures of 800°C. However, in the conventional catalyst at these temperatures the rhodium can migrate into the alumina lattice. It was found that when rhodium was supported on zirconia, the metal showed no loss of surface area after 5 hours at temperatures greater than 900°C⁵⁶. For further protection of the rhodium in the catalyst, a system was devised⁵⁷ where the platinum and rhodium were contained in two different layers. The alumina, ceria and platinum layer was initially deposited, followed by the zirconia, alumina and rhodium layer. The two layer approach improved the removal of hydrocarbons and increased the conversion of carbon monoxide and nitric oxide.

Ceria, known for its oxygen storage capacity in automotive catalysts⁵⁸, was found to deactivate at severe temperatures. However, a cerium zirconium oxide solid solution improved the thermal stability and activity of the ceria⁵⁹.

1.5.2 Natural Gas

The practical process for utilising natural gas is the conversion of the feedstock to synthesis gas, through steam reforming. Synthesis gas is a mixture of carbon monoxide, carbon dioxide and hydrogen, the composition depending on the feedstock and the details of the conversion process. The main use of synthesis gas is in the production of transportation fuels. Hydrocarbons may be formed using the Fischer - Tropsch process (Equation 1) or depending on the stoichiometry, alcohols may be produced (Equations 2 and 3).



In a study of zirconia as a catalyst for the synthesis of methanol^{60,61}, it was observed that methanol was formed from hydrogen and carbon monoxide, in the presence of water vapour, at low and high temperatures. The use of zirconia, as a support, with impregnated copper as the active catalyst was investigated^{62,63,64}. Denise⁶⁵ observed that the Cu/ZrO₂ catalyst with a 1-2% Cu loading produced more methanol, per gram of copper, than the conventional CuO/ZnO/Al₂O₃ catalyst, which used 40 - 50 % copper. Amenomiya⁶⁶ showed that 40% Cu/ZrO₂ gave the highest carbon conversion and best selectivity to methanol, for the different loadings of copper used.

Ichikawa⁶⁷, produced ethanol using a rhodium on zirconia catalyst. The rhodium was deposited as a carbonyl cluster onto the oxide. The selectivity to ethanol was 53% , 27% to methanol and 17% to methane. The conversion of carbon monoxide was 12% and the reaction temperature was 210°C. This system was developed by B.P.⁶⁸ using a Rh/ZrO₂/SiO₂/K catalyst to produce ethanol.

Shell have developed a catalyst for the Fischer - Tropsch process incorporating zirconia⁶⁹. The traditional catalysts used were iron, or cobalt on silica, in comparison to the new catalyst which comprises cobalt on silica and zirconia. Zirconia was introduced to increase the activity of the catalyst without changing the high level of selectivity to higher hydrocarbons. The effect of adding 15% by weight of zirconia to a cobalt silica catalyst was an increase in the activity of more than threefold. The catalyst was prepared by impregnating zirconium tetrapropoxide, by an incipient wetness technique. The sample was then calcined at 500°C, prior to impregnation of the cobalt nitrate solution, followed by calcination.

1.5.3 Pollution Control

The removal of nitrogen oxides from stack gases is important in environmental protection. Ammonia was added to the stack gases to react with the NO_x to produce water and nitrogen. A catalyst containing zirconia, vanadium pentoxide and cobalt (III) oxide was tested in the above reaction ⁷⁰. At atmospheric pressure and a temperature of 380°C , the catalyst was used to treat a flue gas containing NO_x and CO. The catalyst reduced the concentration of both CO and NO_x by 90%. Hydrated zirconia has been used in the removal of atmospheric sulfur ⁷¹. High conversions of the sulfur-containing compounds were obtained.

1.5.4 Sulfated Zirconia-Superacidic Catalysis

The interest in zirconia, modified with small quantities of sulfate ions, has increased greatly in the past few years, due to the exhibition of super acidic properties of zirconia catalysts. In a recent publication, Davis ⁷² reviews the use of sulfated zirconia as a hydrocarbon conversion catalyst. It was concluded that platinum containing sulfated zirconia was a more active catalyst for hydrocarbon isomerisation and cracking than most zeolite cracking catalysts. Therefore, there has been a great interest in these catalysts. The preparation technique, initial calcination and final catalyst treatment played an important role in determining the catalyst activity. Nascimento et al. ⁷³ found that the sulfur content of the catalysts depended upon the calcination temperature and the concentration of acid used to prepare the catalyst. Garin ⁷⁴ and Hosoi ⁷⁵ observed an increase in activity for hydrocarbon isomerisation when platinum was added as opposed to sulfated zirconia. Identification of the nature of the acidity was unsuccessful, however, the data indicated Brønsted acidity to be more likely. Nitta ⁷⁶ found that sulfated zirconia exhibited high activity and selectivity for the conversion of methanol into

hydrocarbons. The activity and selectivity were found to be comparable to those obtained with a HZSM-5 catalyst.

Summary

From the literature, it can be observed that there is a desire for a single phase (either monoclinic or tetragonal), high surface area zirconia catalyst support. The use of dopants provides the best way of stabilising the surface area and phase of zirconia. A full characterisation of these materials is required for its use as a catalyst support. The work in this thesis will try to satisfy the above points.

References

-
- ¹ N. N. Greenwood and A. Earnshaw, *Chemistry of the Elements*, Pergamon 1994.
 - ² D. K. Smith and H. W. Newkirk, *Acta Cryst.*, 18 (1965) p983.
 - ³ G. Teufer *Acta. Cryst.*, 15 (1962) p1187.
 - ⁴ D. K. Smith and C. F. Cline, *J. Am. Ceram. Soc.* 45 (1962) p249.
 - ⁵ O. Ohtaka, T. Yamanaka, S. Kume, N. Hara, H. Asano and F. Izumi, *Proc. Jpn. Acad. B* 66, (1990) p193.
 - ⁶ L. H. Schoenlein and A. H. Heur, *Mechanics of Ceramic*, vol. 6, 1982.
 - ⁷ F. A. Cotton and G. Wilkinson, *Advanced Inorganic Chemistry*, Interscience 1980.
 - ⁸ R.C. Garvie, *J. Phys. Chem.* 65 (1969) p1238.
 - ⁹ B.H. Davis, *Comm. Am. Ceram. Soc.* 1984 C-168.
 - ¹⁰ E. Crucean and B. Rand, *Trans. J. Brit. Ceram. Soc.* 78 (1979) p58.
 - ¹¹ S.S. Jada and N.G. Peletis, *J. Mater. Sci. Lett.* 8 (1989) p241-246.

-
- ¹² T. H. Etsell and S. N. Flengas, *Chem. Rev.*, 70 (1970) p339.
- ¹³ M. Ozawa and M. Kimura, *J. Less Common Metals*, 171(1991) p95-212.
- ¹⁴ R. Franklin, P. Goulding, J. Haviland, R.W. Joyner, I. McAlpine, P. Moles, C. Norman, T. Nowell, *Catalysis Today* 10(1991) p405.
- ¹⁵ B. Bastide, P. Odier and J.P. Coutures, *J. Am. Ceram. Soc.*, 71 [6] (1989) p449-453.
- ¹⁶ C. K. Loong J. W. Richardson and M. Ozawa, *J. Catal.* 157 (1995) p636-644 .
- ¹⁷ P. Singh, S.R. Sainkar, M.V. Kuber, V.G. Gunjekar, R.F. Shinde and S.K. Date, *Materials Letters* Vol. 9 (2), (1990) p65.
- ¹⁸ P. D.L. Mercera, J. G. Van Ommen, E. B. M. Doesburg, A. J. Burgraaf and J. H. Ross, *Applied Catalysis*, 78 (1991) p79-96 and P. D.L. Mercera, J. G. Van Ommen, E. B. M. Doesburg, A. J. Burgraaf and J. H. Ross, *Applied Catalysis*, 71 (1991) p363-391.
- ¹⁹ A.D. Makarov, G. K. Boreskov and V. A. Dzis'ko, *Kin. I Katal.* vol. 2 No. 1 p84-93.
- ²⁰ K. J. Rao and V. S. Nagarajan, *J. Mater. Sci.* 24 (1989) p2140-2146.
- ²¹ S. Soled and G. B. McVicker, *Catalysis Today*, 14 (1992) p189-194.
- ²² H. J. M. Bosman, E. C. Kruissink, J. van dr Spoel and F. van den Brink, *J. Catal.* 148 (1994) p660-672 .
- ²³ J. B. Miller, S. E. Rankin and E. I. Ko, *J. Catal.* 148 (1994) p673-682.
- ²⁴ A. Trunschke, D. L. Hoang and H. Lieske, *J. Chem. Soc. Faraday Trans.*, 91(24) (1995) p4441-4444.
- ²⁵ D.L. Hoand, H. Berndt and H. Lieske, *Catalysis Letters* 31 (1995) p165-172.
- ²⁶ H. Cordatos, T. Binluesin, J. Stubenrauch, J.M. Vohns and R. J. Gorte, *J. Phys. Chem.*, 100 (1996) p785-789.
- ²⁷ A. D. Logan and M. Shelef, *J. Mater. Res.* 9 (1994) p468-475.

-
- ²⁸ J. G. Nunan, H.J. Robota, M. J. Cohn and S. A. Bradley, *J. Catal.* 133 (1992) p309-324 .
- ²⁹ T. Settu and R. Gobinathan, *Bull. Chem. Soc. Jpn.*, 67 (1994) p999-2005.
- ³⁰ K. Urabe, A. Nakajima, H. Ikawa and S. Udagawa, *Advances in Ceramics vol. 24: Science and Technology of Zirconia III*, (1984).
- ³¹ W. S. Postula, A. Akgerman and R. G. Anthony, *Applied Catalysis* 112 (1994) p175-185.
- ³² M. Ozawa, M. Kimura and A. Isogai, *J. Alloys Compounds*, 193 (1993) p73-75.
- ³³ R. Franklin and R. W. Joyner, Unpublished Results.
- ³⁴ G. R. Roa, J. Kasper, S. Meriani, R. di Monte and M. Graziani, *Catalysis Letters*. 24 (1994) p107-122.
- ³⁵ G. R. Roa, J. Kasper, P. Fornasiero, S. Meriani, R. di Monte and M. Graziani, *Stud. Surf. Sci. Catal.* (1994) p397-406.
- ³⁶ G. R. Roa, J. Kasper, P. Fornasiero, S. Meriani, A. Trovarelli, R. di Monte and M. Graziani, *J. Catal.* 151 (1995) p68-177.
- ³⁷ P. D. L. Mercera, Ph. D. Thesis University of Twente 1991.
- ³⁸ A. N. Cormack and S. C. Parker, *J. Am. Ceram. Soc.*, 73 [11] (1990) p3220-3224.
- ³⁹ O. Ruff and F. Ebert, *Z. anorg. allgem. Chem.*, 180 (1929) p19.
- ⁴⁰ R. Cypres, R. Wollast and J. Raucq, *Ber. Deut. Keram. Ger.* 40 (1963) p527.
- ⁴¹ A. Clearfield, *Inorg. Chem.*, 3 (1964) p146.
- ⁴² R.C. Garvie, *J. Phys. Chem.* 65 (1969) p1238.
- ⁴³ T. Mitsuhashi, M. Ichihara and U. Tatsuke, *J. Am. Ceram. Soc.*, 57, (1973) p97.
- ⁴⁴ W. H. Hall, *Proc. Phys. Soc. A* 62 (1949) p741.
- ⁴⁵ J. Bailey, P. Bills and D. Lewis, *Trans. J. Brit. Ceram. Soc.*, 74, (1975) p247.
- ⁴⁶ V. Filipovich and A. Kalinina, *Struct. Glass*, 5, (1965) p34.

-
- ⁴⁷ R. C. Garvie, *J. Phys. Chem.*, 82, (1978) p2.
- ⁴⁸ Y. Murase and E. Kato, *J. Am. Ceram. Soc.*, 66, (1982) p3.
- ⁴⁹ B. H. Davis, R. Srinivasan and R. De Angelis, *J. Mater. Res.* 1 (4) 1986.
- ⁵⁰ K. Tanabe, *Mater. Chem. Phys.*, 13 (1985) p347.
- ⁵¹ K. Shibata, T. Kiyoura, J. Kitagawa, T. Sumiyoshi and K. Tanabe, *Bull. Chem. Soc. Jpn.*, 46 (1973) p2985.
- ⁵² Y. Nakano, T. Iizuka, H. Hattori and K. Tanabe, *J. Catal.*, 57 (1979) p1.
- ⁵³ Y. Nakano, Ph.D. Thesis Hokkaido University 1982.
- ⁵⁴ K. Tanabe, H. Hattori, I. Ichikawa, H. Ikeda, *J. Res. Inst. Catalysis*, 19 (1972) p185.
- ⁵⁵ Y. Nakano, T. Iizuka, H. Hattori and K. Tanabe, *J. Catal.*, 57 (1979) p1.
- ⁵⁶ USP 4 233 189, H. Ghandi (Ford) 1979.
- ⁵⁷ EP 0 139 240, I. Onal (UOP Inc.) 1984, DE 3 737 419, S. Natsumoto 1986, , EP 0 262 962, T. Chiba (Engelhard Corp.) 1987.
- ⁵⁸ H. C. Yao and H. C. Yao and Y. F. Yao, *J. Catal.*, 86 (1984) p254.
- ⁵⁹ M Ozawa, M. Kimura and A. Isogai, *J. Alloys Compounds*, 193 (1993) p73-75.
- ⁶⁰ M. Y. He and J. G. Ekerdt, *J. Catal.*, 87, (1984) p238.
- ⁶¹ H. W. Chen, J. M. White and J. G. Ekerdt, *J. Catal.*, 99 (1986) p293.
- ⁶² B. Denise and R. P. A. Sneed, *Applied Catalysis* 28 (1986) p235.
- ⁶³ G. J. J. Bartley and R. Burch, *Applied Catalysis*, 43 (1988) p141.
- ⁶⁴ D. Gasser and A. Baiker, *Applied Catalysis*, 43 (1988) p141.
- ⁶⁵ B. Denise , O. Cherifi, M. M. Bettahar and R. P. A. Sneed, *Applied Catalysis*, 48 (1989) p365.
- ⁶⁶ Y. Amenomiya, *Applied Catalysis*, 30 (1987) p57.
- ⁶⁷ M. Ichikawa, *J. C. S. Chem. Comm.*, (1978) p556.

-
- ⁶⁸ EP 30 110 W. Ball (B.P.) 1980; EP 79 132, W. Ball (B.P.) 1982.
- ⁶⁹ FR 2 173 041; Shell 1973, GB 2 077 289; H. Bijwaard (Shell) 1981, FR 2 483 911 Shell 1973; GB 2 125 062; A. Hoek (Shell) 1983, EP 0 110 449; A. Hoek (Shell) 1983, EP 0 127 220, J. Minderhoud (Shell) 1984, EP 0 262 962, T. Chiba (Engelhard Corp.) 1987.
- ⁷⁰ JP 62 286 543, I. Kozo 1986.
- ⁷¹ EP 244 301, E. Quemere (Rhone-Poulenc) 1987.
- ⁷² B. H. Davis, R. A. Keogh and R. Srinivasan, *Catalysis Today*, 20 (1994) p219-256.
- ⁷³ P. Nascimento, C. Akratopoulou, M. Oszagyan, G. Coudurier, C. Travers, J. F. Joly and J. C. Vadrine, in L. Guzzi et al. (Editors), *New Frontiers in Catalysis*, Amsterdam 1993, p. 1185-1197.
- ⁷⁴ F. Garin, D. Andriamasinoro, A. Abdulsamad and J. Sommer, *J. Catal.*, 131 (1991) p199.
- ⁷⁵ T. Hosoi, T. Shimidzu, S. Itoh, S. Baba, H. Takaoka, T. Imai and N. Yokoyama, *Am. Chem. Soc., Div. Petr. Chem., Prepr.*, 33 (1988) p562.
- ⁷⁶ M. Nitta, H. Sakoh and K. Aomura, *Applied Catalysis*, 10 (1984) p215.

2. Experimental

2.1 Surface Area Determination

The use of nitrogen adsorption combined with applying the Brunauer, Emmett and Teller equation has been used to determine the surface areas of the zirconia and doped zirconia samples. The surface area and porosity of a solid play complementary roles in the adsorption phenomena. The measurement of the adsorption of gases or vapours yields information on the surface area and pore structure of the samples. The specific surface area is directly proportional to the monolayer coverage of the adsorbed species. The monolayer coverage is defined as the quantity of the adsorbate which can be accommodated in a completely filled single layer of molecules on the surface of the solid. On applying the BET equation to a relevant isotherm, the monolayer coverage can be determined. The surface area of the sample can be determined from knowledge of the size of an adsorbed molecule. From the BDDT classification of isotherms¹, there are five isotherms and the BET equation can be applied only to types II and IV.

The BET Equation

$$\frac{P}{V(P_0 - P)} = \frac{1}{V_m C} + \frac{(C-1)P}{V_m C P_0}$$

P = equilibrium pressure

V = volume of gas adsorbed at equilibrium pressure

V_m = volume necessary to form a monolayer

P₀ = saturated vapour pressure of the adsorbed gas at temperature of measurement

C = constant

A straight line is obtained by plotting $P/V(P_0-P)$ against P/P_0 . The gradient is given by $(C-1)/V_m C$ and the intercept by $1/V_m C$. The surface area can be derived from V_m . The BET equation is only valid for the range $0.05 < P/P_0 < 0.30$, since the isotherm is linear in this range.

The sample was outgassed overnight, over the temperature range 100 to 200°C, until a final pressure of 6×10^{-2} Torr was reached. Helium was used to calibrate the sample volume and nitrogen was used as the adsorbate. The computer controlled system calculated the surface area, monolayer coverage and C constant.

2.2 X - Ray Photoelectron Spectroscopy

X-ray photoelectron spectroscopy is used for the quantitative analysis of the surface composition of the sample^{2,3}. The origin of the characterisation is derived from the photoelectric effect. X-rays, usually K_α Al ($h\nu = 1486$ eV) or K_α Mg ($h\nu = 1254$ eV) bombard the sample, where the photoelectrons are emitted from the near surface region (< 10 nm) of the sample. The kinetic energy of the electrons leaving the sample produces features in the energy spectrum which correspond to the ionisation from core orbitals. These features are characteristic of the elements present near the surface of the material. From the following relationship the binding energies are determined.

$$E_K = h\nu - E_B - \phi$$

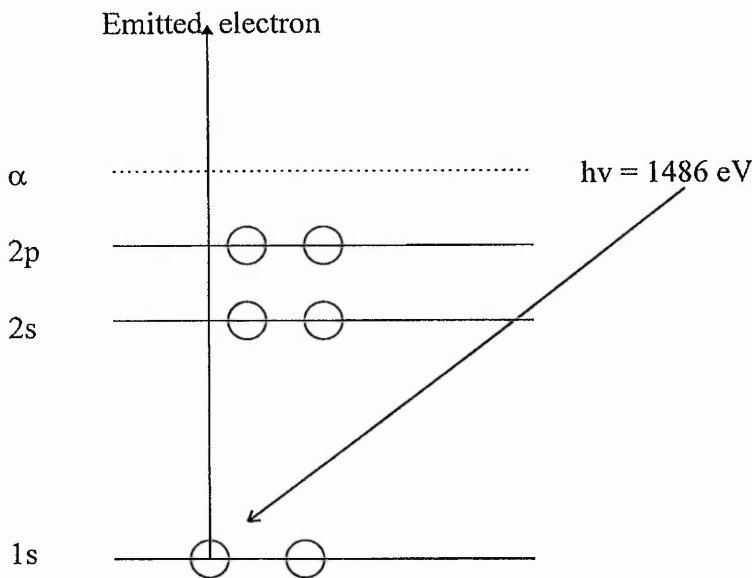
$h\nu$ = x-ray energy

E_B = electron binding energy of a particular core level of the atom

E_K = photoelectron kinetic energy

ϕ = work function

All the elements except for H and He give rise to a photoelectric spectrum in this way.



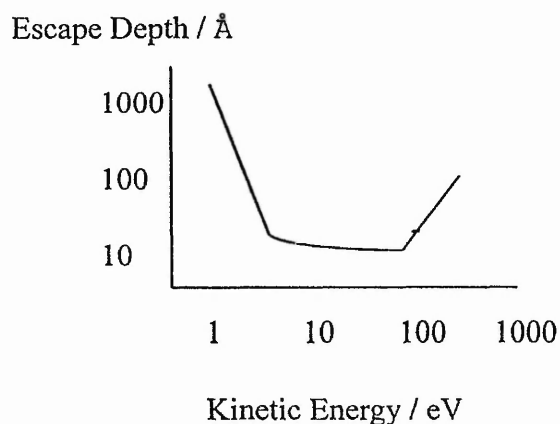
Representation of an incoming X-ray to remove an electron from the 1s level of the atom, where α is the Fermi level.

The x-rays are produced by high energy electron bombardment of the anode (Al or Mg). The bombardment produces a 1s core hole in the Al or Mg atom which is then filled by a 2p to 1s transition and the emission of the x-ray. The emitted electrons from the sample are analysed using hemispherical electrostatic deflectors with final electron collection onto a channel electron multiplier.

The electrons emitted can travel only short distances before losing energy in collisions with atoms. This inelastic scattering process gives rise to the surface sensitivity of XPS. This also relates to the notion of escape depth, which is defined as the thickness of material for which the probability of electron transmission without energy loss is $1/e$. The intensity I of elastically transmitted electrons depends exponentially on the thickness d ,

$$I = I_0 \exp(-d/\lambda)$$

This has been expressed in terms of a universal escape depth curve, where the mean free path of an electron is plotted as a function of kinetic energy.



The binding energy for the core level of an atom varies only by +/- 2%. However, for an atom in different chemical environments, the binding energy is not constant. The binding energy for carbon 1s may vary up to 5eV for different carbon environments in a polymer. The binding energy increases with increasing charge.

The main use for XPS in this project was to determine the quantity of the dopant at the catalyst surface. This was achieved by comparing the relative peak areas for the most intense bands of the dopant and the zirconia. The results obtained refer to a distribution that is homogeneous with depth. The following equation was used:

$$\frac{I_A}{I_B} = \frac{N_A}{N_B} \times \frac{\delta_A}{\delta_B} \times \left[\frac{E_A}{E_B} \right]^{0.6}$$

I = area under peak corrected for number of scans

N_A/N_B = surface ratio of element A to B

δ = photoionisation cross sectional area⁴

E = kinetic energy

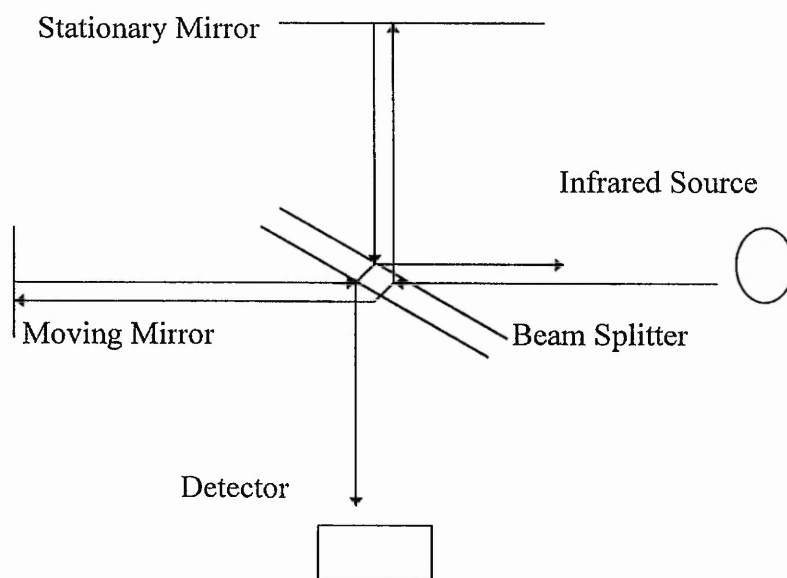
X-ray excited electron spectra were recorded with a VG ESCA3. The powder samples were attached to the probe using double sided tape. Mg K_{α} (1254 eV) and Al K_{α} (1486 eV) radiation was used. The vacuum in the analyser chamber was kept at $< 10^{-8}$ Torr. Carbon 1s BE = 285 eV was used as the reference for all the samples.

2.3 Fourier transform infrared spectroscopy (FTIR)

Pyridine adsorption combined with infrared spectroscopy was undertaken on the silica doped zirconia samples, to investigate the acidic nature of the catalysts.

FTIR spectrometers employ an interferometer to generate the spectrum⁵. The interferometer consists of a moving mirror, fixed mirror and a beam splitter. The infrared source is collimated with slits and the resultant beam is divided in two, with half passing to the fixed mirror and the other half reflected to the moving mirror. After reflection the two beams recombine at the beam splitter and constructively or destructively interfere, depending on the optical paths of the two arms of the interferometer. Part of the beam passes through the sample and is focused onto the detector, which records the interferogram. The interferogram is converted to a spectrum using a Fourier transform mathematical function.

Interferometer Optical System

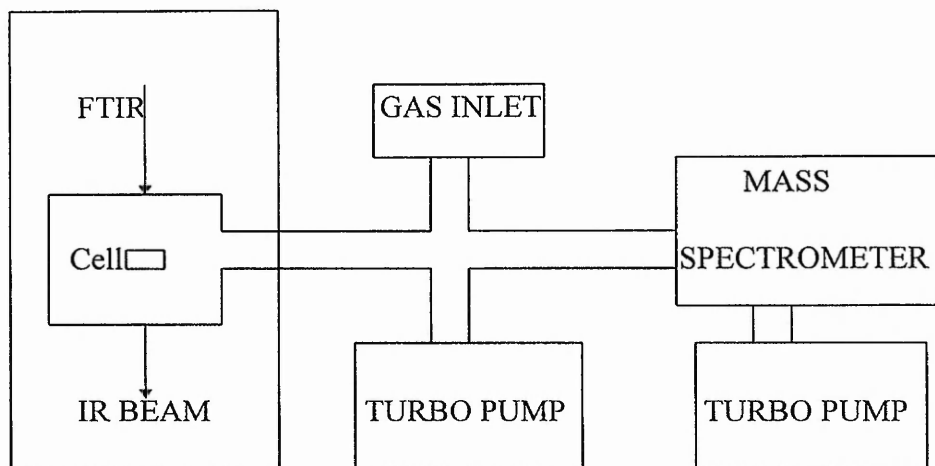


The experimental setup consisted of a vacuum system for sample treatment, mass spectrometer to record the desorption of the adsorbed species and the infra red spectrometer for the measurement of the adsorbed species on the sample. The vacuum system, built in stainless steel, contained a dosing section and a cell, which sat in the infra red beam. The cell was equipped with two calcium fluoride (CaF_2) windows, defining a spectral region of 1200 cm^{-1} to 4000 cm^{-1} . The sample was pressed into a self supporting thin wafer and housed in a gold sample holder, which sat directly in the infra red beam. The sample holder could be heated to 600°C . Thus all the sample treatments could be performed *in situ*. The system was evacuated using a rotary pump and a turbo molecular pump ($<10^{-6}$ mbar). The pressure was measured with a cathode gauge in the high vacuum region, and a Baratron capacitance manometer in the low vacuum range.

The sample was pretreated in vacuum at 400°C , for one hour, before the dosing of pyridine took place at 40°C . The pyridine was admitted into the system via a dosing valve. The adsorbed species were detected using infrared spectroscopy on a Bruker IFS 88 Fourier transform spectrometer equipped with a Mercury Cadmium Telluride detector. The spectra were recorded with a spectral resolution of 4 cm^{-1} . All the spectra were recorded in the transmission mode and the empty cell was used to provide the reference spectra.

Pyridine was dosed over a pressure range of 10^{-3} to 1 mbar. Spectra were recorded until equilibrium was reached at each pressure. The system was then evacuated to 10^{-6} mbar, where upon the temperature programmed desorption of the adsorbed species was recorded by the infra red spectrometer and the mass spectrometer.

Schematic diagram of the infrared experimental set up.



2.4 Powder X-ray Diffraction

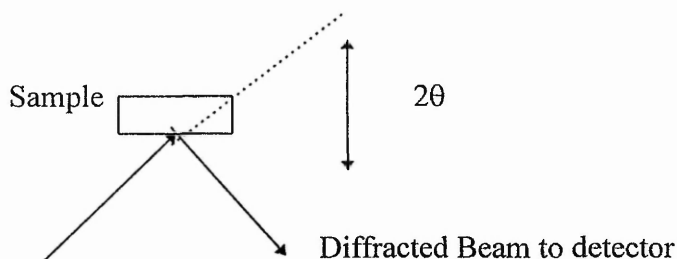
X-ray diffraction (XRD) is a technique used to identify the crystalline phases present in materials and to measure structural properties of the phases such as strain, crystallite size, epitaxy, preferred orientation and defect structure ^{6 7 8}. XRD is non destructive. Materials composed of any element can be studied with XRD, but XRD is most sensitive to elements with high atomic numbers. Amorphous materials have diffraction patterns devoid of the sharp peaks characteristic of crystals and consist of broad features, however, quantitative analysis of the amorphous material is complicated but provides information on local atomic structure. Since, the diffraction pattern from amorphous materials may be weak, thick samples or synchrotron radiation is necessary.

Monochromatic x-rays, produced by bombardment of high energy electrons onto the source, commonly copper, are diffracted by the powder sample in accordance with the Bragg Law.

$$n\lambda = 2d\sin\theta$$

- λ = wavelength of the x-ray source
 d = distance between planes
 2θ = diffracted angle from incidence

Basic features of an XRD experiment



Incident Beam from x-ray source

The intensity of the diffracted x-rays are detected by a position sensitive detector over the desired range for 2θ . Phase identification from the recorded XRD pattern is obtained by comparing the measured d -spacing and the integrated intensities with known standards in the JCPDS Powder Diffraction File. This identification is primary in the zirconia and doped zirconia samples to distinguish between the monoclinic and tetragonal phases.

2.4.1 Determination of phase composition

The determination of the phase composition of the samples was undertaken by comparing the relative ratios for the tetragonal (111) line and the monoclinic (111) and (-111) lines⁹. The volume fraction (V_m) of the monoclinic zirconia phase was calculated from the integrated intensity ratio X_m . Powder x-ray diffraction of the samples was taken in detail over the range $26^\circ < 2\theta < 33^\circ$, since the main monoclinic and tetragonal lines are observed in this region.

$$X_m = \frac{I_m(-111) + I_m(111)}{I_m(-111) + I_m(111) + I_t(111)}$$

and using the non linear relationship proposed by Toraya⁹

$$V_m = \frac{PX_m}{1 + (P-1)X_m}$$

where P is a constant with the value 1.31.

2.4.2 Determination of strain and crystallite size

The strain and crystallite size of the sample can be determined from the line broadening of the tetragonal (111) or the monoclinic (111) peak. The width of the peak is affected by the radiation source, instrumental broadening, crystallite size and strain¹⁰. The Voight^{11 12 13} function, which is a convolution of a Cauchy and Gaussian function, has been used to investigate the line broadening effects due to strain and size. The Cauchy component of the function relates to the crystallite size and the Gaussian function relates to the strain. The Cauchy and Gaussian components are found from the ratio of the full width half maximum (FWHM) of the broadened profile to its integral breadth, which is the area under the peak divided by the intensity. The above literature lead to a procedure for determination of crystallite size strain for zirconia powders¹⁴. The diffraction patterns are collected and the peak area of the desired line is determined. Then a series of subtractions are performed. The $K_{\alpha 2}$ component of the x-ray, which adds to the line broadening, and the background are subtracted, where upon the half height width and peak height are measured. This allows the integral breadth to be calculated. The Cauchy and Gaussian components can then be determined from

equations containing half height breadth and the integral breadth ¹⁵. Both the Cauchy and Gaussian functions are corrected for instrumental broadening. The crystallite size and the strain of the system can then be calculated using the following equations:-

Determination of apparent crystallite size free of strain.

$$D = \frac{\lambda}{\beta_C \cos \theta}$$

β_C = line broadening due to crystallite size

θ = Bragg angle

λ = X-ray wavelength, Å

Determination of strain

$$e = \frac{\beta_G}{4 \tan \theta}$$

β_G = line broadening due to strain

θ = Bragg angle

The Scherrer equation was also used to determine the crystallite size from the line broadening, for a comparison.

$$D = \frac{0.9\lambda}{B \cos \theta}$$

D	=	crystallite size
B	=	line broadening (radians)
θ	=	Bragg angle
λ	=	x-ray wavelength, Å

The diffraction patterns, for the finely ground zirconia and doped zirconia samples were recorded on a Siemens D500 XRD apparatus. The scan range was $26^\circ < 2\theta < 33^\circ$ with a step size of 0.01° and a step time of 5 seconds. The tetragonal (111) line appears at 30° whereas, the monoclinic (111) appear at 31° and (-111) at 28° , using copper as the x-ray source.

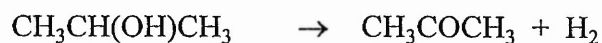
2.5 Microreactor studies

A microreactor has been designed and constructed, with an on line gas chromatograph (GC), to investigate the decomposition of propan-2-ol. The main decomposition routes are:

(1) The dehydration reaction of propan-2-ol to propene and water. This reaction is acid catalysed.



(2) The dehydrogenation reaction of propan-2-ol to acetone and hydrogen. This reaction is base catalysed.

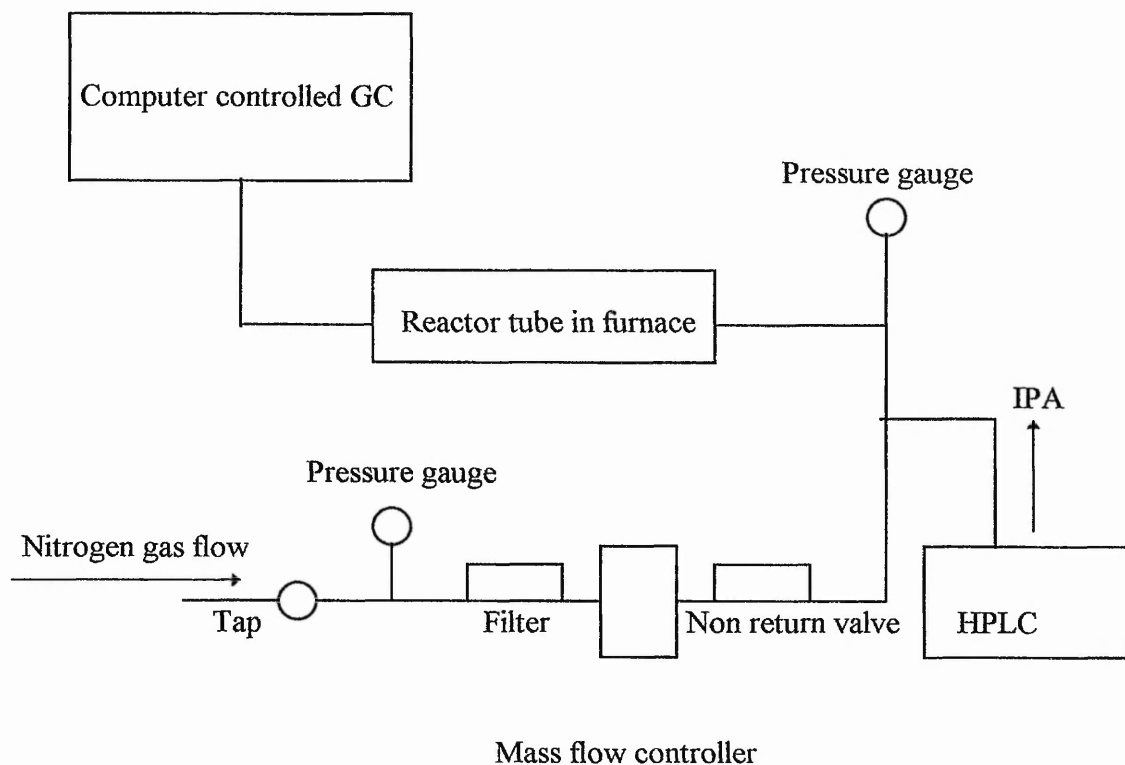


2.5.1 Reactor Design

The microreactor was constructed from 1/4" stainless steel tubing (see schematic below). The gas line, which contained nitrogen as the diluent, consisted of, in order, a tap, pressure gauge, filter, mass flow controller connected to a Brooks controller and a non return valve. The line was then connected to the 1/2" reactor tube, made of stainless steel, which was housed in a Carbolite furnace controlled by an Eurotherm 818 controller. The liquid feed was admitted to the system, using a Kontron 420 high performance liquid chromatography pump (HPLC), at a junction before the furnace and after the non return valve. At the junction of the gas line and the liquid feed, the trace heating of the lines began, to keep the propan-2-ol in the gaseous state. The lines were heated with Isopad heating tape and controlled by Variacs. The trace heated lines continued from the reactor tube to the Varian Star 3400 GC, where the products were analysed. The GC was controlled by an Opus 486 computer. Air actuated Valco valves were used for automated injections of the products, with a Porapak Q column being used for the separation of the products. The carrier gas through the column was nitrogen. The products were detected using a flame ionisation detector (FID). The advantages of using a FID detector are; (1) it has a high sensitivity to virtually all organic compounds, (2) it has little or no response to the inert carrier gases commonly used such as nitrogen or helium, (3) it gives a stable base line and it is not significantly affected by fluctuations in temperature, carrier gas flow rate or pressure, and (4) it has a good linearity over a wide sample concentration range ¹⁶.

One gram of catalyst was used in the microreactor. After calcining at the desired temperature, the material was pelleted between 0.6 and 1.0 mm. The sample was held in the reactor tube using silica wool. The sample was activated at 400°C for one hour. The gaseous flow of IPA was 5ml/min. which was diluted with a 40 ml/min. flow of nitrogen, equivalent to a liquid hourly space velocity (LHSV) = 1. The temperature range of the reaction was approximately 70°. This temperature range provided sufficient to determine accurately the activation energy for the production of propene from propan-2-ol, using the Arrhenius equation.

Schematic diagram of the microreactor.



2.6 Gravimetric Analysis

The progress of many important physical processes can be followed through observation of associated weight changes^{17, 18}. Adsorption, desorption, oxidation, reduction and evaporation can be studied. A microbalance is a highly responsive instrument capable of detecting very small changes in the mass of the specimen. The versatility of using microbalance techniques for the measurement of small mass changes *in situ* has been recognised and it is certain that the mass change observed is actually occurring on the specimen under examination.

Investigating the adsorption of gases on a sample under evacuation, the following processes may occur: (1) chemisorption, where the mass change will be irreversible with a subsequent decrease in pressure and will not proceed beyond a monolayer, (2) physisorption, where the process will be reversible with pressure at constant

temperatures. If the substrate is porous the mass change will be much larger due to the considerable internal surface area.

A C. I. Microbalance was used for the adsorption experiments. The microbalance was connected to a vacuum line and pump by diffusion and rotary pumps. Pyridine was admitted to the system via a dosing valve. The adsorption took place in a static mode, where the gas was admitted into the microbalance region and the system was left to equilibrate. The mass uptake of pyridine was measured as a function of pressure. The system was allowed to equilibrate over a necessary time period (. 30 minutes)The sample was outgassed at 400°C for an hour before the experiment began. The pyridine adsorption experiments were performed at room temperature, the same temperature as the adsorption of pyridine was undertaken in the infrared experiments.

References

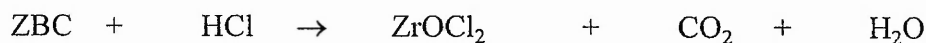
-
- ¹ S. J. Gregg and K. S. W. Sing, *Adsorption Surface Area and Porosity*, Academic Press, London, 2nd Edition 1982.
 - ² C. R. Brundle, C. A. Evans Jr., S. Wilson, *Encyclopedia of Materials Characterisation*, p 282 - 299, Butterworth - Heinemann 1992.
 - ³ D. Briggs and M. P. Seah, *Practical Surface Analysis*, 2nd. Edition, Volume 1, Wiley 1992.
 - ⁴ J. H. Scofield, *J. Electron Spectrosc.*, 8, (1976), p129.
 - ⁵ H. H. Willard, L. L. Merritt, Jr., J. A. Dean and F. A. Settle, Jr., *Instrumental Methods of Analysis*, Wadsworth 7th Edition 1988.
 - ⁶ C. R. Brundle, C. A. Evans Jr., S. Wilson, *Encyclopedia of Materials Characterisation*, p 198 - 213, Butterworth - Heinemann 1992.
 - ⁷ B. D. Cullity, *Elements of X-Ray Diffraction*, Addison - Wesley 1956.
 - ⁸ P. W. Atkins, *Physical Chemistry*, Oxford University Press 3rd Edition 1986.
 - ⁹ H. Toraya, M. Yoshimura and S. Somiya, *J. Am. Ceram. Soc.*, 67 (1984) C-119.

-
- ¹⁰ Th. H. de Keijser, J. I. Langford, E. J. Mittemeijer and A. B. P. Vogels, *J. Appl. Cryst.* 15,(1982) p308 - 314.
- ¹¹ J. I. Langford, *J. Appl. Cryst.*, 11, (1978) p10 - 14.
- ¹² A. Benedetti, G. Fagherazzi, S. Enzo and M. Battagliarin, *J. Appl. Cryst.*, 21, (1988) p536 - 542.
- ¹³ A. Benedetti, G. Fagherazzi, S. Enzo and MS. Polizzi, *J. Appl. Cryst.*, 21, (1988) p543 - 549.
- ¹⁴ C. J. Norman, *Measurement of Crystallite Size and Strain by X-ray line broadening*, Internal Report MEL Chemicals.
- ¹⁵ Th. H. de Keijser, J. I. Langford, E. J. Mittemeijer and A. B. P. Vogels, *J. Appl. Cryst.*, 15, (1982) p308 - 314.
- ¹⁶ A. Braithwaite and F. J. Smith, *Chromatographic Methods*, Chapman and Hall 4th Edition 1994.
- ¹⁷ S. P. Wolsky and A. W. Czanderna, *Microweighing in vacuum and controlled environments*, Elsevier 1980.
- ¹⁸ S. P. Wolsky and E. J. Zdanuk, *Ultra Micro Weight Determination in Controlled Environments*, Wiley 1969.

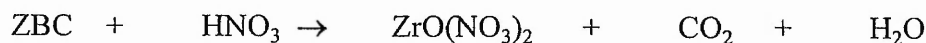
3. Zirconia and Lanthana Doped Zirconia

3.1 Preparation of zirconium oxide.

Zirconium oxide was prepared from two precursors, zirconium hydroxide and zirconium basic carbonate, both supplied by MEL Chemicals. The zirconium hydroxide, XZ0631/01 batch 93/165/01 had the following specification, 0.01% Na, <0.01% Cl, 0.04% SO₃ and 0.02% SiO₂. Zirconium basic carbonate (ZBC) with the following specification, 0.13% SiO₂, 0.13% TiO₂, 0.16% SO₃ and <0.01% Na, was used as a precursor to the zirconium hydroxide. The hydroxide was prepared from the basic carbonate via two similar routes. The zirconium basic carbonate was added to an equal volume mixture of 36% hydrochloric acid and distilled water. Carbon dioxide was evolved and zirconium oxychloride was produced.



In a similar manner, the ZBC was added to an equal volume mixture of concentrated nitric acid and water, to produce zirconium oxynitrate.



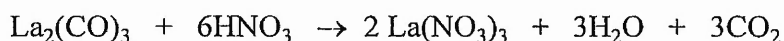
Zirconium hydroxide was produced by precipitation. Ammonium hydroxide (28-30% NH₃ in H₂O) was added dropwise to the solutions, to reach a final pH of 10.0. The zirconium hydroxide precipitated out over the pH range 4 to 10. The mixture was stirred, filtered, washed with distilled water and dried at 110°C overnight.

Zirconium oxide was produced by calcination of the dried hydroxides, over a range of temperatures from 400 to 900°C, in static air for two hours.

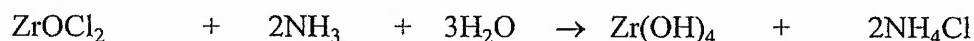
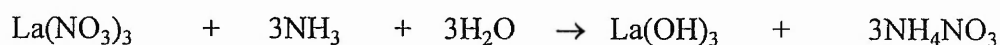
3.2 Preparation of lanthana doped zirconia

3.2.1 Coprecipitation

Lanthanum carbonate ($\text{La}(\text{CO}_3)_3$) 99.9% Molycorp was used as the lanthanum source. Initial experiments were to produce 3 mole % lanthana zirconia samples. Lanthanum carbonate was added to an equal volume mixture of concentrated nitric acid and distilled water, to produce lanthanum nitrate.



Lanthanum nitrate was mixed with zirconium oxychloride, in the required concentrations. A constant pH method was used for the coprecipitation of lanthana and zirconia. The lanthanum nitrate and zirconium oxychloride were added dropwise to an ammonium hydroxide solution at pH 10. The pH of reaction was maintained at 10 by constant addition of ammonia solution. Upon coprecipitation, the reaction mixture was stirred, filtered, washed with distilled water and dried at 110°C overnight. The samples were calcined in static air to give the mixed oxide.



The preparation of 3 mole % lanthana zirconia samples was repeated using a fixed pH of 11.0 and 11.3. The pH of 11.3 was the maximum pH obtained when using 28-30% NH_3 in H_2O . Preparation of 3 mole % lanthana zirconia at constant pH

8.0 was undertaken as well as preparation of 6 mole % lanthana zirconia at constant pH 11.3.

3.2.2 Impregnation

An incipient wetness technique was used to impregnate lanthana on the zirconia to give 3 mole % $\text{La}_2\text{O}_3/\text{ZrO}_2$. The sample was assumed to be 3mole% from the preparation method. Lanthana was introduced as lanthanum nitrate and impregnated on zirconia, previously calcined at 500°C . The sample was dried at 110°C ready for further calcination.

3.3 Surface Area Results

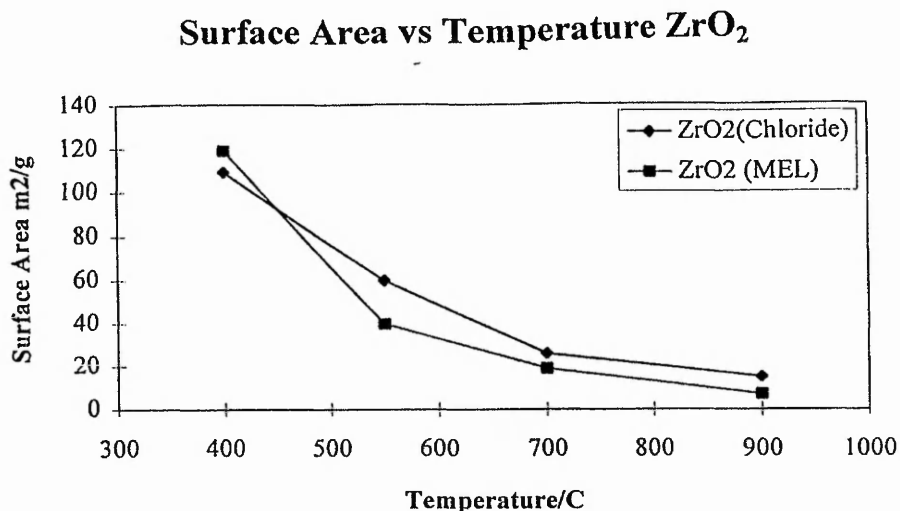
3.3.1 Zirconia BET results

The initial characterisation of the samples was surface area analysis obtained by applying the BET equation ¹. The zirconia samples were calcined over a range of temperatures 400 to 900°C for 2 hours in static air. The error in all the BET results is less than +/- 5%.

Table 3.3.1 *zirconia surface area.*

Calcination Temperature / $^\circ\text{C}$	ZrO_2 (Chloride) $/\text{m}^2\text{g}^{-1}$	ZrO_2 (MEL) $/\text{m}^2\text{g}^{-1}$
400	109	119
550	60	40
700	26	19
900	15	7

Figure 3.3.1 Surface Area for zirconia



From the above results it can be noticed that the MEL zirconia had a slightly larger surface area initially. However, at the highest temperature the MEL oxide had less than half the surface area of the zirconia from the oxychloride. Over the 500°C temperature range, the surface area dropped to a seventh of its original value. Preparation methods of the zirconia play an important role in determining the surface area.

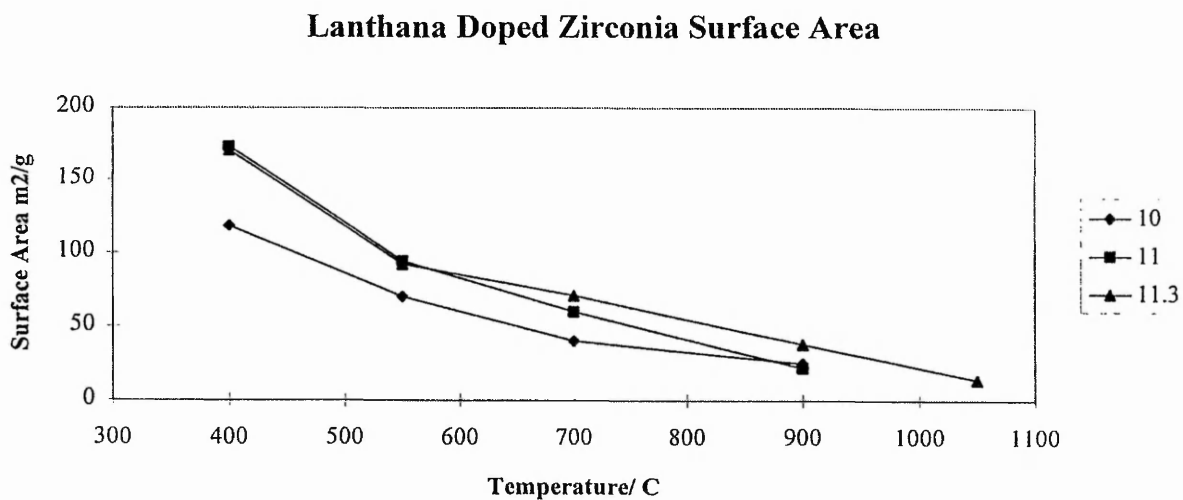
3.3.2 Lanthana doped zirconia BET results

The below results show that the final pH of precipitation played an important role in the stabilisation of the surface area of zirconia. The highest pH of precipitation gives the highest surface area, from 700°C upwards. Below this temperature, pH 11.3 showed similar results to pH 11.0. These two samples were initially greater than the pH 10.0 sample, but at 900°C, pH 10.0 had a marginally higher surface area than pH 11.0. All the samples over the full range of calcination temperatures stabilise the surface area compared to the undoped zirconias. The stabilisation was greater at the higher calcination temperatures, with pH 11.3 giving a surface area two and a half times larger than the zirconia prepared from the oxychloride at 900°C

Table 3.3.2 .1 surface area results for coprecipitated lanthana doped zirconia

Calcination Temperature /C	3mole%La ₂ O ₃ /ZrO ₂ (pH 10.0) m ² g ⁻¹	3mole%La ₂ O ₃ /ZrO ₂ (pH 11.0) m ² g ⁻¹	3mole%La ₂ O ₃ /ZrO ₂ (pH 11.3) m ² g ⁻¹
400	118	173	170
550	70	94	92
700	40	60	71
900	25	22	38
1050	---	---	14

Figure 3.3.2 Coprecipitated lanthana doped zirconia surface area.



Investigation into 6 mole % $\text{La}_2\text{O}_3/\text{ZrO}_2$ at precipitation pH 11.3 gave a surface area of $19 \text{ m}^2 \text{ g}^{-1}$ and 3 mole % $\text{La}_2\text{O}_3/\text{ZrO}_2$ pH 8 had a surface area of $21 \text{ m}^2 \text{ g}^{-1}$, at 900°C .

Table 3. 3. 2. 2. *Surface area for impregnated lanthana doped zirconia*

Temperature $^\circ\text{C}$	Surface area $\text{m}^2 \text{ g}^{-1}$
550	85
700	91
900	35
1050	15

The impregnation preparation stabilised the surface area of zirconia to a similiar extent as the coprecipitation preparation.

3.4 Powder X-Ray Diffraction (XRD) results

3.4.1 Zirconia XRD

XRD patterns were obtained for ZrO_2 (oxychloride) and ZrO_2 (MEL), over the temperature range 400 to 900°C . For both samples, at 400°C the spectra were broad and tetragonal but at higher temperatures, the main phase observed was monoclinic.

3.4.1 Table 1 ZrO_2 (MEL) results.

Temperature / °C	Monoclinic crystallite size nm (Scherrer)	Monoclinic phase %
400	---	0
550	16	54
700	15	84
900	---	98

The monoclinic phase content increased with temperature, to almost 100% monoclinic at 900°C. The phase composition results agree with those reported previously ².

3.4.1 Table 2 ZrO_2 (oxychloride) XRD results.

Temperature / °C	Monoclinic crystallite size nm (Scherrer)	Monoclinic phase %
400	---	0
550	11	90
700	14	89
900	22	95

The phase content was approximately 90% monoclinic at 550°C. As expected the increase in crystallite size with calcination temperature was accompanied by a decrease in surface area. The above samples were further investigated to determine the strain and apparent crystallite size ³.

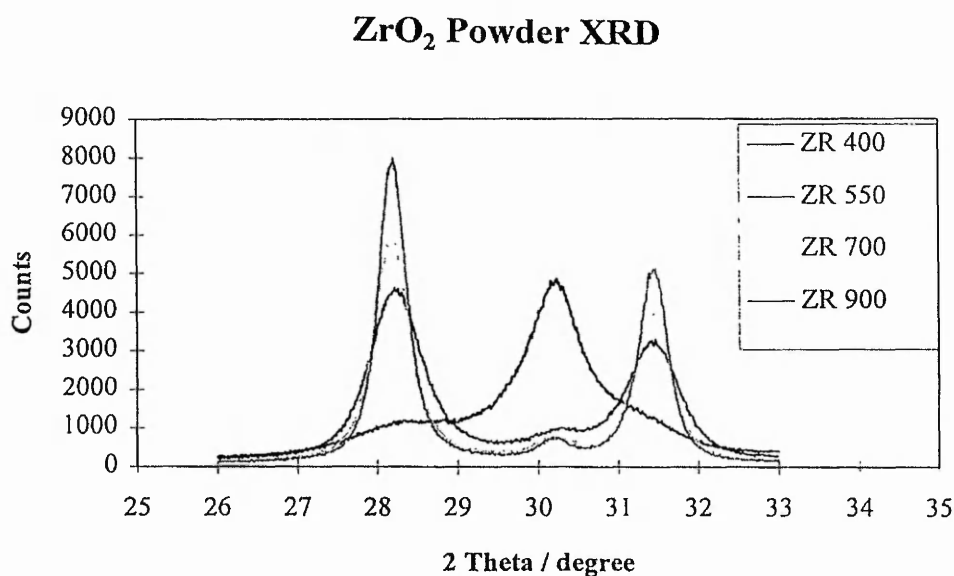
3.4.1 Table 3 *ZrO₂ (oxychloride) XRD results.*

Temperature <i>/ °C</i>	Apparent crystallite size nm	Theoretical Crystallite size from surface area nm	Strain
550	32	18	11.9
700	51	41	8.5
900	28	72	4.3

The strain, which is a measure of the defective nature of the sample relative to a pure defect free sample, decreased with increasing temperature. The sample at high temperatures has fewer defects and becomes more crystalline upon sintering. The drop in the crystallite size at 900°C can possibly be explained due to twinning of the monoclinic zirconia. Twinning⁴ occurs in some crystals in which they have two parts symmetrically related to one another. They are called twinned crystals. The relationship between the two parts of the twinned crystal is described by a symmetry operation bringing one part into coincidence with the other or with an extension of the other. The two main kinds of twinning are distinguished depending on whether the symmetry operation is 180° rotation about an axis called the twin axis, or reflection across a plane, called the twin plane. The plane on which the two parts of a twinned crystal are united is called the composition plane. Therefore, the measured result is not a true result since only part of the crystal and not the full crystal is participating in the broadening. The crystallite size of twinned crystals cannot be determined accurately using powder XRD.

3.4.1 Graph 1 Powder XRD of ZrO_2 (oxychloride) over range $26^\circ < 2\theta < 33^\circ$.

The monoclinic peaks appear at $2\theta = 28^\circ$ (-111) and 31.5° (111), whereas, the tetragonal peak appears at 30° (111)⁵. The counts observed increased with calcination temperature, indicating increasing sample crystallinity.



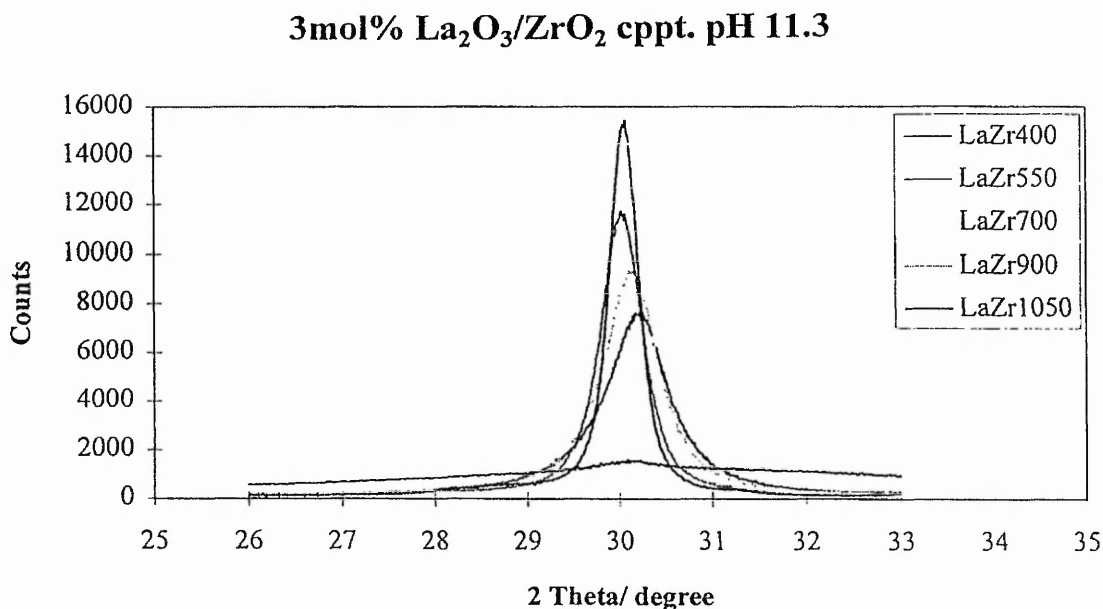
3.4.2 Lanthana XRD results

3.4.2 Table 1 The Crystallite size, calculated from the Scherrer equation⁶, and the monoclinic percentage,⁷ for lanthana doped zirconia coprecipitated samples.

Temp. / °C	3mol% La ₂ O ₃ /ZrO ₂ pH 10.0		3mol% La ₂ O ₃ /ZrO ₂ pH 11.0		3mol% La ₂ O ₃ /ZrO ₂ pH 11.3	
	Size nm	% monoclinic	Size nm	% monoclinic	Size nm	% monoclinic
550	22	0	10	0	11	0
700	22	0	12	0	13	0
900	18	0	19	16	16	Trace

All the samples show a high concentration of the tetragonal phase. Generally, the crystallite size increases with calcination temperature. The pH 11.3 samples were investigated further for the strain and apparent crystallite size.

3.4.2 Graph 1 Powder XRD of 3mol% La₂O₃/ZrO₂ pH 11.3



3.2.4 Table 2 Size and strain^{8 9 10} for pH 11.3 lanthana zirconia samples.

Temperature / °C	Apparent crystallite size nm	Strain
550	14	8.7
700	18	8.0
900	26	6.5
1050	25	3.3

The strain of the samples decreased with increasing calcination temperature. The sample contained oxygen vacancies due to the charge imbalance of using a +3 oxide. The oxygen vacancy concentration decreases with increasing temperature due to the sample sintering. Comparing the lanthana strain results to the zirconia

results, it was observed that at 900°C the zirconia had less strain than in the lanthana system. This was attributed to the oxygen vacancies in the latter.

The crystallite size of La₂O₃/ZrO₂ pH 11.3 calcined at 1050°C was lower than at 900°C. This was due to the tetragonal particles which increased in size above 30nm transforming to the monoclinic phase ¹¹. Subsequently the number of tetragonal crystallites decreased. Therefore, the shift in the size distribution of the tetragonal crystallites caused the average tetragonal crystallite size to decrease. Tetragonal crystallite sizes were not been observed over 30 nm, in agreement with Garvie's theory ¹².

From the surface area data, the theoretical crystallite size was calculated using the following equation. The equation can be applied to cubic non porous crystallites¹¹. The density of tetragonal zirconia was taken as 6.10 g cm⁻³ and 5.56 g cm⁻³ for monoclinic zirconia ¹³.

$$S.A. = \frac{6}{\rho D}$$

S.A. = surface area m²g⁻¹

ρ = density of tetragonal zirconia gm⁻³

D = cubic size

3.4.2 Table 3 *Calculated crystallite size for 3mol%La₂O₃/ZrO₂ pH 11.3*

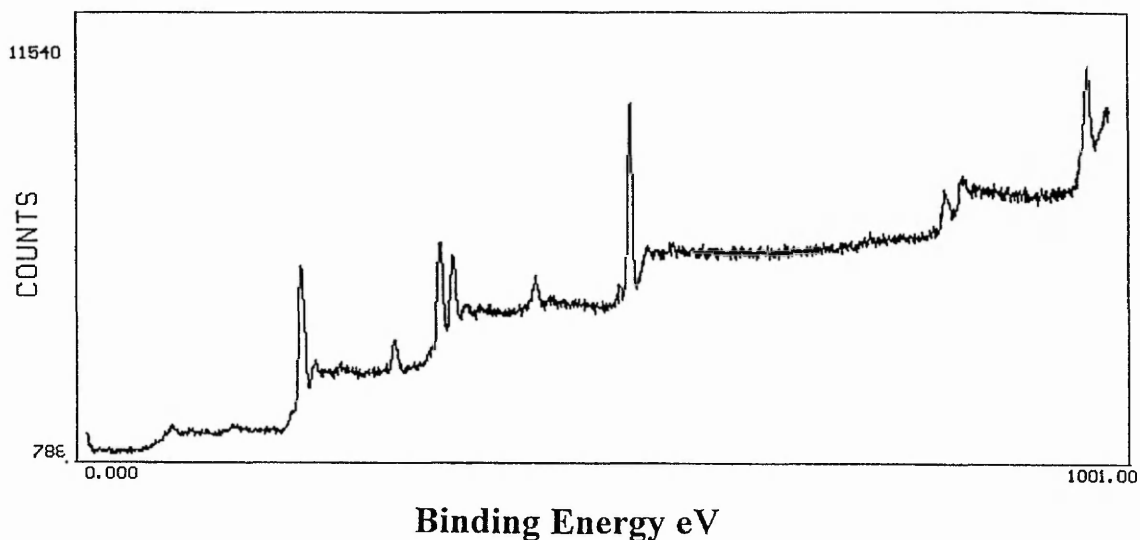
Measured surface area/ m ² g ⁻¹	Measured crystallite size /nm	Calculated size from surface area /nm
92	14	11
71	18	14
38	26	26

From the data it was observed that that the determination of crystallite size from the line broadening method slightly over estimated the size, in comparison to the theoretical size. However, there is reasonable agreement.

The impregnation preparation stabilised the monoclinic phase up to 700°C, with approximately 50% monoclinic at 900°C and 100% tetragonal at 1050°C. This stabilisation of the monoclinic phase by the impregnation preparation is in agreement with Mercera's work ¹⁴.

3.5 X-ray Photoelectron Spectroscopy (XPS)

The spectra showed only carbon as an impurity in the samples. The main peaks observed were Zr 3d, La 3d, O 1s and C 1s¹⁵



The peaks in the above spectrum of 3mol% $\text{La}_2\text{O}_3/\text{ZrO}_2$ calcined at 550°C were assigned as below.

Assignment	Binding Energy eV
Zr 3d	184
Zr 3p _{3/2} 3p _{1/2}	333 348
O 1s Auger	531 976
C 1s	285
La 3d _{5/2} 3d _{3/2}	837 855

3.5.1 Coprecipitated XPS results

3.5.1 Table 1 *binding energies and La/Zr surface ratio for 3 mole % La₂O₃/ZrO₂ pH 11.3*

Calcination Temperature / °C	Binding Energy eV		La/Zr Surface Ratio
	Zr 3d	La 3d	
400	184.5	838.6, 856.1	0.056
550	184.5	836.4, 855.4	0.064
700	184.8	837.2, 854.1	0.069
900	184.4	837.1, 857.9	0.129
1050	187.3	841.0, 857.9	0.145

The La/Zr surface ratio increased with calcination temperature. Dopant enrichment at the surface was observed upon sintering, with the greatest increase in the surface dopant occurring over the temperature range 700 to 900°C. At, 1050°C, the surface ratio was almost five times greater than if an homogeneous mix of the oxides was obtained (3mol%). Even at the lowest temperature, the surface ratio is twice that of an homogeneous mix. The coprecipitation method was used to investigate the possibility of an homogeneous preparation of doped zirconia. XPS provided an excellent tool for the investigation of the inhomogeneity of the system.

3.5.2 The effect of pH of preparation on La/Zr surface ratio

Preparation pH's 8.0, 10.0 and 11.3 calcined at 900°C were used to investigate the effect of pH on surface concentration.

Table 3.5.1 Surface ratio for varying pH preparations for 3 mole % $\text{La}_2\text{O}_3/\text{ZrO}_2$.

pH	Binding Energies eV		La/Zr Surface Ratio
	Zr 3d	La3d	
8.0	184.6	839.1, 854.2	0.166
10.0	184.7	838.5, 854.9	0.153
11.3	184.4	837.1, 853.7	0.129

Increasing the pH of coprecipitation decreases the surface ratio of lanthana to zirconia.

3.5.3 XPS results of impregnated samples

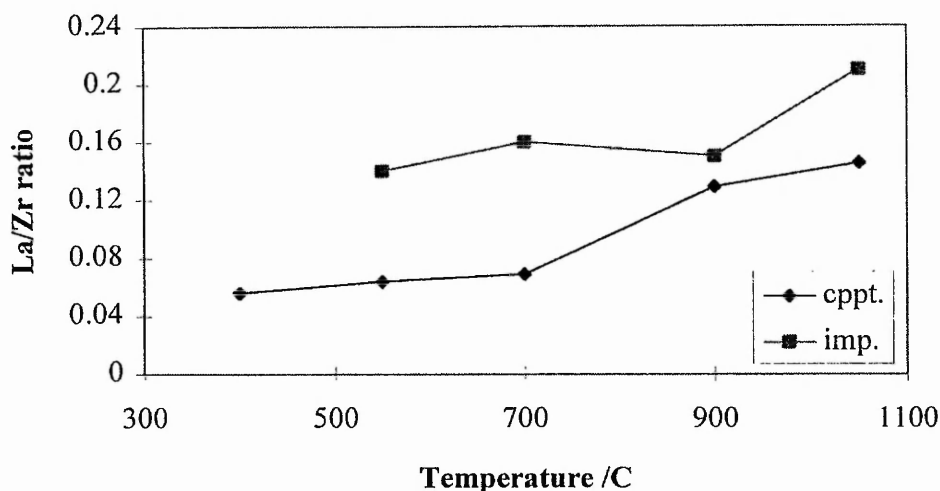
By the nature of the preparation, the impregnated samples were expected to have larger La/Zr surface ratios and this was indeed observed.

Table 3.5.3 Lanthana impregnated XPS results.

Temperature $^{\circ}\text{C}$	La/Zr surface ratio
550	0.14
700	0.16
900	0.15
1050	0.21

The temperature range 550 to 900 $^{\circ}\text{C}$ had little effect on the surface ratio. The ratio was approximately five times higher than the homogeneous mix of 3 mole %. This ratio was equivalent to the coprecipitated sample calcined at 1050 $^{\circ}\text{C}$. The ratio did increase at the highest temperature to seven times the homogeneous mix.

La/Zr Surface Ratio



3.6 Discussion

The surface area of zirconia is stabilised against sintering by the addition of dopants ¹⁶, and the method of preparation affects the stabilisation ¹⁷. A high surface area monoclinic zirconia was produced by impregnation, whereas, a high surface area tetragonal zirconia system was achieved by coprecipitation. Therefore, a tailored material can be achieved by dopant addition.

From the BET results for the coprecipitated samples, increasing the pH of precipitation produces an increase in the surface area of the calcined catalysts. If the pH of precipitation could be increased beyond 11.3 an increased surface area might be achieved. The pH of coprecipitation can be increased by using a different base, such as sodium hydroxide or potassium hydroxide. The use of potassium and sodium hydroxides have been used to investigate the precipitation of zirconia up to final pH's of 13 and 14 ¹⁸. However, using such bases, problems can arise in ensuring all the alkali metals are removed from the samples. Alkali impurities may affect the oxide and may detract from the properties of the introduced dopant. The stabilisation may be affected by the impurities.

From the work of Franklin² on the coprecipitation of lanthana and zirconia, it was observed that at 700°C, 4 and 8 mol% La₂O₃/ZrO₂ had surface areas of 58 and 74 m²g⁻¹ respectively. These coincide with the above experimental results, where at 700°C the 3 mol% La₂O₃/ZrO₂ coprecipitated sample had a surface area of 71 m²g⁻¹.

The impregnated preparation surface area results gave similar surface area results to coprecipitation results. However, the monoclinic phase was stabilised as opposed to the tetragonal phase. The stabilisation of the monoclinic phase by dopants was observed by Mercera¹⁴. He showed that 4 mol% LaO_{1.5}/ZrO₂ was greater than 90% monoclinic at 900°C with a surface area of 37m²g⁻¹. The above results at 900°C show only 50% monoclinic with a surface area of 35m²g⁻¹.

Of the two preparation methods, the impregnation route readily stabilised the surface area but did not fully stabilise a single phase, whereas the coprecipitation method stabilised a single phase. Using the coprecipitation preparation method, the dopant in the bulk must stabilise the tetragonal phase and from the impregnation method the dopant on the surface must stabilise the surface area.

The addition of dopants retards the crystallisation of zirconia, which starts usually around 400°C¹⁹. From the powder x-ray diffraction results, at 400°C for the zirconia sample prepared from the oxychloride precursor, the sample phase was mainly tetragonal, giving a broad diffraction pattern. However, for 3mol. % La₂O₃/ZrO₂ coprecipitated sample at pH 11.3, the phase was not identifiable and the sample was amorphous. However at, 550°C the coprecipitated sample is tetragonal, with the crystallisation of the zirconia retarded up to 150°C. The crystallite size limit of detectability using XRD is approximately 3 nm with small particles not being observed². Therefore, in the coprecipitated sample, the effect of the dopant keeps the particles sufficiently small so as not to be detected by XRD. However, at 400°C, the particle size in pure ZrO₂ was already starting to increase. This is in line with the surface area of the doped sample (170 m²g⁻¹) being much larger than the surface area than that of pure zirconia (109 m²g⁻¹), as a consequence of this increased crystallite size.

Ozawa ¹¹, records the retardation of the crystallisation of amorphous zirconia by the addition of lanthana and other rare earth oxides. The effect of the retardation was found to increase with increasing dopant concentration. A number of rare earth oxides were investigated and it was found that increasing the ionic radius of the metal increased the retardation of the crystallite phase. Lanthana retarded the crystallisation to the greatest extent since it had the largest ionic radius studied. This led to the conclusion that crystallisation by the diffusion of ions in the precursor was inhibited more greatly by doping with rare earth cations with large ionic radii. From Ozawa's results, 10 mol% $\text{La}_2\text{O}_3/\text{ZrO}_2$ retarded the crystallisation of zirconia to approximately 500°C from 400°C for undoped zirconia. These results are in agreement with the above experimental results.

The results of determining the crystallite size for the measured surface area, assuming cubic non-porous samples, showed good agreement for the coprecipitated lanthana samples at pH 11.3. This suggested that the coprecipitated samples were non porous and the surface area was solely related to the crystallite size. However, for the monoclinic zirconia prepared from the oxychloride precursor, the results were not concurrent with a non porous system (3.4.1 Table 3), suggesting the samples had some porosity. The crystallite size, determined from XRD by removing the line broadening due to the strain from the monoclinic (111) peak, would give a much smaller surface area of less than $40 \text{ m}^2\text{g}^{-1}$ than the measured area of $60 \text{ m}^2\text{g}^{-1}$, if non porous at 550°C . Therefore, the sample showed some degree of porosity. Upon calcination at 700°C , the crystallite size determined from XRD and the theoretical size determined from the surface area measurement, became closer, suggesting that the porosity was reduced upon heat treatment. Therefore, sintering took place and the crystallite size played a more dominant role in determining the surface area. Mercera ⁷ records that undoped monoclinic zirconia contained meso and macro pores. From Mercera's BET results the absence of micropores was indicated. The specific pore volume was found to decrease with increasing calcination temperature. Agreement is found between Mercera and the above results.

The crystallite sizes for the tetragonal coprecipitated lanthana zirconia lie below the limit of Garvie's ⁴ critical crystallite size for tetragonal zirconia, which states that the crystallite size must be below 30 nm. None of the tetragonal samples investigated had sizes larger than 30 nm. The monoclinic zirconia sample at 550°C, had a crystallite size of 32 nm and the tetragonal zirconia sample, at 550°C, had a crystallite size of 14 nm. Monoclinic zirconia had an initial crystallite size greater than that required for the tetragonal phase.

From the XPS experiments, it was observed that the ratio of lanthana to zirconia in the surface region was greater than that of the bulk ratio of 3mol%. The near surface region can be determined for the individual atoms from the relationship of the kinetic energy of the emitted electron with its escape depth, which can be estimated from the universal curve ²⁰. The near surface region is usually in the order of a few atomic layers. The dopant enrichment at the surface was expected in the impregnation technique, due to the nature of the preparation. However, the coprecipitation technique might have been expected to provide a homogeneous method of preparation, but initially at 400°C, the surface ratio was twice that expected from the bulk ratio. Migration of the dopant to the surface occurred at the lowest calcination temperature. For the coprecipitated samples, the surface ratio remains approximately constant up to 700°C, but over the temperature range 700 to 900°C the ratio increased to approximately 13 %.

These results are in contrast with the impregnated samples, whose surface ratio remained constant, at approximately 16%, until 900°C. However, over the temperature range 900 to 1050°C, the ratio increases to 21%. The increases in surface ratios were not easily explainable. For the coprecipitated sample over the temperature range 700 to 900°C, the surface area decreased from 71 to 38 m²g⁻¹, the crystallite size increased from 18 to 26 nm and the phase remained tetragonal. The increase in surface ratio was not accompanied by any drastic change in the physical properties measured for the coprecipitated sample. For the impregnated sample over the temperature range 900 to 1050°C, the surface area drops from 35 to 15 m²g⁻¹ and the phase changes from approximately 50% monoclinic to the majority of the phase being tetragonal. The impregnated sample surface ratio

increase may be related to the increasing amount of the tetragonal phase. The temperature increase must be the dominant role in the increased surface lanthana to zirconia ratio due to the large surface ratio of La/Zr at high temperatures.

Migration of the dopant to the surface or near surface region, due to the effect of temperature, was accompanied by an increased crystallite size and a reduced surface area. The increase in dopant concentration at the surface, due to temperature, has been observed by Ingo ²¹, where he investigated the impurities silicon and sodium in a CeO₂/Y₂O₃/ZrO₂ mixed oxide system. The surface ratios of silicon to zirconium and sodium to zirconium were found to increase over the temperature range 910 to 1460°C. The enrichments at the surface were many times the bulk values.

Varying the pH of coprecipitation for the preparation of 3mol. % La₂O₃/ZrO₂ from 8.0 to 11.3 gave an increase in surface area when the samples were calcined at 900°C. The increase in surface area was accompanied by a decrease in the lanthana to zirconia surface ratio.

3.6 Table 1 *Surface area and surface ratio results for varying pH of preparation for 3mol% La₂O₃/ZrO₂ calcined at 900°C.*

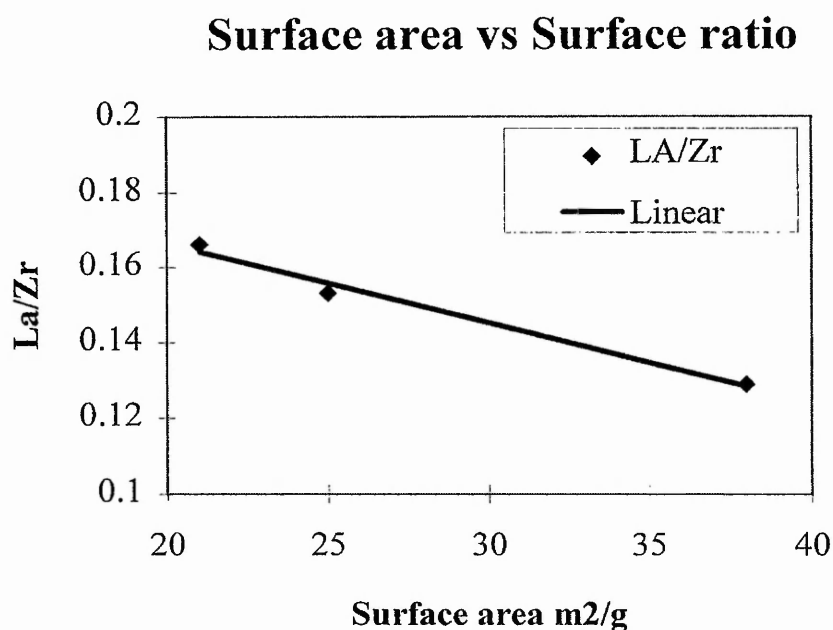
pH	Surface Area m ² g ⁻¹	La/Zr surface Ratio
8.0	21	0.166
10.0	25	0.153
11.3	38	0.129

The inverse relationship between the surface ratio and surface area was found to be linear.

Using the above result to design a zirconia mixed oxide with high surface area, the pH of coprecipitation must be as high as possible but the surface content of the dopant must be kept low. The pH of preparation can be increased by the use of sodium or potassium hydroxide and the lanthana to zirconium surface ratio can be

reduced by using less dopant. However, a minimum amount of dopant is required to stabilise the tetragonal phase. Franklin ¹ prepared 1mol% $\text{La}_2\text{O}_3/\text{ZrO}_2$ which was only 33% tetragonal at 700°C.

3.6 Graph 1 *Surface area against surface area with variation of pH. R^2 factor = 0.98.*



3.7 Characterisation Conclusions

From the full characterisation of the physical properties of the mixed oxides, the following conclusions may be drawn;

- (1) the addition of 3 mol% La_2O_3 to ZrO_2 stabilises the surface area.
- (2) the monoclinic or tetragonal phase of zirconia can be stabilised depending on the preparation method.
- (3) the addition of a rare earth cation retards the crystallisation of zirconia.

(4) Garvie's criteria for critical crystallite size for tetragonal zirconia are met.

(5) a design for a high surface area mixed oxide has been discussed including the pH of preparation and surface dopant to zirconia ratio.

References

-
- ¹ S. J. Gregg and K. S. W. Sing, *Adsorption, Surface Area and Porosity*, Academic Press 1967.
- ² R. Franklin and R. W. Joyner, Unpublished Results.
- ³ C. Norman, *Interim Report*, MEL Chemicals.
- ⁴ B. D. Cullity, *Elements of X-ray diffraction*, Addison-Wesley 1956.
- ⁵ JCPDS Files.
- ⁶ B. D. Cullity, *Elements of X-ray Diffraction*, Addison - Wesley 1956.
- ⁷ H. Toraya, M. Yoshimura and S. Somiya, *J. Am. Ceram. Soc.*, 67 (1984) C-119.
- ⁸ Th. H. de Keijser, J. I. Langford, E. J. Mittermeijer and A. B. P. Vogels, *J. Appl. Cryst.* 15, (1982) p308-314.
- ⁹ J. I. Langford, *J. Appl. Cryst.*, 11, (1978) 10-14.
- ¹⁰ A. Benedetti, G. Fagherazzi, S. Enzo and M. Battagliarin, *J. Appl. Cryst.* 21, (1988) p536-542.
- ¹¹ R. C. Garvie, *J. Phys. Chem.*, 65, (1969) p1238
- ¹² R. C. Garvie, *J. Phys. Chem.*, 82, (1978) p219.
- ¹³ C. D. Hodgman, R. C. Weast and S. M. Selby, *Handbook of Chemistry and Physics*, Chemical Rubber Publishing Co..
- ¹⁴ P. D.L. Mercera, J. G. Van Ommen, E. B. M. Doesburg, A. J. Burgraaf and J. H. Ross, *Applied Catalysis*, 78 (1991) p79-96 and P. D.L. Mercera, J. G. Van Ommen, E. B. M. Doesburg, A. J. Burgraaf and J. H. Ross, *Applied Catalysis*, 71 (1991) p363-391.

-
- ¹⁵ D. Briggs and M. P. Seah, *Practical Surface Analysis*, 2nd. Edition, Volume 1, Wiley 1992.
- ¹⁶ R. Franklin, P. Goulding, J. Haviland, R. W. Joyner, I. McAlpine, P. Moles, C. Norman and T. Nowell, *Catalysis Today*, 10 (1991) p405-407.
- ¹⁷ M. A. C. G. van de Graaf and A. J. Burgraaf, *Am. Ceram. Soc., Science and Technology of zirconia II*, 1984.
- ¹⁸ B. H. Davis, *Am. Ceram. Soc. Comm.* (1984) c-168.
- ¹⁹ M Ozawa and M. Kimura, *J. Less Comm. Metals*, 171 (1991) p195-212.
- ²⁰ M. P. Seah and W. A. Dench, *Surface and Interface Analysis*, 1, (1979) p2-11.
- ²¹ G. M. Ingo, *Appl. Surf. Sci.*, 70/71 (1993) p235-239.

4. Silica doped zirconia

4.1 Preparation of silica doped zirconia

4.1.1 Coprecipitation

The addition of silica to zirconia using a coprecipitation technique was investigated. Parameters of the preparation method were varied to give a detailed analysis on the effect of preparation on the stabilisation of the surface area of the doped zirconia. Two coprecipitation methods were used as well as two final pH's of precipitation. Therefore, four sets of samples were prepared. The two methods used were a constant pH and a rising pH, with the final required pH's of 10.0 and 11.3. The constant pH method maintained the pH during precipitation, whereas the rising method gradually increased the pH to the final desired pH.

The silica source used was tetraethylorthosilicate (TEOS $\text{Si}(\text{OC}_2\text{H}_5)_4$ Aldrich 99%) and the dopant concentration was 3.5 wt%. Tetraethylorthosilicate was mixed with the zirconium oxynitrate, which was prepared from zirconium basic carbonate. Depending on the preparation method used, ammonia solution was added to the reaction mixture dropwise, or the reaction mixture was added to the ammonia solution dropwise. When ammonia was added to the reaction mixture, this constituted the rising pH method. The products started to precipitate out at pH approximately 4 and the coprecipitation continued to final pH's of 10.0 and 11.3. When the reaction mixture was added to the ammonia solution, this constituted the constant pH method. The ammonia solution was initially set at either pH 10.0 or 11.3, where coprecipitation occurred instantly. The desired pH was maintained by constant addition of ammonia solution during the reaction. Upon reaching the desired pH the products were stirred, filtered, washed with distilled water and dried at 110°C overnight. Calcination took place in static air for two hours in the temperature range 400 to 1050°C.

4.1.2 Impregnation

The samples were prepared using the incipient wetness technique. Zirconium hydroxide was precipitated from zirconium oxynitrate solution using ammonium hydroxide to a final pH of 10.0. The hydroxide was filtered, washed and dried in the oven overnight at 110°C. The hydroxide was calcined at 500°C for two hours to give the oxide. Tetraethylorthosilicate in ethanol was used to impregnate the zirconium hydroxide. The sample was stirred and then dried in the oven at 110°C. Calcination took place in static air for two hours over the temperature range 550 to 1050°C. 3.5wt% SiO₂/ZrO₂ and 5wt% SiO₂/ZrO₂ were prepared by impregnation. Volume ratios of ethanol to TEOS of 1: 0.45 and 1: 0.79 were used to give 3.5 and 5wt% SiO₂/ZrO₂ respectively

4.2 Surface Area Results

The surface area of the silica doped zirconia catalysts were performed using nitrogen adsorption and applying the BET method ¹.

4.2 Table 1 3.5wt% SiO₂/ZrO₂ coprecipitated samples.

Calcination Temperature /°C	pH = 11.3 constant /m ² g ⁻¹	pH = 10.0 constant /m ² g ⁻¹	pH = 11.3 rising /m ² g ⁻¹	pH = 10.0 rising /m ² g ⁻¹
400	157	174	159	169
550	88	120	92	102
700	52	79	79	79
900	27	26	37	38
1050	9	4	6	13

The addition of silica stabilised the surface area of zirconia (4.2 Table 1 and 2) relative to pure zirconia (Chapter 3 3.3.1 table 1). The variation in coprecipitation methods affected the final results, with the rising pH method stabilising the surface area to a greater extent

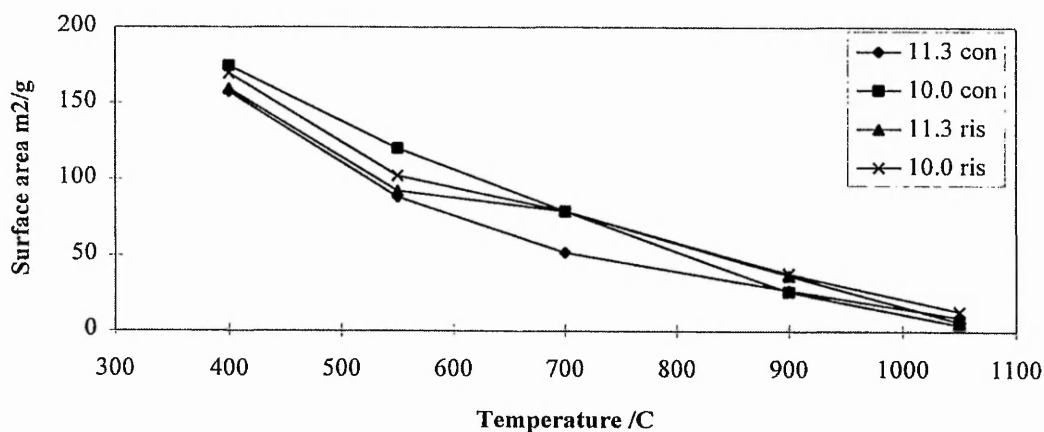
than the constant pH method. This became mostly evident in the higher calcination temperatures of 900 and 1050°C. The impregnation preparation stabilised the surface area to a greater extent up to 900°C, but above this temperature the surface area dropped to a similar level as the coprecipitation results. The increase in dopant concentration stabilised the surface area to a greater extent². The method of preparation played a dominant role in the surface area stabilisation³.

4.2 Table 2 Impregnated silica samples surface areas.

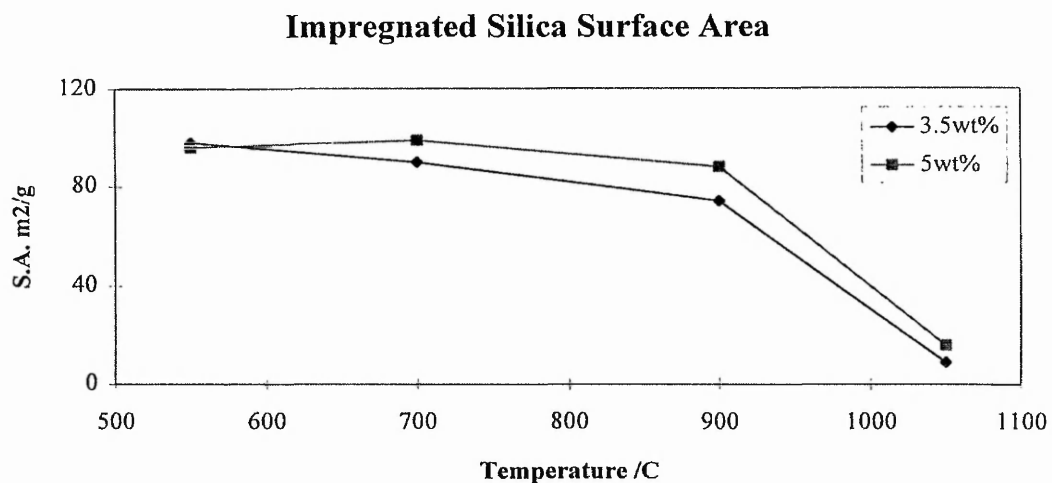
Calcination Temperature /°C	3.5wt% SiO ₂ /ZrO ₂ /m ² g ⁻¹	5wt%SiO ₂ /ZrO ₂ /m ² g ⁻¹
550	98	96
700	90	99
900	74	88
1050	9	16

4.2 Graph 1 Silica doped zirconia coprecipitated surface area results.

Coprecipitated silica/zirconia surface areas



4.2 Graph 2 Impregnated silica zirconia surface area results.



4.3 Powder x-ray diffraction results

Powder x-ray diffraction studies were performed to determine the phase composition⁴ and crystallite size⁵ of the doped zirconia systems.

4.3.1 Coprecipitated XRD results

4.3 Table 1

3.5wt%SiO₂/ZrO₂ pH10 rising

Temp. /°C	Crystal Size/ nm	Phase	Strain
400		A	
550	14	T	10.3
700	14	T	9.0
900	20	T	7.6
1050	27	T	4.1

4.3 Table 2

3.5wt%SiO₂/ZrO₂ pH 11.3 rising

Temp. /°C	Crystal Size /nm	Phase	Strain
400		A	
550	12	T	5.6
700	13	T	6.0
900	14	T	4.7
1050	35	T+m	4.0

4.3 Table 3

3.5wt% SiO₂/ZrO₂ pH 10 constant

Temp. /°C	Crystal Size/ nm	Phase	Strain
400		A	
550	10	T	7.1
700	14	T	8.4
900	19	T	6.3

4.3 Table 4

3.5wt%SiO₂/ZrO₂pH11.3 constant

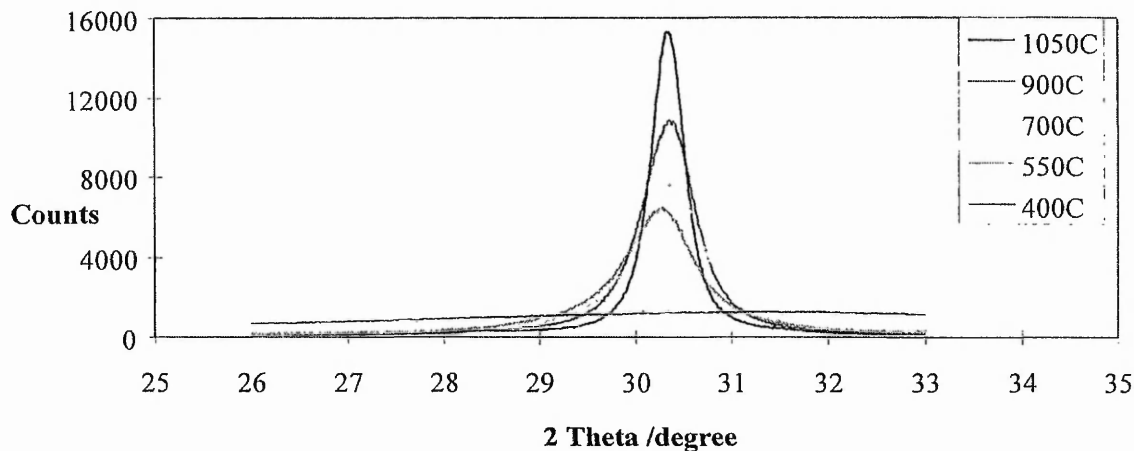
Temp. /°C	Crystal Size /nm	Phase	Strain
400		A+t	
550	11	T	4.0
700	12	T	3.8
900	17	T	4.7

Where, A = amorphous, T = tetragonal, M = monoclinic and lower case relates to trace amounts of phase.

The coprecipitation method of preparation stabilised the tetragonal phase of zirconia. From the powder XRD pattern only the tetragonal (111) peak was observed over the range $28^\circ < 2\theta < 31^\circ$ and peaks for the monoclinic phase were not observed. At 1050°C, the phase was 100% tetragonal (4.3 Graph 1). However, the sample did not become crystalline until 550°C. The crystallite sizes for the four sets of samples were similar at the respective calcination temperatures, and increased with temperature. This correlates with the surface areas being similar at the same calcination temperatures, since there is a relationship between surface area and crystallite size. The strain decreased with increasing temperature, indicating fewer defects in the larger crystallites.

4.3 Graph 1 Powder XRD patterns for 3.5wt%SiO₂/ZrO₂ pH 10 rising

3.5wt%SiO₂/ZrO₂ cppt. pH 10 rising



From inspection of the powder XRD pattern, the increased crystallinity can be observed with temperature. The tetragonal (111) peak increases and becomes sharper, indicating a crystallite size increase derived from the application of the Scherrer equation ⁶

4.3.2 XRD results for impregnated samples

4.3 Table 5 3.5wt% SiO₂/ZrO₂

Calcination Temperature /°C	Monoclinic Crystallite Size /nm	Monoclinic Phase Content /%
550	9.6	94
700	9.4	92
900	10.7	89
1050	16.9	35

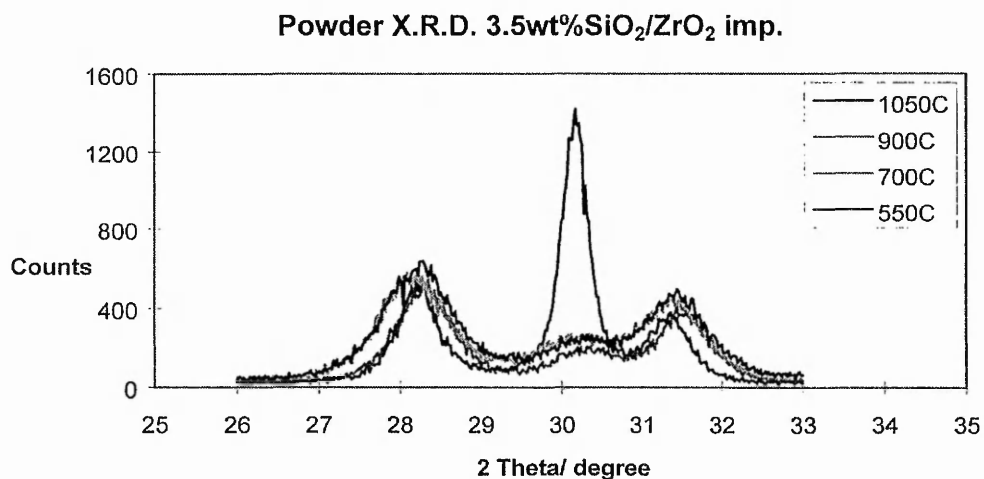
4.3 Table 6 5wt% SiO₂/ZrO₂

Calcination Temperature °C	Monoclinic Crystallite Size/nm	Monoclinic Phase Content %
550	9.1	96
700	10.2	98
900	9.9	91
1050	14.8	26

The impregnation preparation technique stabilised the monoclinic phase of zirconia. The phase was stable up to 900°C, however, at 1050°C the main phase was tetragonal (4.3 Graph 2). This series was not calcined at 400°C since the precursor to the impregnated sample was zirconium hydroxide which had already been calcined at 500°C to give zirconia.

The crystallite sizes for the two dopant concentrations remained constant and were similar up to 900°C. Over the temperature range 900 to 1050°C, the crystallite size increased, in line with the decrease in surface area at the highest calcination temperature. From inspection of 4.3 Graph 2, the phase transformation can be clearly observed. The three monoclinic patterns look similar and not very crystalline.

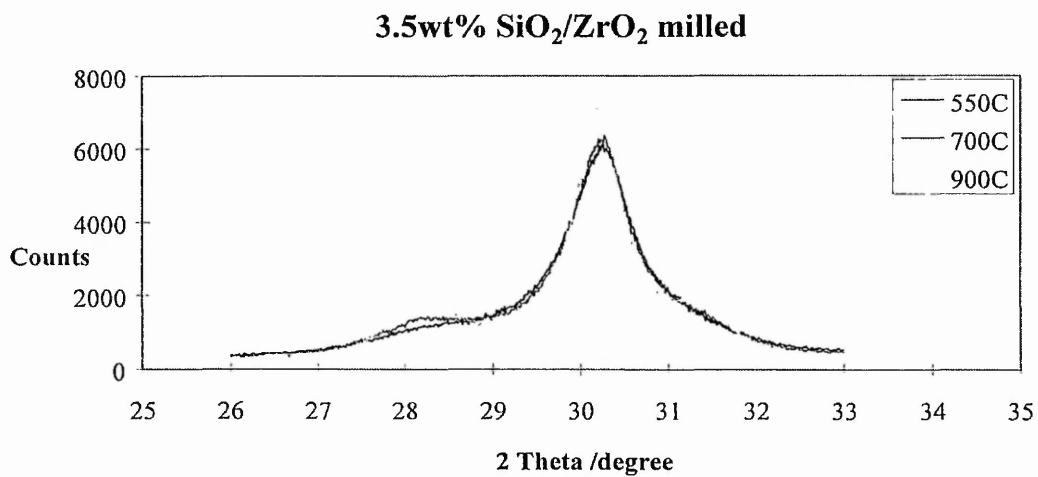
4.3 Graph 2 3.5 wt% Impregnated $\text{SiO}_2/\text{ZrO}_2$



4.3.3 Milled silica zirconia samples

3.5 wt% $\text{SiO}_2/\text{ZrO}_2$ pH 10.0 rising samples calcined at 550, 700 and 900°C were milled to investigate the tetragonal to monoclinic phase change. The samples were milled for one hour then the powder XRD pattern was recorded. It can be clearly seen that the effect of milling produced a transformation to the monoclinic phase but with the major phase remaining tetragonal

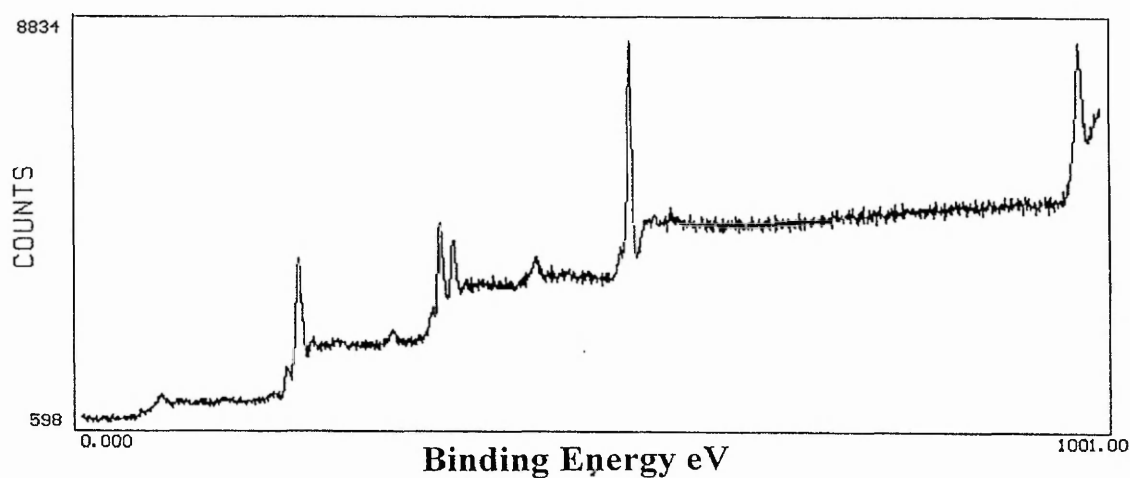
4.3 Graph 3 3.5wt% SiO₂/ZrO₂ pH 10 rising milled samples.



4.4 X-ray photoelectron spectroscopy results

XPS was used to determine the ratio of silicon to zirconium at the catalyst surface⁷. The aim of the investigation was to correlate the effect of preparation method and calcination temperature with the amount of dopant at the surface or near surface region. The main peaks observed were Zr 3d, C 1s, O 1s, Si 2p and Si 2s⁸. Carbon was present as an impurity.

Standard XPS spectrum of silica doped zirconia.



The peaks in the above spectrum of 3.5wt% SiO₂/ZrO₂ coprecipitated and calcined at 1050°C are assigned below.

Assignment	Binding Energy eV
Zr 3d	184
Zr 3p _{3/2} 3p _{1/2}	333 348
O 1s Auger	531 976
C 1s	285
Si 2p 2s	104 155

4.4 Table 1 Surface Si/Zr ratios for coprecipitated samples.

Temperature /°C	pH = 10.0 rising	pH = 11.3 rising	pH = 10.0 constant	pH = 11.3 constant
Precursor	0.05	0.07	0.10	0.06
550	0.09	0.10	0.14	0.07
700	0.11	0.10	0.14	0.09
900	0.27	0.14	0.18	0.15
1050	0.31	0.32	0.40	0.45

The precursors were the mixed hydroxides of silicon and zirconium before calcination.

The concentration of dopant at the surface or near surface region increased with calcination temperature (4.4 Graph 1). The surface enrichment of the dopant increased only gradually to 900°C. Over the temperature range 900 to 1050°C the dopant concentration at the surface increased by the greatest extent. The theoretical bulk ratio for 3.5wt% SiO₂/ZrO₂ was 0.075. Therefore, the observed surface ratios are all above the theoretical bulk ratio. However, the majority of the ratios for the precursor materials are lower than the theoretical bulk ratio, indicating that the preparation method allows the sample to go into the bulk and the temperature effect causes migration of the dopant to

the surface, or the dopant is in big discrete separate particles and spreads on the effect of calcination.

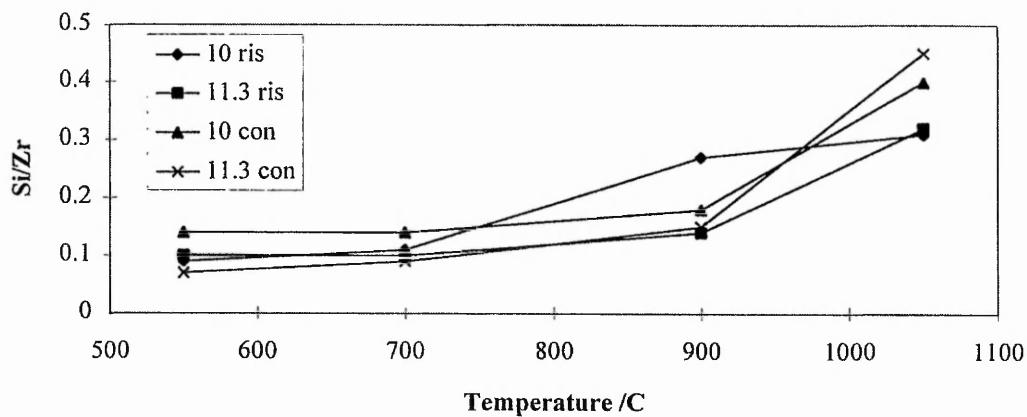
4.4 Table 2 Surface Si/Zr for impregnated samples.

Calcination Temperature °C	Si/Zr 5wt%	Si/Zr 3.5wt%
Precursor	0.19	0.13
550	0.17	0.11
700	0.16	0.12
900	0.17	0.11
1050	0.41	0.36

For the impregnated samples, the surface or near surface concentration of dopant remains constant up to 900°C. The surface ratios were larger than the theoretical bulk ratios, as was expected from the nature of the preparation. The theoretical bulk ratio for 5wt% SiO₂/ZrO₂ was 0.11. Over the temperature range 900 to 1050°C, a dramatic increase in surface dopant enrichment was observed (4.4 Graph 2). The ratios at this high temperature were similar to those from the coprecipitation preparation.

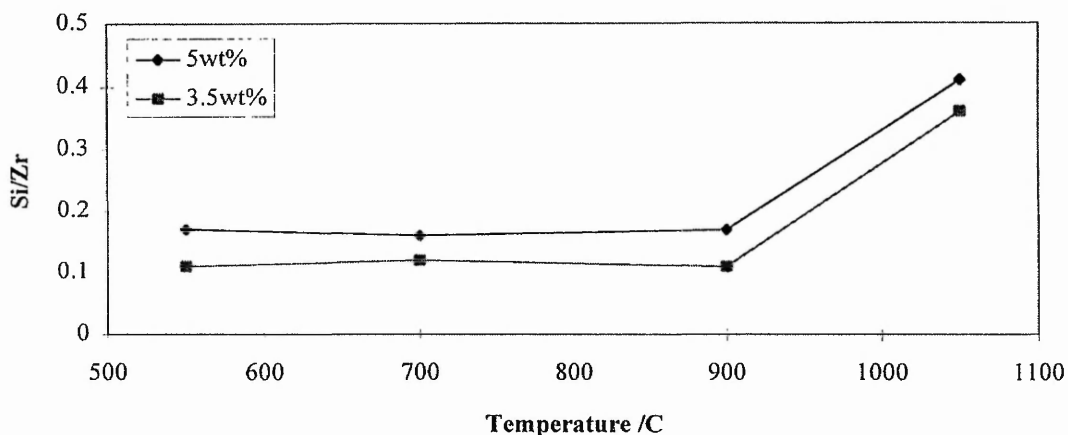
4.4 Graph 1 Surface ratio Si/Zr for coprecipitated 3.5wt% SiO₂/ZrO₂

Si/Zr coprecipitated samples



4.4 Graph 2 Surface ratio Si/Zr impregnated 3.5 and 5 wt% SiO₂/ZrO₂.

Si/Zr Impregnated Samples



4.4 Table 3 Binding energies for Zr 3d and Si 2p for coprecipitated samples.

Temperature °C	pH 10 rising		pH 10 con.		pH 11.2 rising		pH 11.2 con.	
	BE eV		BE eV		BE eV		BE eV	
	Zr 3d	Si 2p	Zr 3d	Si 2p	Zr 3d	Si 2p	Zr 3d	Si 2p
Precursor	183.6	102.4	184.6	104.0	183.8	102.8	183.2	103.5
550	183.6	103.0	183.9	103.4	183.7	104.8	183.2	103.0
700	184.1	103.9	183.9	103.2	183.5	102.9	183.8	103.8
900	183.7	103.8	184.6	103.3	185.2	104.2	184.5	103.5
1050	184.4	103.9	183.5	104.7	184.0	103.8	183.7	104.2

The binding energies for silicon 2p and zirconium 3d were similar and within experimental error, indicating that the zirconium and silicon were in fixed oxidation states over the calcination temperature range. Both metals were in the +4 oxidation state

and consistent with the literature values ⁹. The binding energies were calculated by calibrating for C 1s at B.E. = 285 eV.

4.5 Discussion of Characterisation

The surface area of zirconia is stabilised by the addition of silica as a dopant ¹⁰. The method of preparation played an important role in determining the stabilisation³. Tetragonal high surface area zirconia is produced by coprecipitation whereas, monoclinic high surface area zirconia is produced by impregnation ¹¹. A higher surface area zirconia can be prepared, relative to pure zirconia, in either the tetragonal or monoclinic phase by predetermining the preparation method.

For the coprecipitation preparations, the rising pH method improves the surface area to a greater extent than the constant pH method. With the constant pH method, the products precipitated immediately on contact with the high pH ammonia solution. However, the rising method produced a gradual coprecipitation over a range of pH's.

The surface areas for 3.5wt% SiO₂/ZrO₂ pH 10.0 rising at 550 and 900°C are 102 and 38 m²g⁻¹, whereas the ZrO₂ surface areas at the two temperatures are 60 and 15 m²g⁻¹. This shows a significant stabilisation by the dopant. However, the silica doped zirconia at pH 10.0 rising has very similar, almost identical surface area results to those of 3mol% La₂O₃/ZrO₂ constant pH 11.3 (Chapter 3). Each dopant has its individual preparation method to maximise the surface area but the stabilised surface areas remained similar for the different dopants. As in the case of lanthana coprecipitated zirconia, silica coprecipitated zirconia stabilises the tetragonal phase 100%.

The impregnation preparation method for doping zirconia with silica gives extremely high surface areas up to 900°C. For 3.5wt% SiO₂/ZrO₂, the surface area is 74 m²g⁻¹, which is double the coprecipitated results for either silica or lanthana as the dopant, and five times greater than that of zirconia at 900°C. However, over the temperature range

900 to 1050°C it is observed that the surface area dropped to a similar value as for the coprecipitation preparation. The surface area is increased by increasing the loading of the dopant up to 5wt%, but the drop in the surface area still occurred over the range 900 to 1050°C.

The monoclinic phase of zirconia is stabilised up to 900°C by the impregnated dopant, but at 1050°C the phase is mainly tetragonal. The change in phase coincides with the drop in surface area, over the temperature range 900 to 1050°C. These silica doped zirconia results contradict the work of Soled¹², who prepared various dopant concentration of silica zirconia samples by bulk preparation and surface impregnation. He concluded that the surface areas of zirconium silicon oxides were essentially independent of the preparation method. Whereas the above results show the importance of the preparation methods in determining the surface areas of zirconia. Soled investigated the samples at only one calcination temperature of 500°C, where he found that 5 atomic % silica zirconia prepared by impregnation or bulk substitution stabilised the tetragonal phase in contrast to the above results, which show the impregnation technique stabilising the monoclinic phase. For both preparations Soled observed that for 1 atomic % silica, the phase was monoclinic indicating that there was a minimum amount of dopant required to stabilise the tetragonal phase (i.e. > 1%).

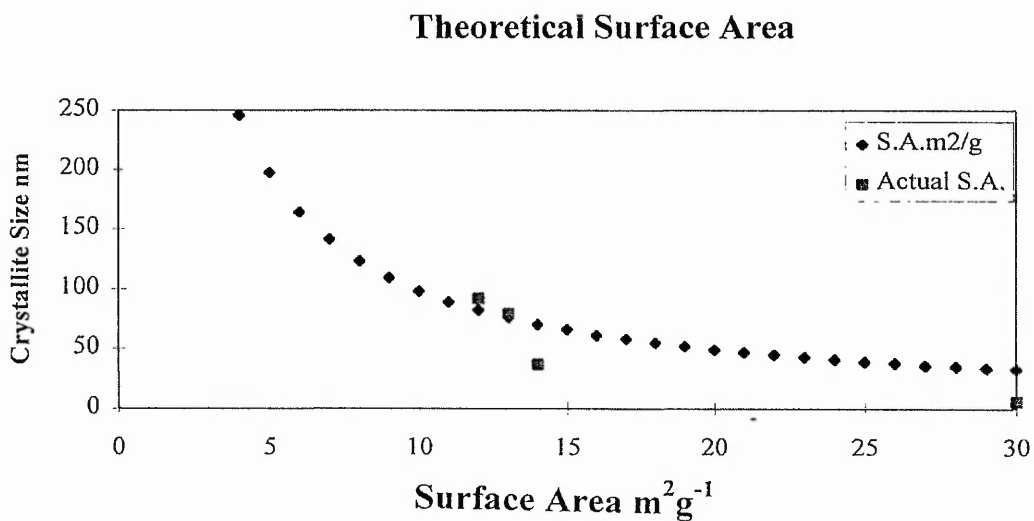
The addition of the dopant to zirconia, using the coprecipitation method, retards the crystallisation of zirconia. Pure zirconia gives the powder XRD pattern of tetragonal zirconia at 400°C, whereas the coprecipitated samples after calcination at 400°C are x-ray amorphous. Powder XRD patterns for tetragonal zirconia are observed at 550°C for the doped materials¹³, as was also the case for lanthana doped zirconia¹⁴.

The crystallite size was determined by separating the influence of strain from the line broadening^{15 16 17}. The coprecipitated samples showed increasing crystallite size with increasing calcination temperature. This is of course expected due to sample sintering in conjunction with loss of surface area. Calculating (see Chapter 3) the theoretical surface areas (4.5 graph 1) from the crystallite sizes shows that at the initial low calcination

temperatures, the theoretical surface area is smaller than the measured indicating the presence of porosity¹⁸. However, at high calcination temperatures, the theoretical surface area is greater than the measured surface area. This discrepancy is possibly due to the development of an internal surface area in the powder, inaccessible to nitrogen adsorption, owing to sintering when the sample is heated¹⁹ or more likely due to particle aggregation.

The impregnated samples with monoclinic phases have similar crystallite sizes of 10 nm and surface areas of approximately $90 \text{ m}^2\text{g}^{-1}$ up to 900°C . The theoretical surface area for monoclinic 10 nm non porous cubic or spherical crystallites is $100 \text{ m}^2\text{g}^{-1}$.

4.2 Graph 1 *Theoretical surface area from crystallite size for non porous spherical or cubic crystallites.*



Garvie's²⁰ criterion for the observation of tetragonal zirconia is not met in all the silica doped zirconia samples. One silica coprecipitated zirconia (3.5wt% $\text{SiO}_2/\text{ZrO}_2$ pH 11.3 rising calcined 1050°C) has a 100% tetragonal phase with a crystallite size of 35 nm. This is larger than Garvie's maximum crystallite size for tetragonal zirconia of 30 nm, where above this crystallite size the tetragonal crystallites transformed to monoclinic crystallites. However, Garvie's experiments were performed on pure zirconia and not on

doped systems. The dopant effect stabilising the phase and surface area may extend to the crystallite size.

The surface ratios for silicon to zirconium were calculated from XPS characterisation, to investigate the effect of temperature on the dopant enrichment at the surface or near surface region. For the coprecipitated samples, the precursors to the oxides gave similar ratios to the theoretical bulk ratio from the preparation criteria. However, the surface enrichment increases gradually with calcination temperature to 900°C. Over the temperature range 900 to 1050°C, the surface ratio increases by the greatest amount to over approximately 1/3 of the surface being the dopant. The coprecipitation preparation of the precursors ($\text{Si(OH)}_4/\text{Zr(OH)}_4$) provides a homogeneous mix of the dopant in the bulk before calcination.

Samples prepared by impregnation show a constant surface ratio from the precursors to 900°C. However, at 1050°C, the surface area increases dramatically to over a 1/3 dopant coverage, as was the case with the coprecipitated samples. The high coverage of dopant at 1050°C can be explained by including the crystallite size and surface area of the samples. At low calcination temperatures, the samples have small crystallite sizes and large surface areas with a known surface dopant concentration, from the impregnation preparation. However, at a high calcination temperature, the crystallites grow and the surface area decreases but the amount of dopant at the surface remains constant. The increase in crystallite size and decrease in surface area means that the same amount of dopant gives a low Si/Zr ratio at 400°C but gives a high surface ratio. at 1050°C due to the decrease in surface area. For example assume a non porous cube has length 1 unit and a silicon surface coverage of 1 surface unit per cube. When the temperature is increased and 8 cubes sinter to form one large cube of length 2 units then the surface area for the 8 individual cubes drops from 48 units to 24 units. Assuming all the silica that was on the surface of the original cubes migrates to the surface of the new larger cube then 8 units of silica are on the surface. Therefore in the small individual cubes the surface ratio was 1 silica unit to 6 surface area units and in the large cube the surface ratio is 8 silica units to 24 surface area units. The drop in surface area and increase in crystallite size is

accompanied by an increase in the surface silicon to zirconium surface ratio. This allows the possibility of phase separation but there must be some interaction between the silica and zirconia due to the acidity at the highest calcination temperatures.

4.6 Infrared spectroscopy combined with pyridine adsorption to investigate the acidic nature of the surface

The use of pyridine adsorption on silica impregnated zirconia combined with infrared spectroscopy has been undertaken to investigate the nature of the acidity of the mixed oxide surface. The infrared spectrum of pure zirconium dioxide is opaque below 800 cm^{-1} and exhibits no distinct features between 800 and approximately 3650 cm^{-1} ²¹. However, bands observed at 3775 , 3680 and 3670 cm^{-1} are characteristic of hydroxyl groups on the surface of zirconia. The bands at 3775 and 3670 cm^{-1} are characteristic of hydroxyls associated with monoclinic zirconia, whereas, the band at 3680 cm^{-1} is associated with hydroxyls on tetragonal zirconia²². The nature of the hydroxyl band at 3775 cm^{-1} was originally thought to be a singularly coordinated OH species on monoclinic zirconia and the two bands close together at 3680 and 3670 cm^{-1} for tetragonal and monoclinic zirconia respectively, related to triply coordinated OH groups²³. However, a more recent investigation by Knozinger²⁴ suggested that there were two surface hydroxyl species. One is related to tetragonally coordinated O^{2-} anions and the other hydroxyl is related to trigonally coordinated O^{2-} anions. Since only the monoclinic phase has trigonally coordinated O^{2-} anions, the higher wavenumber hydroxyl group at 3775 cm^{-1} was associated to the monoclinic phase. However, both monoclinic and tetragonal zirconia have tetragonally coordinated O^{2-} anions. Therefore, the two similar wavenumber hydroxyls at 3680 and 3670 cm^{-1} were associated with the hydroxyl related to the tetragonally coordinated O^{2-} anion.

The spectrum of pure silica is dominated by an intense sharp peak at 3747 cm^{-1} due to isolated noninteracting surface silanol groups (singular SiOH and geminal Si(OH)_2)²¹.

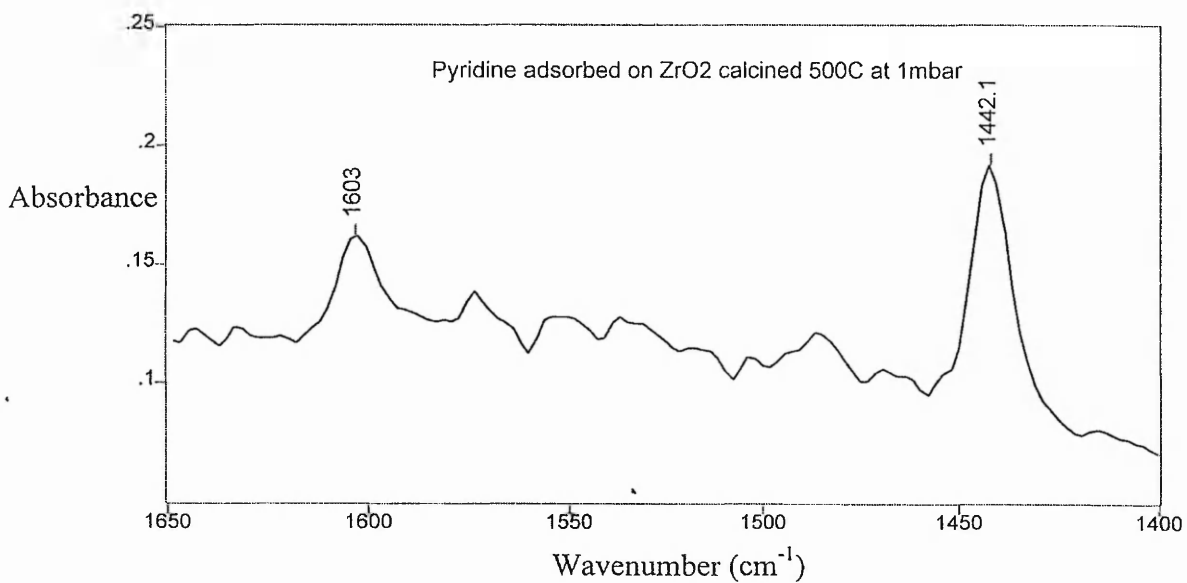
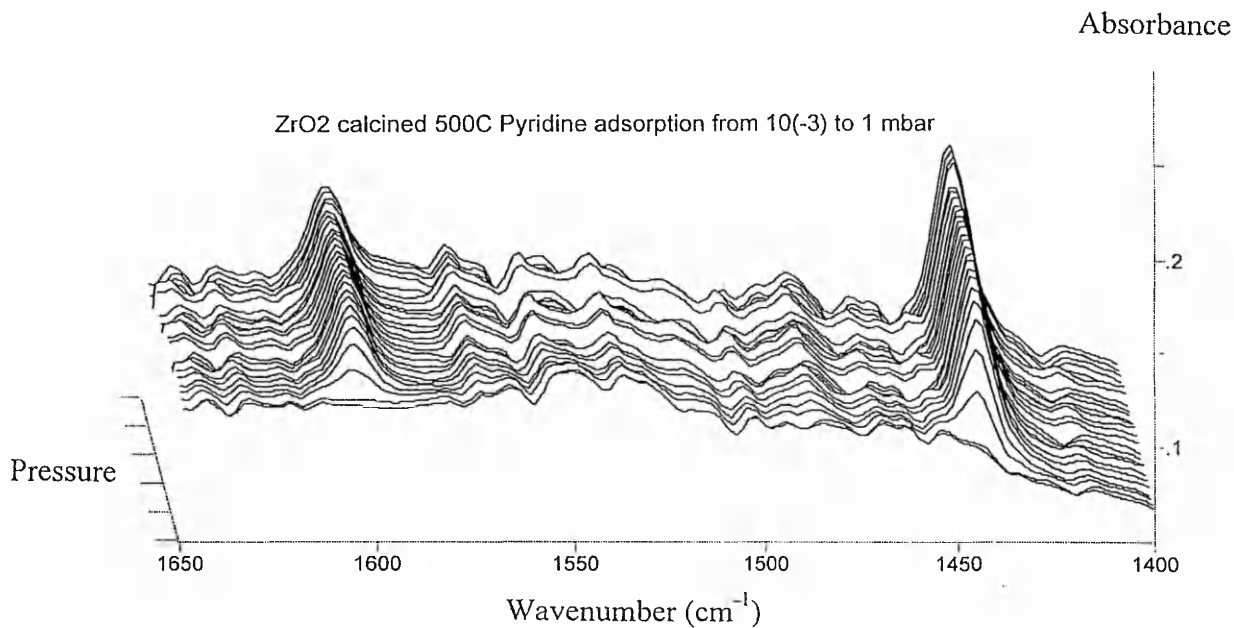
Pyridine has been used as a probe molecule to study the acid sites of oxide surfaces²⁵. Pyridine is used as an acidic probe since it possesses a lone pair of electrons on the nitrogen which is available for donation to other species during bonding and also pyridine can accept a proton from another species. Pyridine bonds to the surface in three different

modes; (1) involving a transfer of a proton from a surface hydroxyl to the pyridine molecule and occurs, with the surface acting as a Brønsted acid, (2) involving coordination of the pyridine molecule through the electron lone pair to the metal of the oxide and takes place with the solid acting as a Lewis acid. This bonding can also be classed as σ -bonding due to the pair of electrons in the bond being entirely donated by the pyridine molecule (3) and finally hydrogen bonding occurring through the interaction of the nitrogen atom with the hydroxyl group on the surface. Hydrogen bonding is the weakest form of interaction²⁶, and can be removed by pumping the system or heating at approximately 470K.

The interaction of the lone pair on the nitrogen of pyridine with a Lewis site results in the 8a normal vibrational mode of pyridine being observed in the range 1590 to 1615 cm^{-1} while the 19b normal mode is found between 1440 and 1465 cm^{-1} ²⁷. Further, less intense Lewis bands are observed at approximately 1490 and 1576 cm^{-1} ²⁸. The interaction of pyridine with a proton of a Brønsted site results in the formation of a pyridinium ion with bands in the regions 1638-1642 cm^{-1} and 1535-1540 cm^{-1} . Hydrogen bonded bands are observed over the range 1580-1590 cm^{-1} .

The samples investigated were ZrO_2 calcined 500°C, 3.5wt% $\text{SiO}_2/\text{ZrO}_2$ impregnated calcined 700 and 900°C and 5wt% $\text{SiO}_2/\text{ZrO}_2$ impregnated calcined 700 and 900°C. The samples proved difficult to press into self supporting thin wafers especially in the case of pure zirconia, as silica may act as a binder. The samples gave low transmission in the experiments.

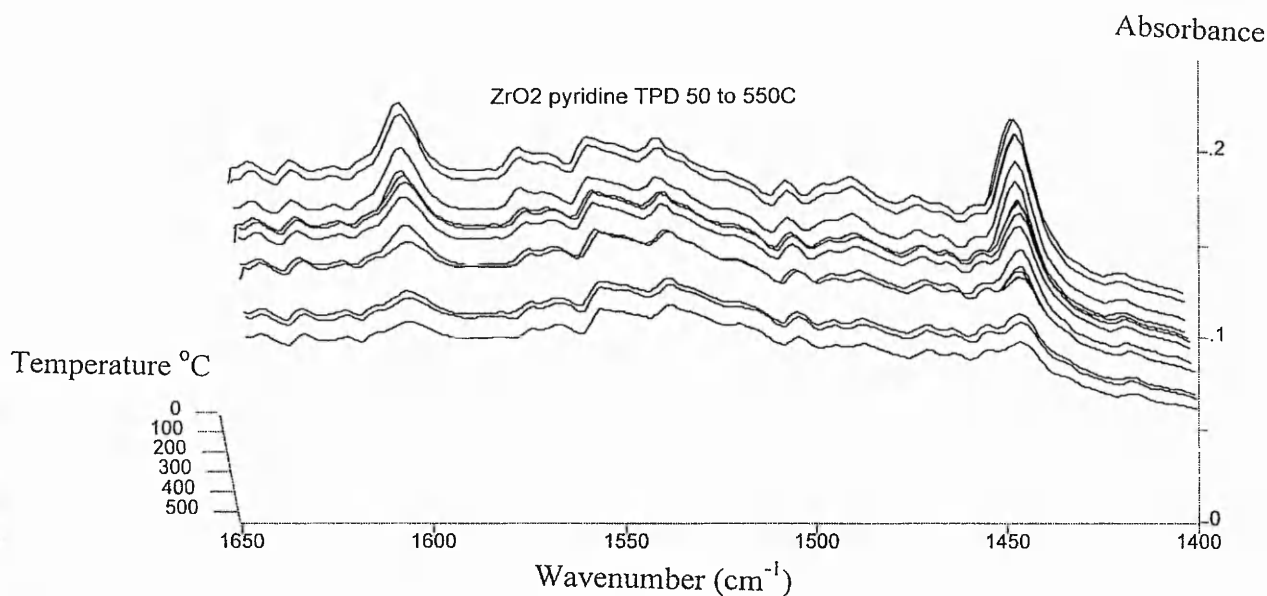
Spectra 1 *Pyridine dosed onto ZrO₂ calcined 500°C from 10⁻³ to 1 mbar*



The infra-red spectrum of pure zirconia was featureless, no hydroxyl groups were observed. However, upon the addition of pyridine to the system two bands appeared at 1604 and 1442 cm⁻¹. These bands correspond to pyridine interacting with Lewis acid sites

on the oxide surface. The above two bands were the only bands observed up to a pressure of 1 mbar of pyridine

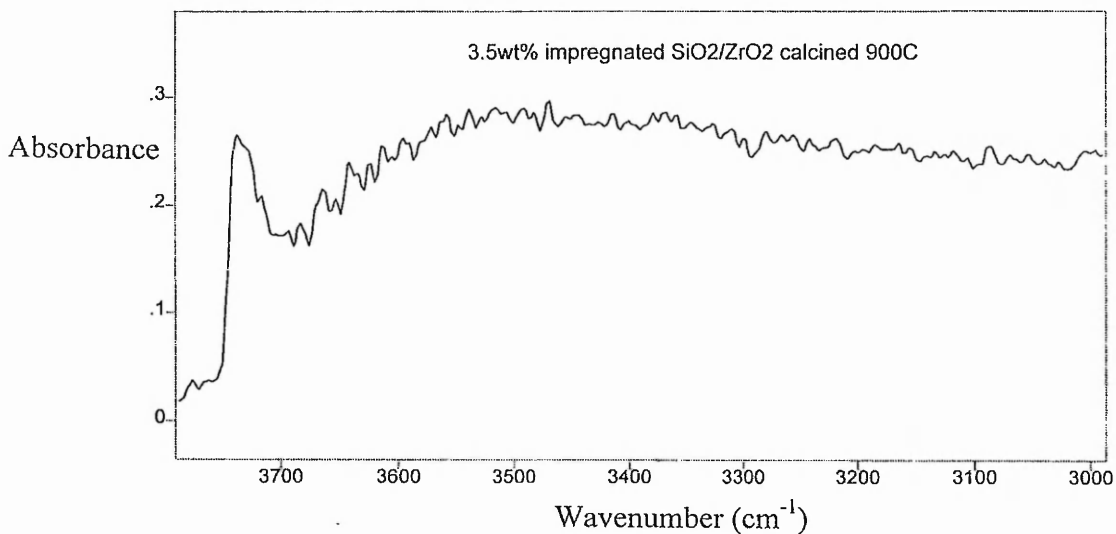
Spectra 2 TPD of pyridine on ZrO_2 calcined $500^\circ C$



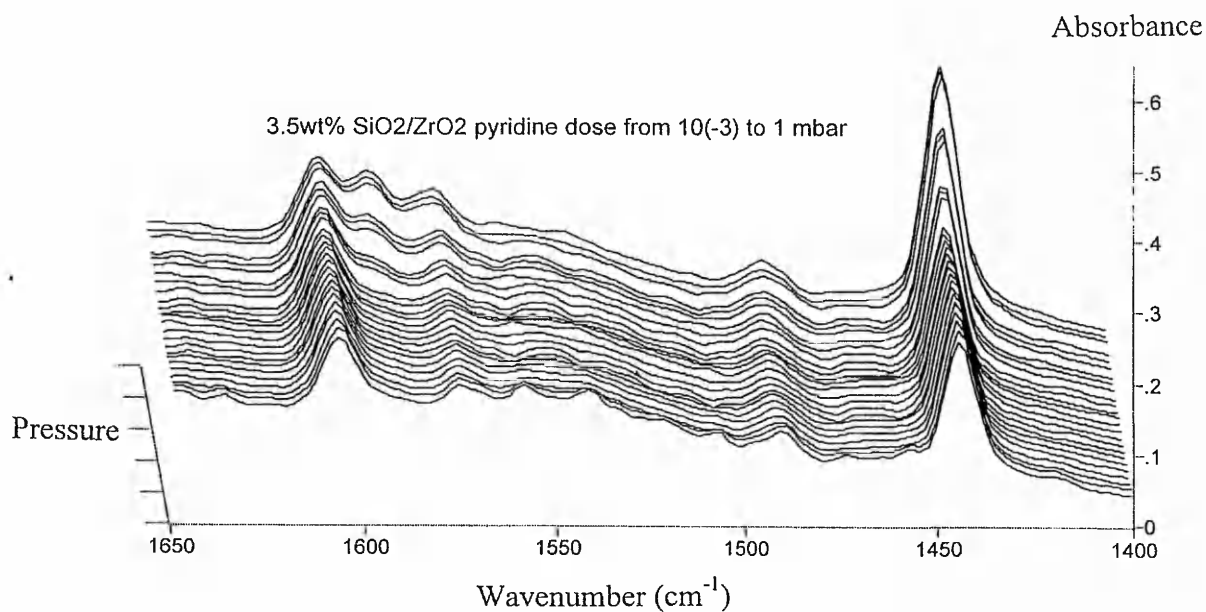
During the temperature programmed desorption the intensity of the bands relating to pyridine at Lewis acid sites gradually decreased. The pyridine was fully removed from the surface at approximately $400^\circ C$. The dosing of pyridine up to a pressure of 1 mbar produced only two bands at 1443 and 1605 cm^{-1} . These were the bands associated with Lewis acid sites. Bands for the formation of a pyridinium ion were not observed (1540 and 1640 cm^{-1}). However, this result was expected since hydroxyl groups were not observed for zirconia at 3775 , 3680 or 3670 cm^{-1} . Bands were not observed for hydrogen bonding of pyridine. There were no hydroxyls on the surface for the pyridine to form hydrogen bonds.

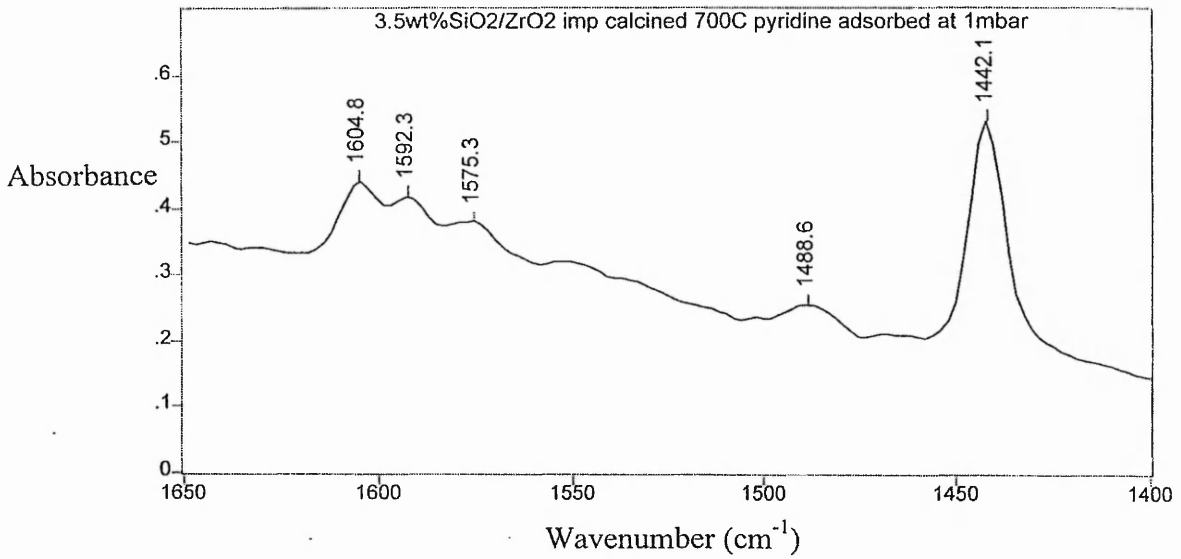
Filimov and Knozinger^{23, 24} observed hydroxyl groups for zirconia. However, for a detailed spectroscopic study the zirconia surface was hydroxylated *insitu* with water vapour making the bands easier to detect. The surface hydroxyls were removed by heating in vacuum to over $700^\circ C$. This was reversible since at room temperature, the addition of water rehydroxylated the surface.

The infra-red spectrum of the silica impregnated zirconia was featureless except for one band at 3737 cm^{-1} which was due to a hydroxyl group related to silica. The spectrum below was recorded at room temperature and the silica hydroxyl band can be observed.



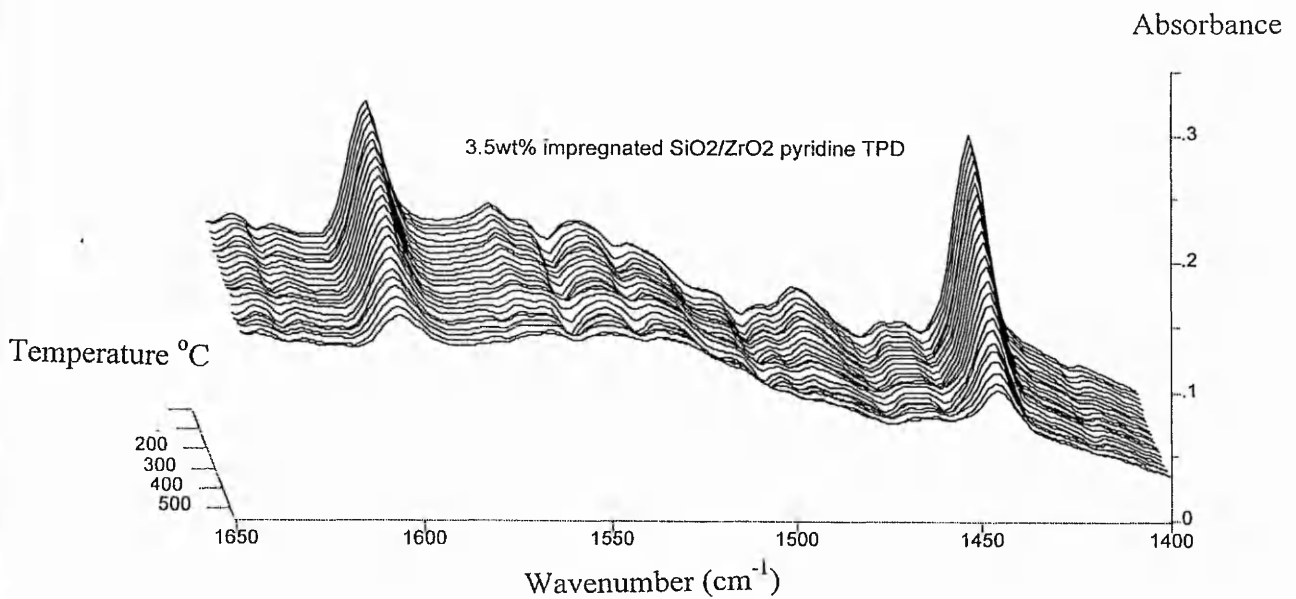
Spectra 3 3.5wt%SiO₂/ZrO₂ imp. cal. 700°C Pyridine dose

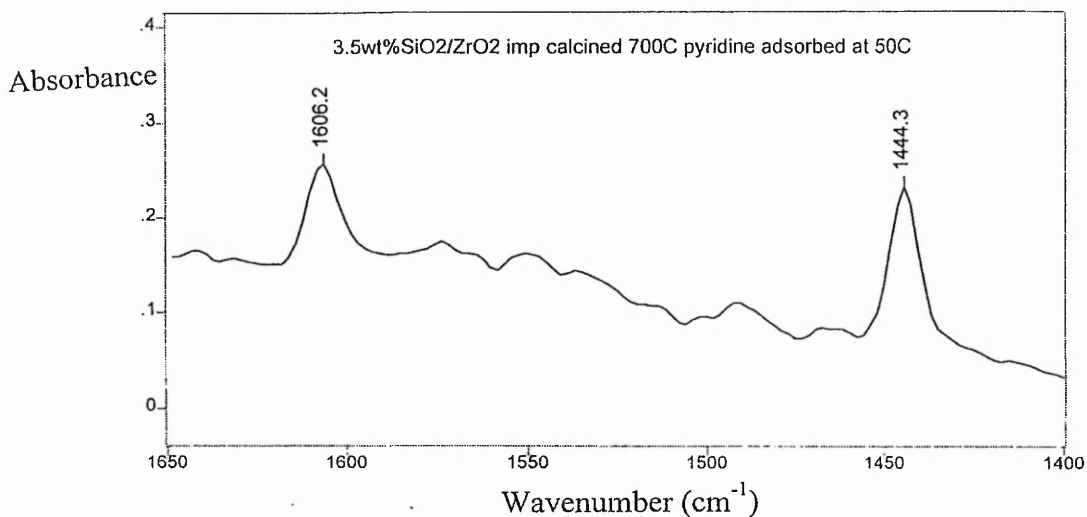




The above spectra shows the bands appearing upon dosing of pyridine onto silica zirconia and produces five bands at a pressure of 1 mbar, 1442, 1489, 1575, 1592 and 1605 cm⁻¹.

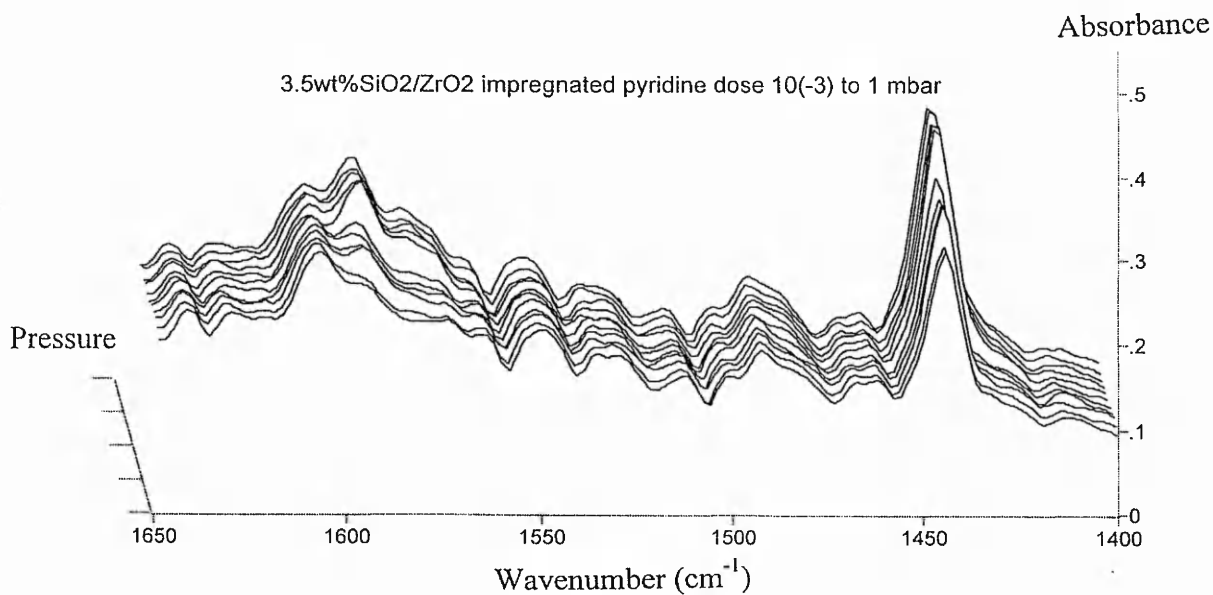
Spectra 4 3.5wt% SiO₂/ZrO₂ imp. cal 700°C pyridine TPD

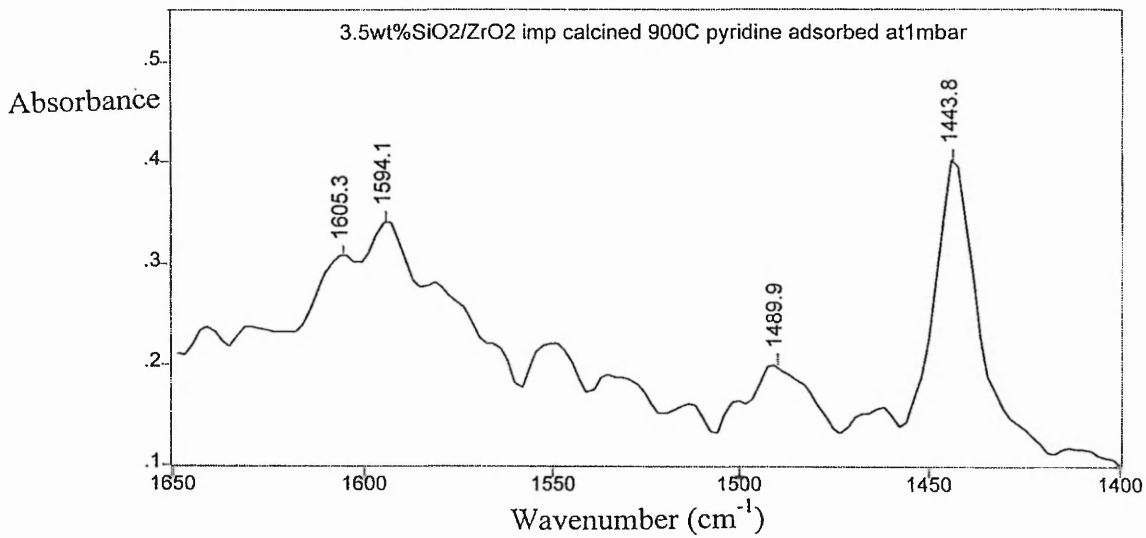




From the above spectra, the pyridine desorbs gradually over the temperature range 50 to 550°C. However, at the start of the desorption experiment after evacuating the system to 10⁻⁶ mbar only the two Lewis acid site bands remain at 1444 and 1606 cm⁻¹.

Spectra 5 3.5wt% SiO₂/ZrO₂ imp. cal 900°C pyridine dose

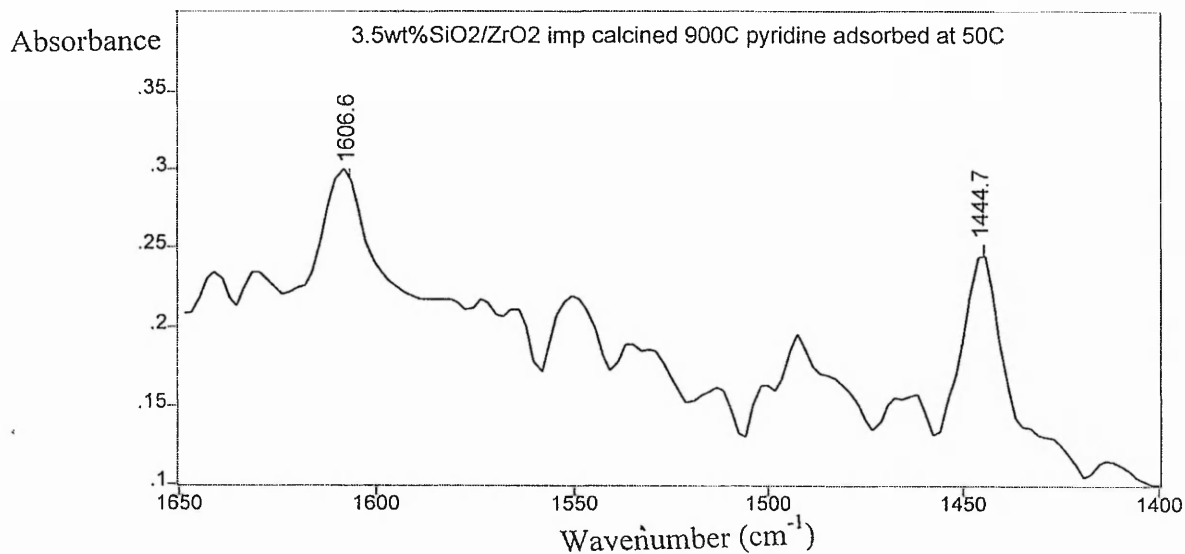
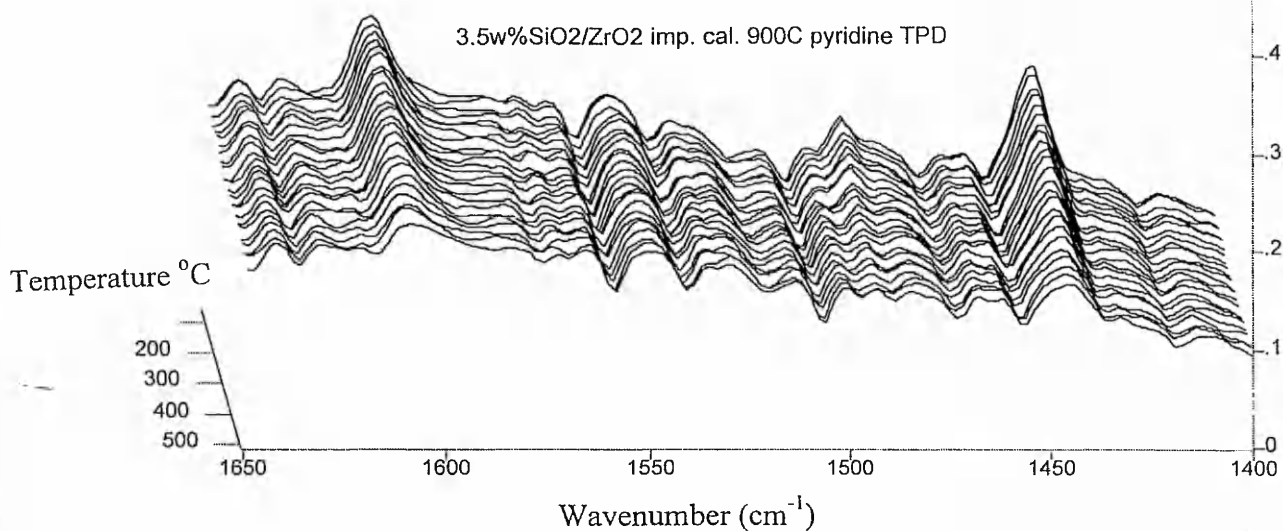




From the above spectra, at low dosing pressures the two main bands were at 1444 and 1605 cm⁻¹. However, at the higher dosing pressures a large band appeared at 1594 cm⁻¹, becoming larger than the band at 1605 cm⁻¹.

Spectra 6 3.5wt%SiO₂/ZrO₂ imp cal 900°C pyridine TPD

Absorbance

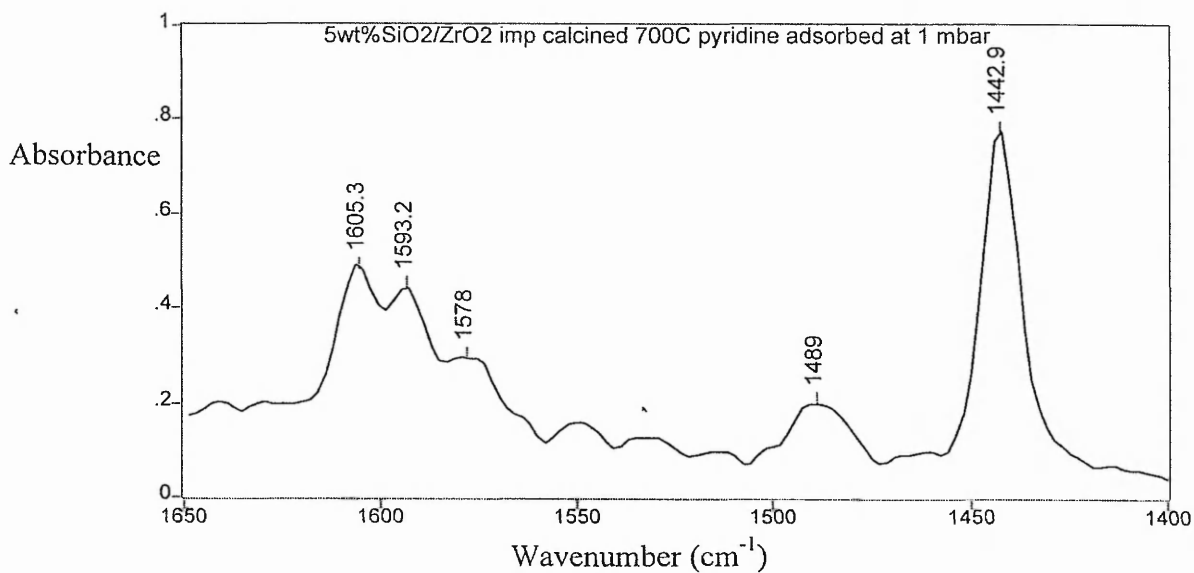
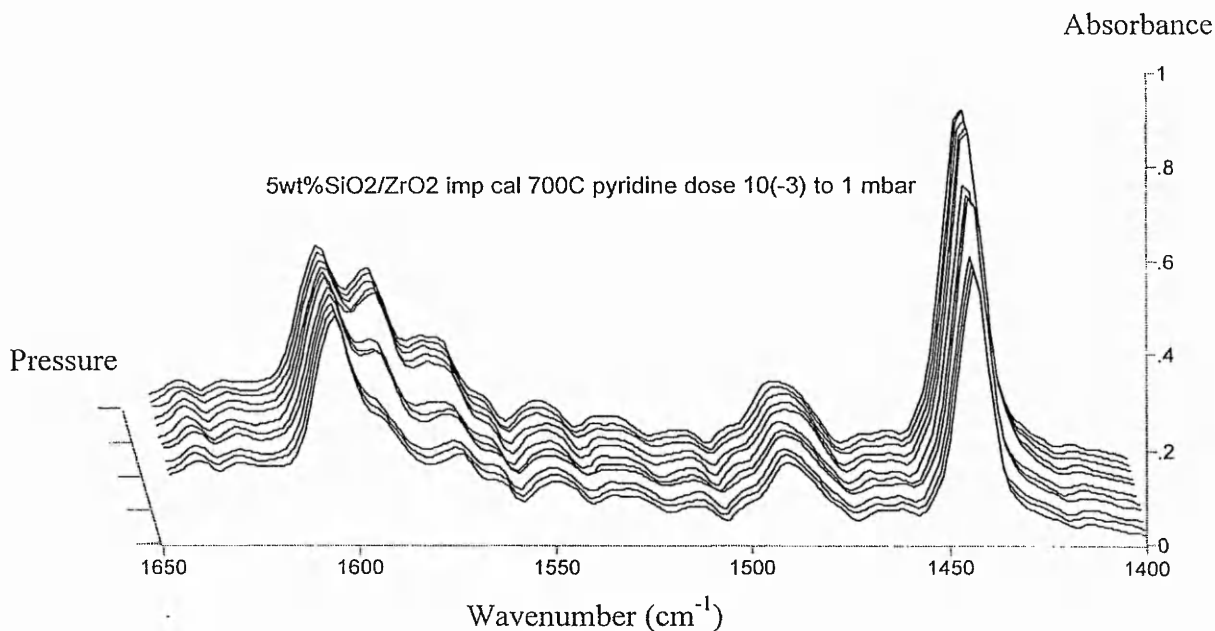


The dosing of pyridine on 3.5wt% SiO₂/ZrO₂ impregnated samples calcined at 700 and 900°C produced the main bands associated with Lewis acid centres at approximately 1444 and 1605 cm⁻¹. Both samples showed a band at approximately 1593 cm⁻¹ relating to hydrogen bonding between pyridine and the surface. Hydrogen bonding was able to take place due to silica hydroxyl groups on the surface which were observed at 3737 cm⁻¹.

Bands for a pyridinium ion were not observed indicating the lack of Brønsted acidity. Therefore, the silica hydroxyls do not contribute to Brønsted acidity, as was observed by Dang²¹.

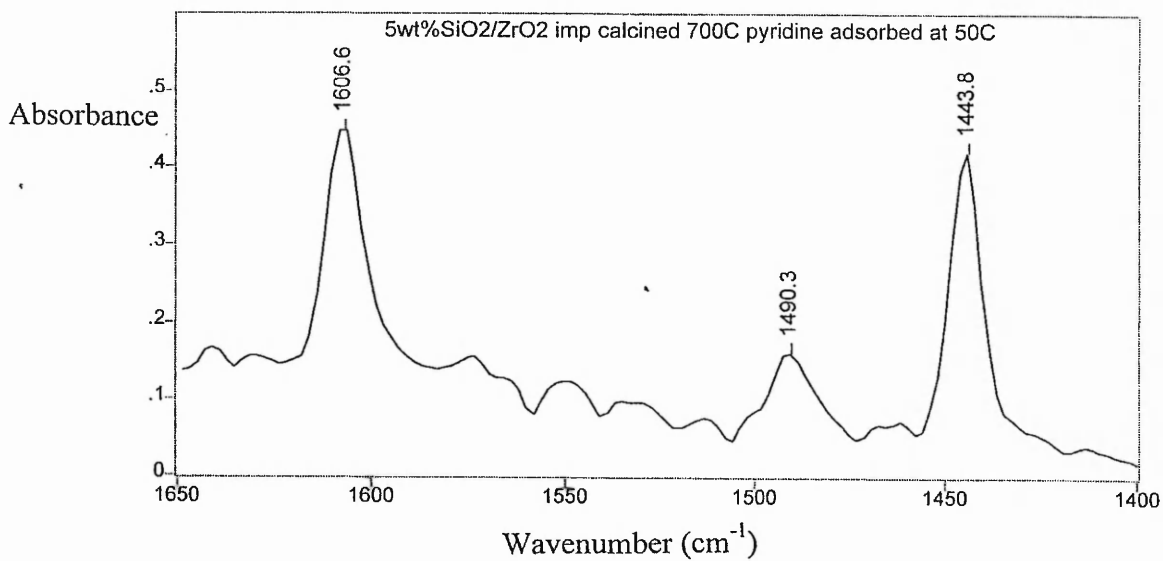
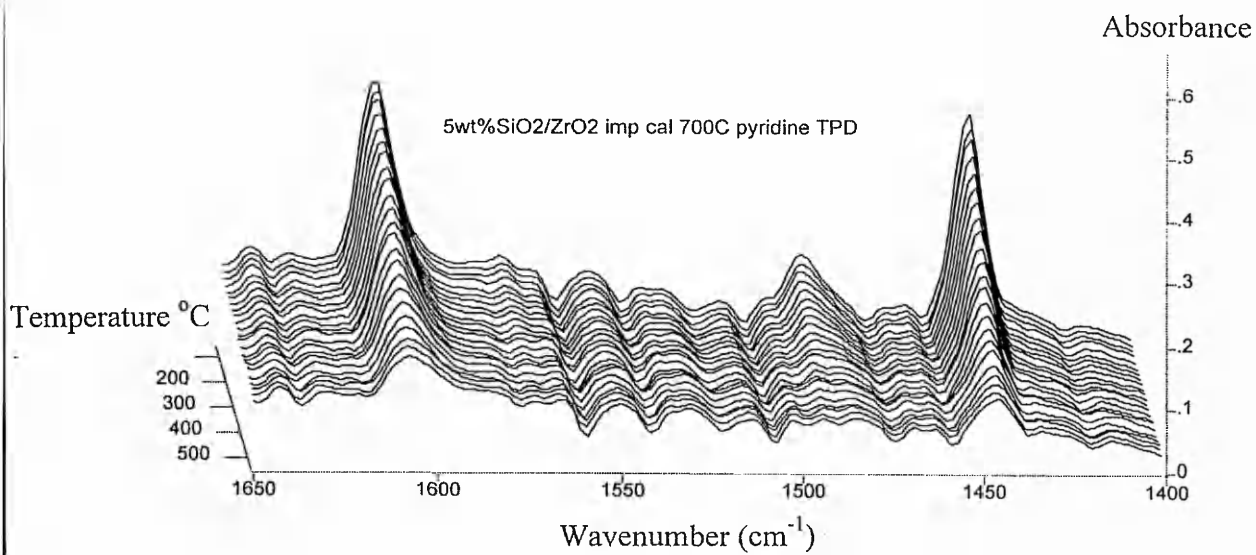
The band which corresponds to hydrogen bonding between pyridine and the surface at 1593 cm^{-1} , in the sample calcined at 900°C , grew larger than the adjacent Lewis acid centre band (1605 cm^{-1}) between the lone pair on the nitrogen and the surface. This did not occur in the sample calcined at 700°C . However, in both systems pumping over a period of time gave a spectrum containing two bands at approximately 1444 and 1605 cm^{-1} prior to the temperature programmed desorption. These bands gradually decreased with increasing temperature but were still observed at the final temperature of 550°C , indicating that pyridine was still adsorbed on the sample.

Spectra 7 5wt%SiO₂/ZrO₂ imp. cal. 700°C pyridine dose



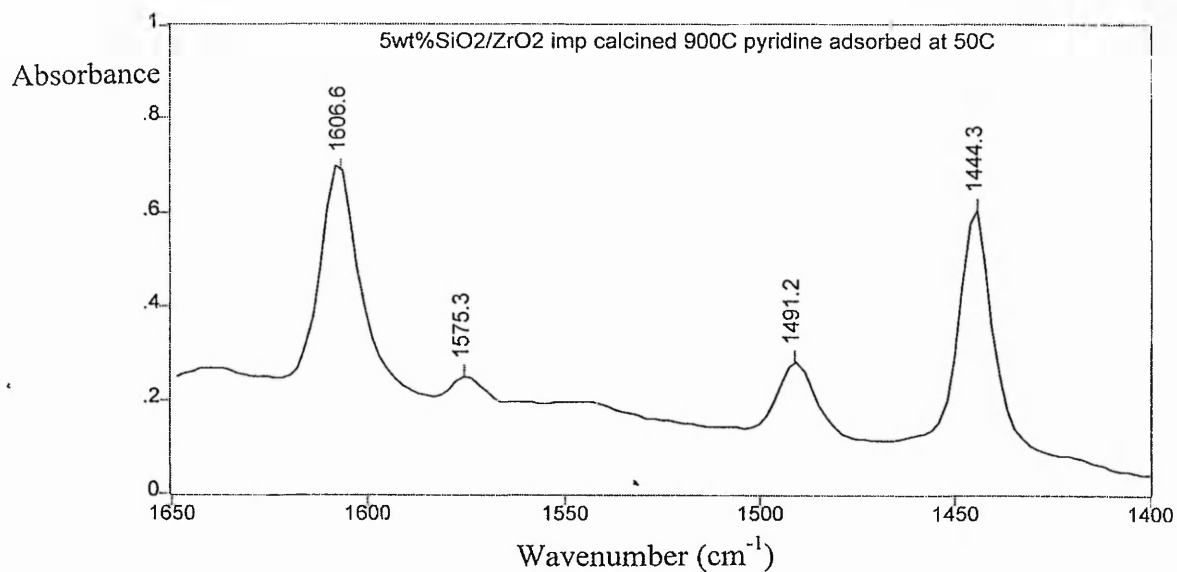
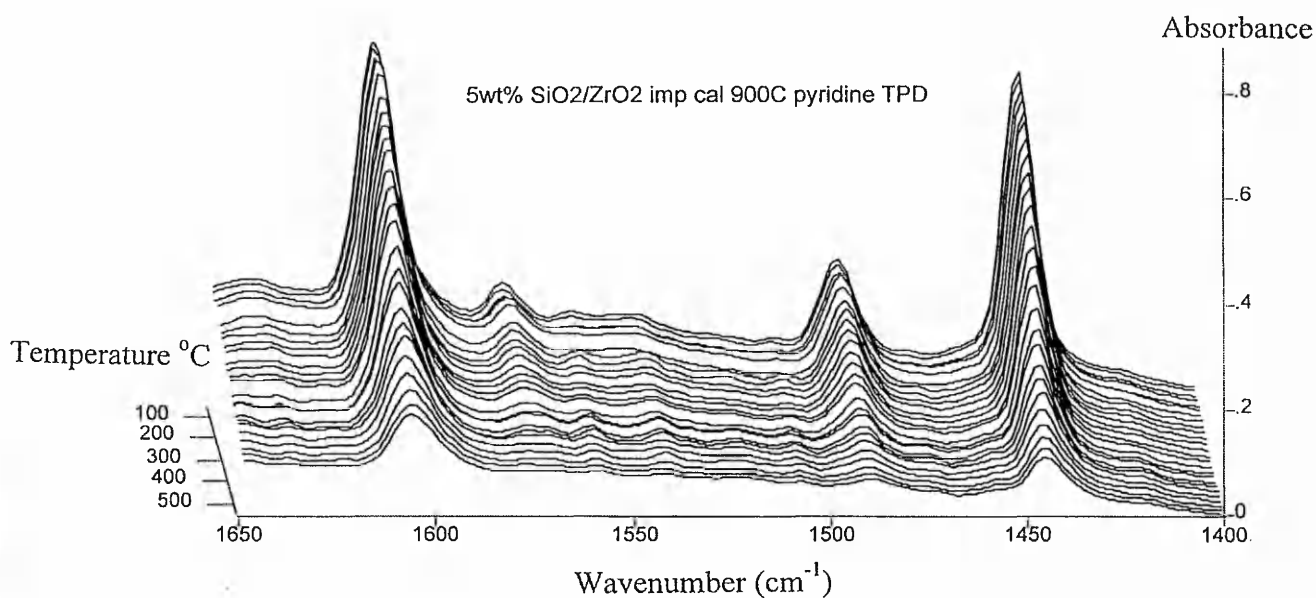
From the above spectra for 5wt% SiO₂/ZrO₂ impregnated calcined at 700°C, five main bands appear upon dosing of pyridine, at 1443, 1489, 1578, 1593 and 1606 cm⁻¹.

Spectra 8 5wt%SiO₂/ZrO₂ imp. cal. 700°C pyridine TPD



From the above spectra, the two bands at 1444 and 1607 cm^{-1} decrease with increasing temperature.

Spectra 9 5wt%SiO₂/ZrO₂ imp. cal. 900°C pyridine TPD



Four bands were observed at the start of the TPD for 5wt% SiO₂/ZrO₂ impregnated calcined 900°C at 1444, 1491, 1575 and 1607 cm⁻¹. The middle two bands disappear however, pyridine was still adsorbed on the surface at 550°C.

The dosing of pyridine on 5wt% SiO₂/ZrO₂ impregnated samples calcined at 700 and 900°C showed bands corresponding to Lewis acid centers and hydrogen bonded pyridine, as in the 3.5wt% samples. Upon evacuation, the sample calcined at 700°C had two main peaks at 1606 and 1443 cm⁻¹ decreasing with increasing temperature. The sample calcined at 900°C had four bands related to Lewis acid centres decreasing with increasing. As in the case of 3.5wt% samples bands for pyridinium ions were not observed, therefore, Brønsted acidity did not occur on the sample and in the presence of silica hydroxyl groups. Pyridine was observed on the samples at 550°C, indicating strong Lewis acid centres

Brønsted acid sites have been observed on zirconia and on silica zirconia systems. Hertl²⁹ using ammonia and pyridine adsorption reactions combined with infra-red spectroscopy showed that three polymorphs, tetragonal, monoclinic and amorphous zirconia had both Lewis and Brønsted acid activity. Using the diffuse reflectance infra-red method, Hertl observed bands due to NH₄⁺ and PyH⁺ showing the presence of surface Brønsted acidity. For silica zirconia systems, Anderson³⁰ only observed the presence of Brønsted acidity when the silica zirconia system was sulfated. Only Lewis acidity was observed before sulfating the sample. The system was investigated using both pyridine and ammonia as probe molecules and the characteristic PyH⁺ band at 1540 cm⁻¹ and NH₄⁺ broad band over the range 1450-1400 cm⁻¹ were observed.

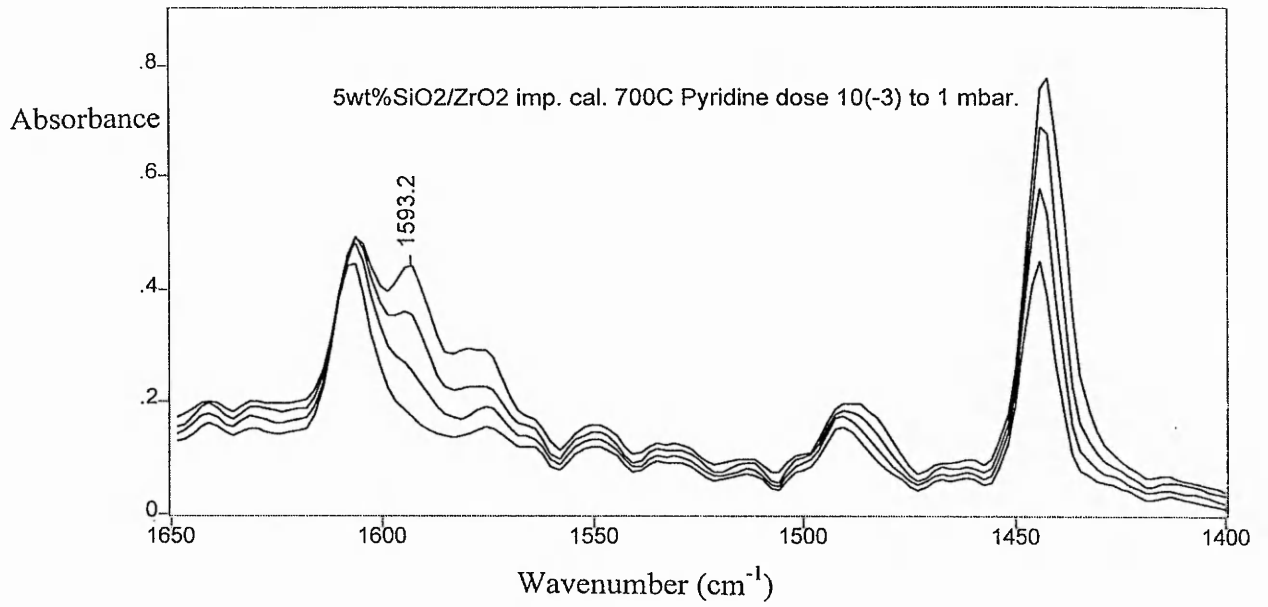
4.6.1 Semiquantification of acid sites on the surface

From the infrared experiments combined with pyridine adsorption, a relationship between the equilibrium dosing pressure and an area for a given infrared band could be obtained. The band investigated was at approximately 1443 cm⁻¹ and was due to pyridine adsorbed at a Lewis acid surface site. Increasing the equilibrium dosing pressure increased the band area. The system was investigated over the pressure range 10⁻³ to 1 mbar (see spectra set 7), with the infrared spectrometer. Upon completion of the dosing experiments, the

system was pumped to 10^{-6} mbar where upon the temperature programmed desorption of pyridine began. The decrease of the band area at 1443 cm^{-1} was investigated during heating.

To quantify the amount of pyridine adsorbed on Lewis acid surface sites a gravimetric method was employed. A C. I. microbalance connected to a dosing and pumping system was used in the gravimetric experiments. Silica zirconia samples were activated *in situ* in a gravimetric apparatus before pyridine was dosed over the pressure range of 10^{-3} to 2 mbar. The experiment was performed in static mode, where the pyridine was dosed into the microbalance compartment and left to equilibrate. The mass of pyridine adsorbed was measured as a function of equilibrium pressure. To ensure an accurate calibration between the infrared and gravimetric experiments, equilibrium pressures used in the calibration of the amount of pyridine on Lewis acid sites were kept below 10^{-2} mbar. At and above the equilibrium pressure of 10^{-2} mbar, hydrogen bonding occurs on the surface which was observed during the infrared spectroscopy experiments. Spectra 10 below shows the emergence of the band at 1593 cm^{-1} relating to hydrogen bonding of the pyridine with the surface. The band started to grow at 10^{-2} mbar. Therefore, any mass uptake in the gravimetric experiments at and above 10^{-2} mbar was a combination of pyridine at Lewis sites and pyridine hydrogen bonding to the surface. For the temperature programmed desorption experiments only Lewis acid bands appeared therefore, the calibration must only contain the appropriate adsorption modes of pyridine.

Spectra 10 *5wt%SiO₂/ZrO₂ calcined 700°C pyridine dose.*



Gravimetric Analysis Results

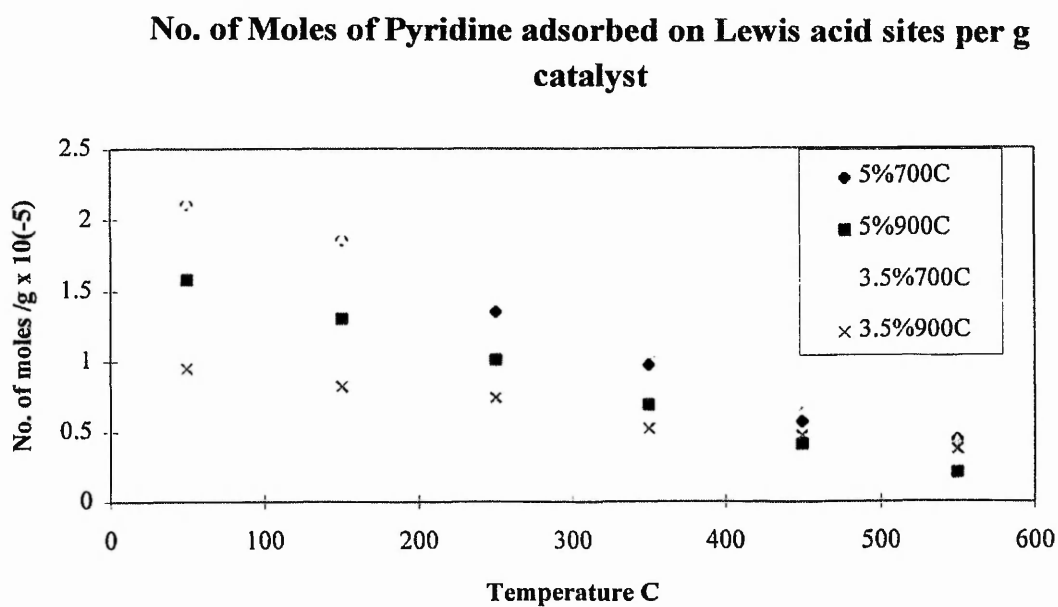
80.32 mg of 5wt% SiO₂/ZrO₂ impregnated calcined 900°C was used in the gravimetric experiment. The adsorption experiment was performed at room temperature and the mass adsorbed mg per sample.

Equilibrium Pressure mbar	Mass Adsorbed mg
1 x 10 ⁻³	0.08
2 x 10 ⁻³	0.13
5 x 10 ⁻³	0.18
6 x 10 ⁻³	0.21
8 x 10 ⁻³	0.33
1.0 x 10 ⁻²	0.43
1.2 x 10 ⁻²	0.52
2.7 x 10 ⁻²	0.92
1.6 x 10 ⁻¹	1.25
3.5 x 10 ⁻¹	1.36
7.6 x 10 ⁻¹	1.57
1.1	1.69
1.5	1.80

From the gravimetric results at 10⁻³ mbar, the number of moles of pyridine on one gram of catalyst can be calculated, since the above results are in mg per mass of sample recorded at room temperature. From the use of Avogadro's number the number of pyridine molecules adsorbed on one gram of catalyst at 10⁻³ mbar is known. Combining these results with the infrared results gives a semiquantitative analysis of the amount of pyridine adsorbed on the catalyst over the temperature range of room temperature to 550°C. The area under the peak relating to

pyridine at Lewis acid sites (1443 cm^{-1}) at a pressure of 10^{-3} mbar is known from the infrared experiments, which varies with temperature and relates to a mass of pyridine adsorbed from the gravimetric experiments. Therefore, a semiquantitative calibration can be performed to relate the number of molecules adsorbed on Lewis acid sites over the temperature programmed desorption range by following the decrease in the peak area at 1443 cm^{-1} . Problems may arise due to the different pressure transducers used in the two experiments, the infrared and the gravimetric analysis. The problems arising in the accuracy and the calibration of the pressure transducers make the calibration only semiquantitative. The calibration gives an indication of the number of acid sites on the surface of the samples and their strength as the temperature was raised. The results from the previous table relate to the number of moles of pyridine adsorbed on one gram of catalyst at room temperature and from the calibration the number of moles of pyridine adsorbed at various temperatures can be calculated.

4.6.1 Graph 1 *Variation of amount of pyridine on Lewis acid site with temperature.*



The above graph depicts the decrease in the amount of pyridine on the surface of the catalysts as a function of temperature. The number of moles of pyridine on the surface was calculated by using the calibration from the gravimetric experiments and relating them to the decrease in the peak area of the Lewis band at 1443 cm^{-1} , as a function of temperature. From the lowest temperature (50°C) on the above graph, the samples calcined at 700°C have a greater concentration of pyridine adsorbed and therefore a greater number of Lewis sites per gram of catalyst. However, normalising the results for surface area and converting the number of moles of pyridine to the number of molecules of pyridine adsorbed per unit area, gave the following results below.

4.6.1 Table 1 *The number of pyridine molecules per nm^2 is listed for the various samples*

Temp. $^\circ\text{C}$	5%SiO ₂ /ZrO ₂ 700 $^\circ\text{C}$	5%SiO ₂ /ZrO ₂ 900 $^\circ\text{C}$	3.5%SiO ₂ /ZrO ₂ 700 $^\circ\text{C}$	3.5wt%SiO ₂ /ZrO ₂ 900 $^\circ\text{C}$
50	0.13	0.11	0.13	0.08
250	0.08	0.07	0.09	0.06
550	0.03	0.01	0.03	0.03

The surface area of the impregnated samples were known, therefore, the number of pyridine molecules adsorbed on the surface at the various temperatures were calculated from the results in 4.6.1 Graph 1. With increasing temperature, the amount of pyridine adsorbed decreased. At the experimental temperature of 50°C , the number of molecules of pyridine adsorbed was similar for all the samples. However, upon increasing the experimental temperature, the number of molecules adsorbed on all the samples became more uniform. This indicated that the strength of the acid sites at elevated temperatures was similar across the range of samples. Pyridine remained adsorbed on the surface at 550°C , indicating strong acid sites as opposed to pure zirconia where no pyridine remained at this temperature. There were stronger acid sites on silica doped zirconia than on pure zirconia.

4.7 Conclusions

- (1) The surface area of zirconia is stabilised when silica is used as the dopant.
- (2) The tetragonal phase of zirconia was stabilised by doping the system using a coprecipitation method of preparation, whereas, the monoclinic phase was stabilised when the impregnation method of preparation was used.
- (3) Garvie's criteria for tetragonal crystallite size was met for the silica doped system in the majority of cases.
- (4) The acidity of the surface of the silica zirconias was investigated and Lewis acid sites were observed but Brønsted acid sites were not.
- (5) The impregnated samples investigated using infrared spectroscopy combined with pyridine adsorption had similar acid site concentrations when normalised for the surface area.
- (6) The acid sites on the silica doped zirconia were stronger than pure zirconia, since pyridine remained adsorbed on the mixed oxide at 550°C, whereas for pure zirconia at this temperature no pyridine was observed.

References

-
- ¹ S. J. Gregg and K. S. W. Sing, *Adsorption, Surface Area and Porosity*, Academic Press, London, 2nd Edition 1982.

-
- ² R. Franklin, P. Goulding, J. Haviland, R. W. Joyner, I. McAlpine, P. Moles, C. Norman and T. Nowell, *Catalysis Today*, 10 (1991) p405-407.
- ³ M. A. C. G. van de Graaf and A. J. Burggraaf, Am. Ceram. Soc., *Science and Technology of zirconia II*, 1984.
- ⁴ H. Toraya, M. Yoshimura and S. Somiya, J. Am. Ceram. Soc., 67 (1984) C-119.
- ⁵ C. J. Norman, *Measurement of Crystallite Size and Strain by X-ray line broadening*, Internal Report MEL Chemicals.
- ⁶ B. D. Cullity, *Elements of x-ray diffraction*, Addison-Wesley 1956.
- ⁷ C. R. Brundle, C. A. Evans Jr., S. Wilson, *Encyclopedia of Materials Characterisation*, p282-299, Butterworth-Heinemann.
- ⁸ D. Briggs and M. P. Seah, *Practical Surface Analysis*, 2nd Edition, Volume 1, Wiley 1992.
- ⁹ C. D. Wagner, W. M. Riggs, L.E. Davis and J. F. Moulder, *Handbook of photoelectron spectroscopy*, Published Perkin Elmer.
- ¹⁰ J. B. Miller, S. E. Rankin and E. I. Ko, J. Catal., 148, (1994) p673-682.
- ¹¹ P. D. L. Mercera, Ph. D. Thesis, Universite Twente 1991.
- ¹² S. Soled and G. B. McVicker, *Catalysis Today*, 14 (1992) p189-194.
- ¹³ M Ozawa and M. Kimura, J. Less Comm. Metals, 171 (1991) p195-212.
- ¹⁴ Chapter 3.
- ¹⁵ Th. H. de Keijser, J. I. Langford, E. J. Mittemeijer and A. B. P. Vogels, J. Appl. Cryst. 15, (1982) p308 - 314.
- ¹⁶ J. I. Langford, J. Appl. Cryst. 11, (1978) p10 - 14.
- ¹⁷ A. Benedetti, G. Fagherazzi, S. Enzo and M. Battagliarin, J. Appl. Cryst. 21, (1988) p536 - 542.
- ¹⁸ P. D. L. Mercera, Ph. D. Thesis, Universite Twente 1991.

-
- ¹⁹ R. C. Garvie, *J. Phys. Chem.*, 65 (1969) p1238
- ²⁰ R. C. Garvie, *J. Phys. Chem.*, 82, (1978) p219.
- ²¹ Z. Dang, B. G. Anderson, Y. Amenomiya and B. A. Morrow, *J. Phys. Chem.*, Vol. 99, No. 39, (1995) p14437-14443.
- ²² H. J. M. Bosman, Ph. D. Thesis, Technische Universiteit Eindhoven 1993.
- ²³ N. E. Tret'yakov, D. V. Pozdnyakov, O. M. Oranskaya and V. N. Filimonov, *Russian Journal of Physical Chemistry*, 44 [4], (1970).
- ²⁴ K. Jacob, E. Knozinger and S. Benfer, *J. Mater. Chem.*, 3[6], (1993) p651-657.
- ²⁵ E. P. Parry, *J. Catal.*, 2, (1963) p371-379.
- ²⁶ M. C. Kung and H. H. Kung, *Catal. Rev.-Sci. Eng.*, 27[3], (1985) p425-460.
- ²⁷ J. Connerton, R. W. Joyner and M. B. Padley, *J. Chem. Soc. Faraday Trans.*, 91[12], (1991) p1841-1844.
- ²⁸ T. Kataoka and J. A. Dumesic, *J. Catal.*, 112, (1988) p66 - 79.
- ²⁹ W. Hertl, *Langmuir* 5, (1989) p96-100.
- ³⁰ B. G. Anderson, Z. Dang and B. A. Morrow, *J. Phys. Chem.*, Vol. 99, No. 39, (1995) p14444-14449.

5. Ceria doped zirconia.

5.1 Preparation of ceria doped zirconia

5.1.1 Coprecipitation

The addition of ceria to zirconia prepared by coprecipitation was investigated, with respect to stabilising the surface area of zirconia. Ceria zirconia ($\text{CeO}_2/\text{ZrO}_2$) samples were prepared with 16, 20 and 50wt% of the dopant. The ceria source was cerium carbonate (Aldrich), which was dissolved in equal volumes of concentrated nitric acid and distilled water, before being added to the zirconium oxynitrate solution, which was prepared from zirconium basic carbonate. A second set of samples were prepared with the same % of dopant and in the same manner but with excess concentrated nitric acid and distilled water being used but still in equal volumes. These samples are called $\text{CeO}_2/\text{ZrO}_2$ dilute system. This was performed to investigate the effect of excess solvent on the surface area of the samples and to see if a more homogeneous mix of the ceria in the zirconia lattice could be produced.

The cerium nitrate and zirconium oxynitrate solutions were well mixed before initiating the coprecipitation. Ammonium hydroxide (28-30% NH_3 in H_2O) was added dropwise to the solution to begin the coprecipitation and was added continuously until a final pH of 10.0 was reached. The coprecipitation began at pH approximately 4 and continued with increasing pH. The mixture was stirred, filtered, washed with distilled water and dried at 110°C overnight to produce the hydroxide precursor. Calcination took place in static air for two hours over the temperature range 550 to 1050°C to produce the binary mixed oxides.

5.1.2 Impregnation

The samples were prepared using the incipient wetness technique. Zirconium hydroxide was precipitated from zirconium oxynitrate using ammonium hydroxide (28-30% NH_3 in H_2O) to a final pH of 10.0. The hydroxide was stirred

filtered, washed with distilled water and dried at 110°C overnight to produce the hydroxide. Cerium nitrate was impregnated onto the hydroxide to give a loading of 16wt% ceria. The mixture was stirred and dried at 110°C. Calcination took place in static air for two hours over the temperature range 550 to 1050°C to produce the binary mixed oxide.

5.2 Surface area results.

The surface area measurements of ceria doped zirconia were performed using nitrogen adsorption and applying the BET equation ¹.

5.2 Table 1 Surface area m^2g^{-1} for coprecipitated and impregnated ceria doped zirconia.

Temp./°C	16% cppt.	20% cppt.	50% cppt.	16%imp
550	55	62	39	63
700	20	34	15	26
900	6	10	3	12

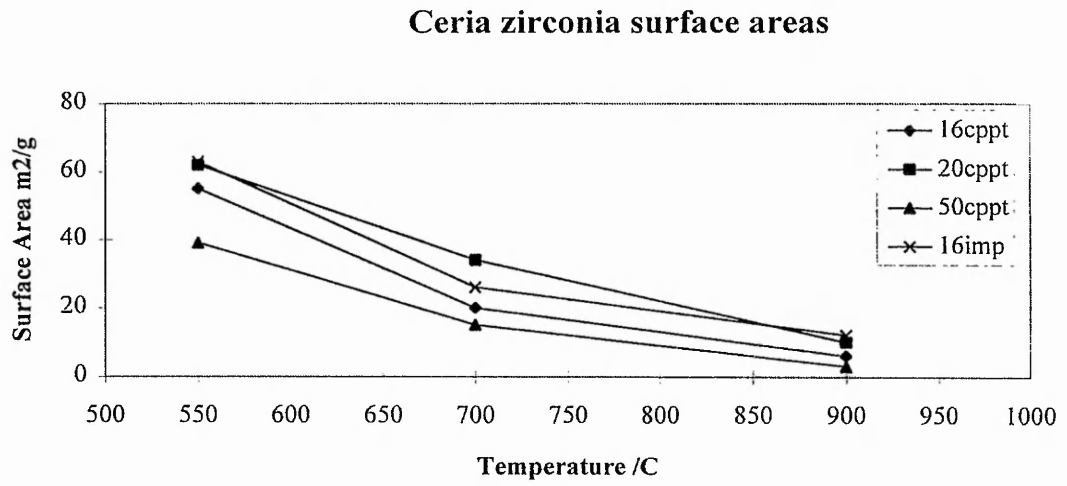
5.3 Table 2 Surface area m^2g^{-1} for ceria zirconia dilute coprecipitated system.

Temp/°C	16% dil.	20% dil.	50% dil.
550	75	58	53
700	37	29	30
900	19	9	5
1050	4	<3	<3

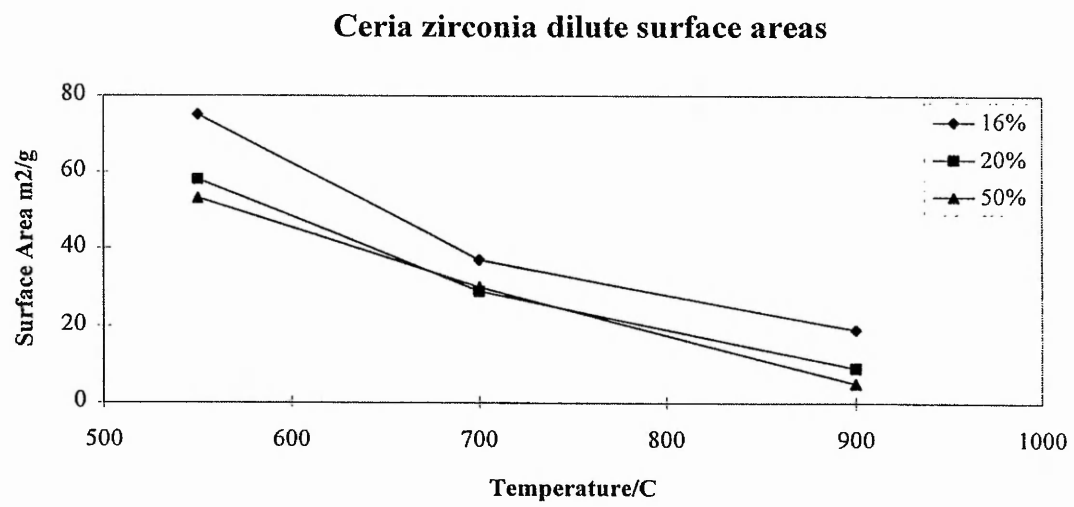
The effect of excess solvent is to increase the surface areas for the 16 and 50 wt% sets, however, the 20% results remained similar. The lower the amount of dopant,

the higher the surface area. The impregnated samples have similar surface areas to the coprecipitated samples.

5.2 Graph 1 Surface area for impregnated and coprecipitated ceria zirconia



5.2 Graph 2 Surface area for ceria zirconia dilute system



5.3 Powder XRD results

Powder XRD was undertaken to determine the crystallite size² and the phase³ of the samples.

5.3 Table 1 Phase identification for coprecipitated and impregnated ceria zirconia samples.

Sample	550°C	700°C	900°C	1050°C
16% imp.	T	T	T + m	T + m
16% cppt.	T	T + m	T + m	T + m
20% cppt.	T	T + m	T + m	T + m
50% cppt.	T	T	T	T + m

T = tetragonal, m = monoclinic.

5.3 Table 2 Crystallite size for coprecipitated and impregnated ceria zirconia samples (nm).

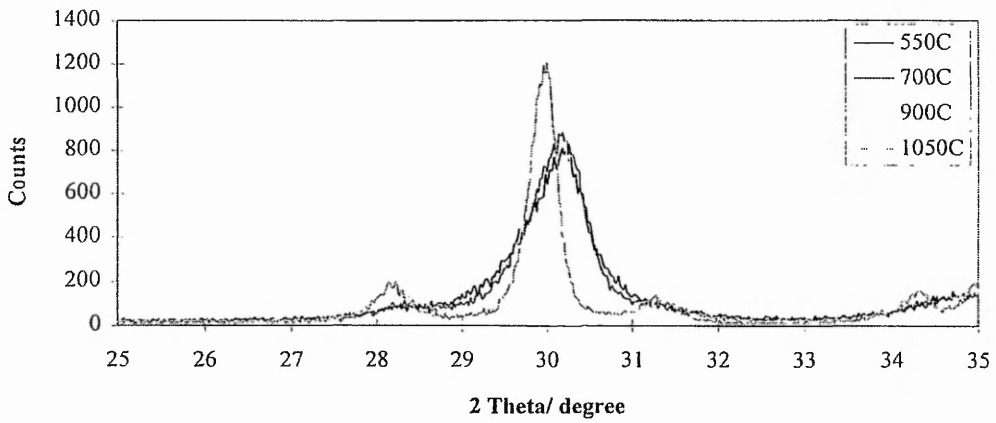
Sample	550°C	700°C	900°C	1050°C
16% imp.	11.5	12.0	15.4	26.6
16% cppt.	10.0	11.5	14.8	23.9
20% cppt.	9.4	10.5	14.9	21.6
50% cppt.	4.5	5.2	7.5	13.6

The crystallite sizes increase with calcination temperature.

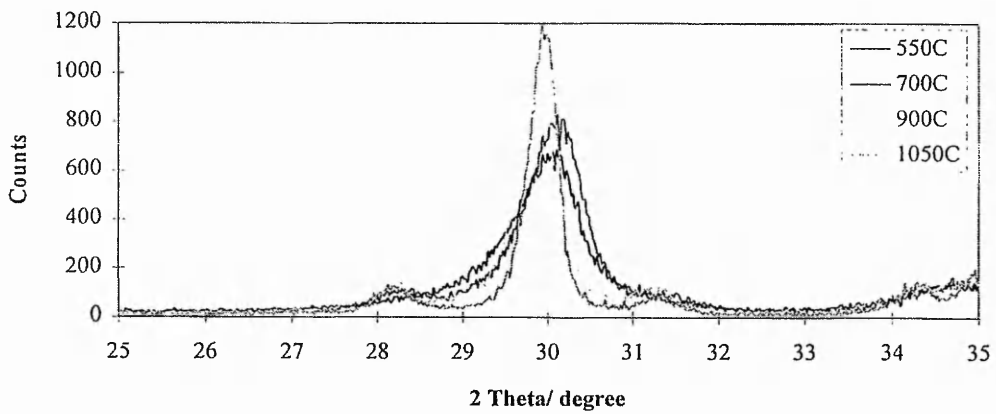
The major phase in all cases is tetragonal, with the monoclinic phase being a trace phase in some of the samples. The concentration of the monoclinic phase did not exceed 10% even in the samples calcined at the highest temperature, 1050°C. The phase compositions were determined as discussed in Chapter 2.

5.3 Graphs 1 -4 Powder XRD patterns for ceria - zirconia coprecipitated and impregnated samples

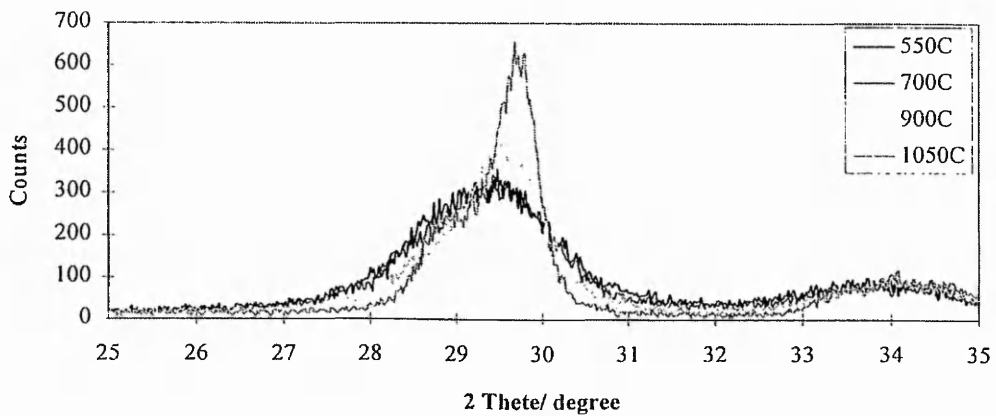
16% CeO₂/ZrO₂ cppt. XRD



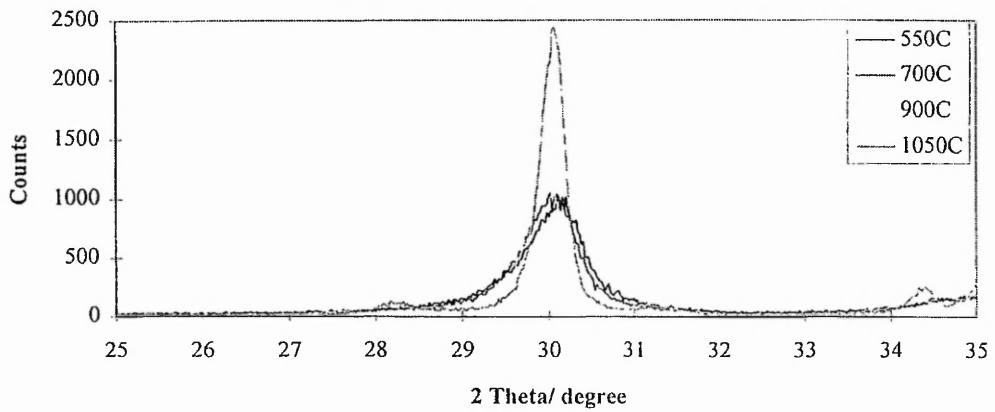
20% CeO₂/ZrO₂ cppt. XRD



50% CeO₂/ZrO₂ cppt. XRD



16% CeO₂/ZrO₂ imp. XRD



5.3 Table 3 Phase identification for ceria zirconia dilute system

Sample	550°C	700°C	900°C	1050°C
16% cppt.	T	T	T	T
20% cppt.	T	T	T	T
50% cppt.	T	T	T	T + m

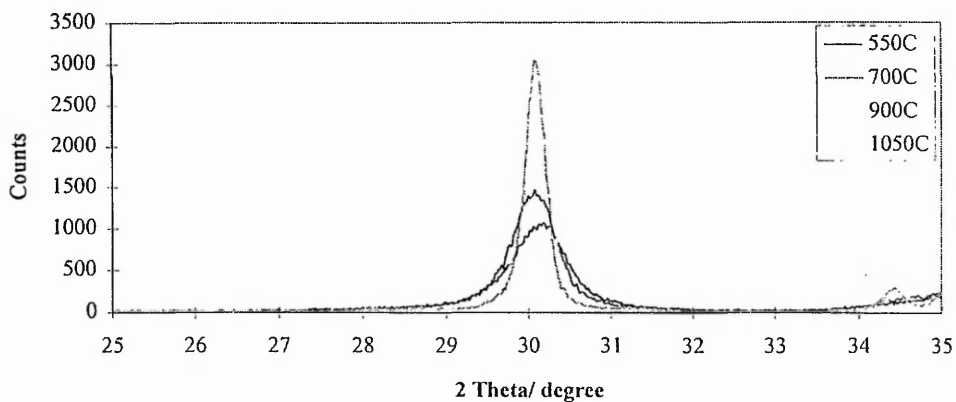
5.3 Table 4 Ceria zirconia dilute system crystallite size (nm) from powder XRD

Sample	550°C	700°C	900°C	1050°C
16% cppt.	10.9	13.3	21.0	31.3
20% cppt.	7.9	9.1	15.3	28.5
50% cppt.	5.1	5.5	10.1	18.9

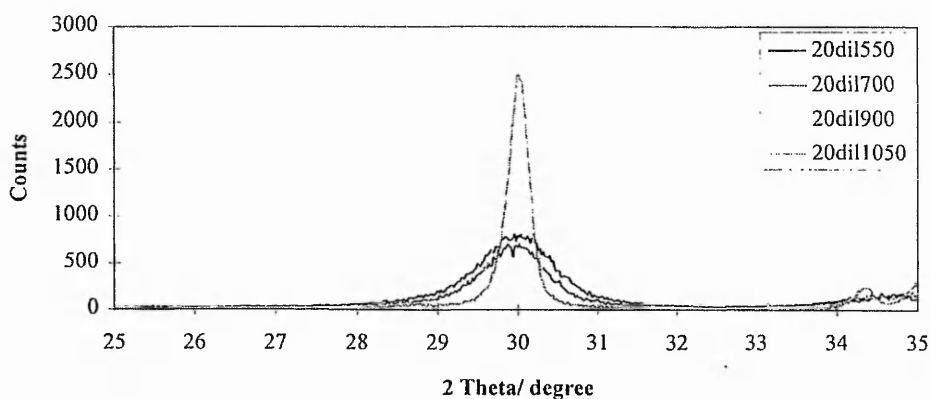
The tetragonal phase is the most dominant.

5.3 Graphs 5-7 Powder XRD patterns for ceria zirconia dilute system

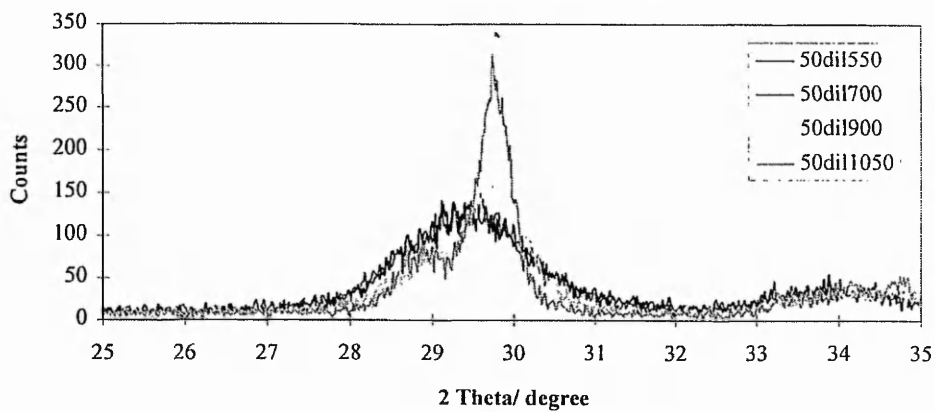
16% CeO₂/ZrO₂ dilute XRD



20% CeO₂/ZrO₂ dilute XRD

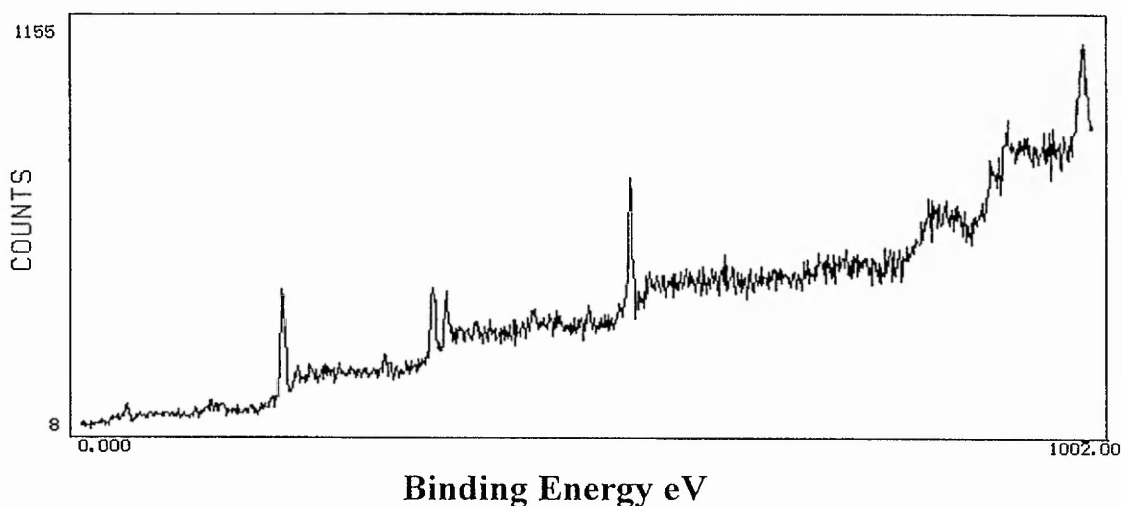


50% CeO₂/ZrO₂ dilute XRD



5.4 XPS results

X-ray photoelectron spectroscopy studies were performed to determine the surface molar ratio of cerium to zirconium for 16, 20 and 50wt% CeO₂/ZrO₂. Ce 3d_{5/2} and Zr 3d⁴ peaks were used to determine the surface ratios. The results are expressed as Ce/Zr surface molar ratio. 16, 20 and 50 wt% CeO₂/ZrO₂ are equivalent to 12, 15 and 42 mole % CeO₂/ZrO₂.



The above XPS spectrum is of 16wt% CeO₂/ZrO₂ coprecipitated and calcined at 1050°C. The main features of the spectrum are assigned below.

Binding Energy eV	Assignment of Peak
183	Zr 3d
285	C 1s
333 348	Zr 3p _{3/2} 3p _{1/2}
531	O 1s
882 900	Ce 3d _{5/2} 3d _{3/2}

5.4 Table 1 *Ce/Zr surface ratios*

Temperature /°C	16wt% CeO ₂ /ZrO ₂ cppt.	20wt% CeO ₂ /ZrO ₂ cppt.	50wt% CeO ₂ /ZrO ₂ cppt.	16wt% CeO ₂ /ZrO ₂ imp.
Precursor	0.10	0.16	0.41	0.17
550	0.10	0.14	1.14	0.11
700	0.14	0.13	0.95	0.15
900	0.13	0.19	1.47	0.19
1050	0.22	0.22	1.24	0.21

5.4 Table 2 *Ce/Zr surface ratios*

Temperature /°C	16wt%dil. CeO ₂ /ZrO ₂	20wt%dil. CeO ₂ /ZrO ₂	50wt%dil. CeO ₂ /ZrO ₂
Precursor	0.10	0.10	0.39
550	0.10	0.21	1.17
700	0.13	0.22	1.18
900	0.19	0.30	0.99
1050	0.28	0.28	0.89

5.5 Discussion

The addition of ceria to zirconia only increases the surface area of pure zirconia , over the temperature range 550 to 900°C, in the sample prepared from the dilute precursor to a weight of 16%. The addition of ceria to zirconia did not stabilise the surface area to the same extent as when lanthana or silica were used as dopants.

The addition of 50wt% CeO₂ to ZrO₂ decreased the surface area compared to pure zirconia (Chapter 3). The least amount of dopant used produces the greatest surface area stabilisation. The nature of the preparation proves to have little effect on the surface area for ceria doped zirconia.

The surface area results are consistent with the literature, where Settu⁵ prepared a 10 mole % CeO₂/ZrO₂ sample which had a low surface area, 7 m²g⁻¹ at 600°C and 2 m²g⁻¹ at 800°C. Using less dopant, Franklin⁶ prepared samples with surface areas around 20 m²g⁻¹ at 950°C for 1, 2 and 3 mole % CeO₂/ZrO₂. Therefore, preparing samples with lower amounts of ceria gives the greater surface areas.

The addition of ceria to zirconia stabilises the tetragonal phase of zirconia. The dilute preparation samples retards the onset of the monoclinic phase up to 1050°C. However, the standard coprecipitation prepared samples show trace amounts of monoclinic zirconia at temperatures as low as 700°C. The dilute preparation may produce a more disperse dopant in the bulk which can retard the onset of the tetragonal to monoclinic phase transformation. Impregnating ceria onto uncalcined zirconia (zirconium hydroxide) stabilises the tetragonal phase. During previous impregnation preparations of silica and lanthana on zirconia, the dopant was impregnated onto zirconium oxide and then recalcined to give the monoclinic phase. Therefore, tailoring the sample precursor before impregnation can determine the final phase obtained.

As expected the crystallite size of the samples increases with increasing calcination temperature. The crystallite sizes do not exceed Garvie's⁷ critical crystallite size of 30 nm, above which the tetragonal crystallites transform to monoclinic crystallites. For the 50wt% CeO₂/ZrO₂ samples, the crystallite sizes were smaller than the other samples, this may possibly be due to the system becoming close to a phase boundary or becoming two phases as opposed to simple nucleation and growth.

The coprecipitation and dilute coprecipitation preparations of ceria / zirconia produce a homogeneous mix of the dopant with zirconia, as can be observed by the precursor XPS results. 16, 20 and 50wt% CeO₂/ZrO₂ relates to 12, 15 and 42

mole % CeO₂/ZrO₂ and from XPS experiments to determine the Ce/Zr surface ratios for the precursor samples, the following ratios were determined 0.10, 0.16 and 0.41 respectively. Therefore, coprecipitation and dilute coprecipitation appear to produce a well mixed binary oxide before calcination. However, upon calcination, surface enrichment of the dopant is observed, as was the case for silica and lanthana doped zirconia. As was expected, the precursor for the impregnated 16wt% CeO₂/ZrO₂ had a high Ce/Zr surface ratio of 0.17, which increased with calcination temperature.

5.6 Conclusions

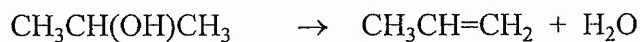
- 1 The addition of ceria to zirconia does not stabilise the surface area to the same extent as lanthana and silica as dopants.
- 2 The addition of silica does stabilise the tetragonal phase of zirconia up to 1050°C.

References

-
- ¹ S. J. Gregg and K. S. W. Sing, *Adsorption, Surface Area and Porosity*, Academic Press, London 2nd Edition 1982.
 - ² C. J. Norman, *Measurement Crystallite Size and Strain by X-ray line broadening*, Internal Report MEL Chemicals.
 - ³ H. Toraya, M. Yoshimura and S. Somiya, *J. Am. Ceram. Soc.*, 67 (1984) C-119.
 - ⁴ D. Briggs and M. P. Seah, *Practical Surface Analysis*, Wiley 1992.
 - ⁵ T. Settu and R. Gobithan, *Bull. Chem. Soc. Jpn.*, 67, (1994) p1999-2005.
 - ⁶ R. Franklin and R.W.Joyner, Unpublished results.
 - ⁷ R.C Garvie, *J. Phys. Chem.* 65 (1969) p1238.

6 Reactor Studies

Propan-2-ol decomposition is widely used to characterise the acid-base or redox properties of catalysts ^{1 2}. The two main routes of decomposition are to propene and acetone.



For propene formation three mechanisms are considered; (1) E₁ (Brønsted H⁺ site), (2) E₂ (acid - base pair site) and (3) E_{1cb} (concerted acid - base pair site). For acetone formation, two mechanisms are considered; (1) an alkoxy intermediate with abstraction of the H on C_α as the rate determining step and (2) the formation of an enolate intermediate with the abstraction of a H on C_β as the rate determining step.

6.1 Mechanisms for Decomposition

E₁ mechanism

The reacting molecule may undergo elimination reactions in which the formation of the carbocation is the rate determining step ³. A stable carbocation is formed upon the elimination of the hydroxyl group.

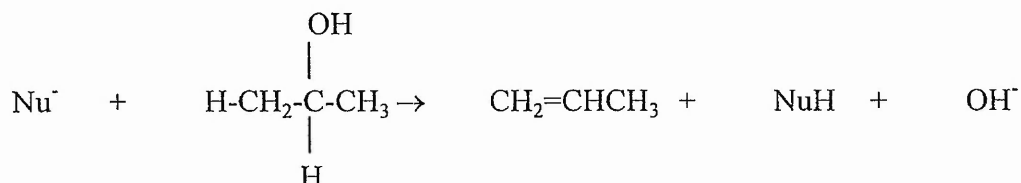


AOH is a Brønsted acid.

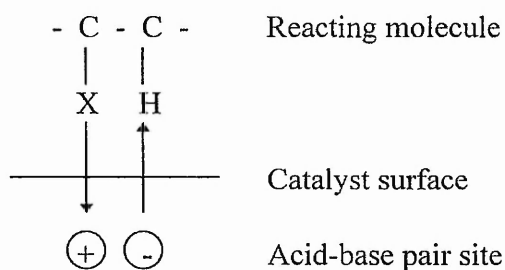
Generally it is tertiary alcohols which dehydrate to the alkene via the E₁ mechanism, due to the high stability of the intermediate carbocation. The E₁ mechanism requires strong acid sites, usually Brønsted sites.

E₂ mechanism

Both the reacting molecule and the nucleophile participate in the single step bimolecular elimination mechanism. A nucleophile removes one group as a group on the adjacent carbon departs.



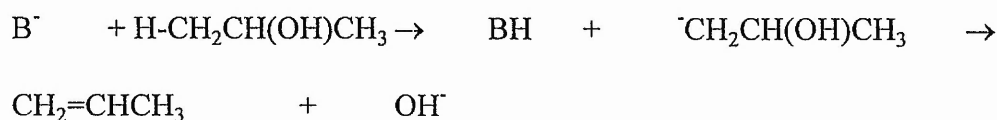
The nucleophile is commonly a base which abstracts a proton from C_β to the hydroxyl group. This works through an acid - base pair site. This E₂ mechanism has been described by Noller⁴ as an adsorbed structure on the catalyst surface, with the reaction taking place at the acid-base pair site.



X is the leaving group.

E_{1cb} mechanism

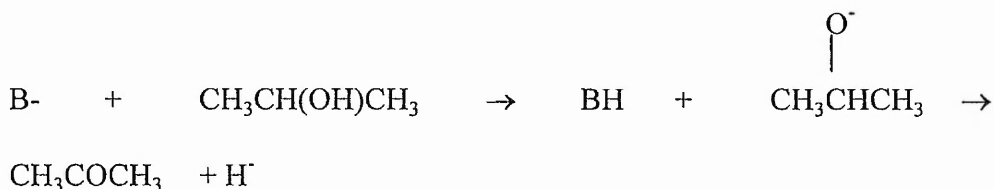
A base abstracts a H from the C_β to form a carbocation. Then the hydroxyl group departs to form the alkene. Again this is considered as an acid - base pair mechanism.



Knozinger ⁵ and Roca ⁶ investigated the dehydration of alcohols on alumina and silica in view of the above mechanisms. The E₁ mechanism was favoured. The reasons for this were; (1) the samples investigated had a low surface oxygen basicity which was not strong enough to initiate the proton abstraction from a C-H bond. This disfavoured the E₂ mechanism. (2) the bond dissociation energy for a heterolytic bond rupture of the C-H bond to form a carbanion (E_{1cb}) was considerably greater than that for the heterolytic bond breaking of the C-O bond, which leads to the formation of the carbocation (E₁). (3) the E₁ mechanism requires strong acid sites and Brønsted acid sites were observed due to surface hydroxyls.

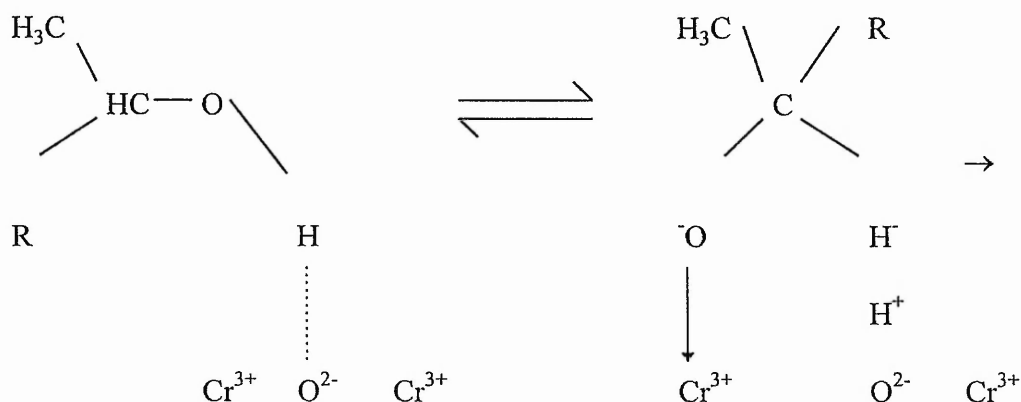
Alkoxy intermediate

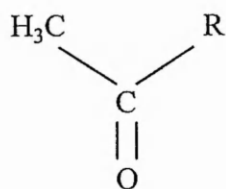
A base abstracts the H of the hydroxyl group forming the alkoxy intermediate. Subsequent removal of the H from C_α forms the ketone.



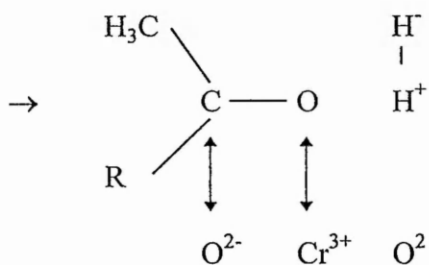
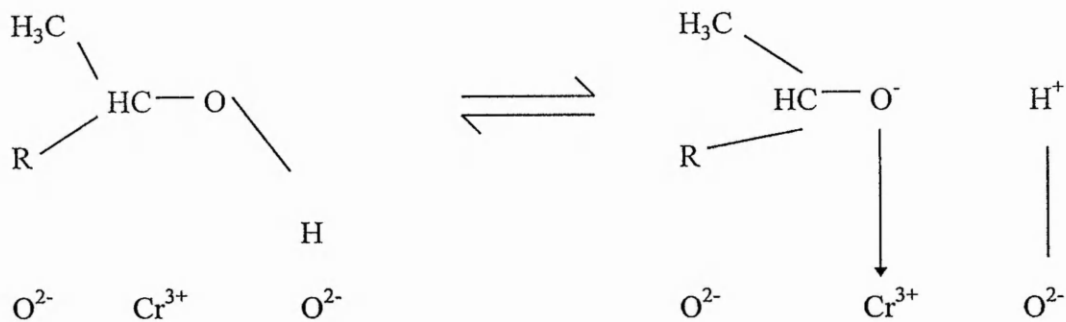
This mechanism has been investigated for the dehydrogenation of alcohols on chromia ⁷ and the following reaction schemes were proposed for the formation of acetone.

(1)



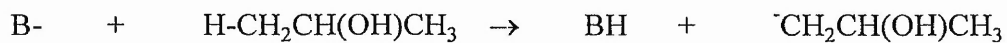


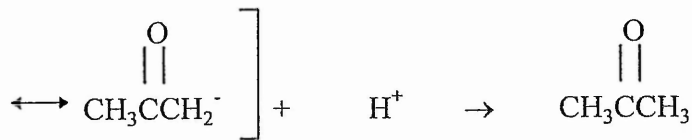
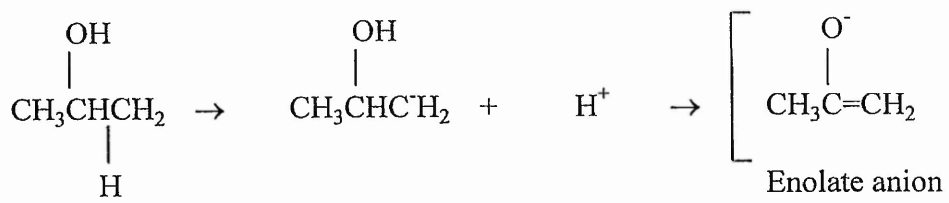
(2)



Enolate intermediate

A base abstracts a H from C_β to the hydroxide group, which leads to an enolate intermediate⁸.





Enolate anion

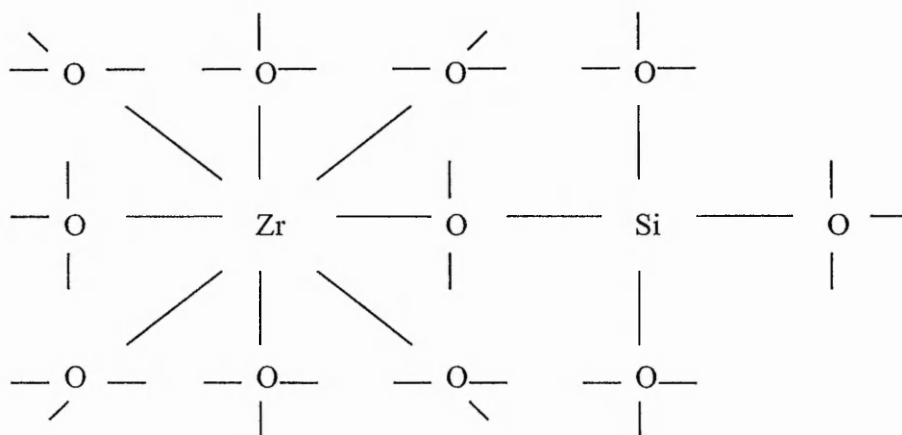
6.2 Binary Metal Oxide Acidity

Binary metal oxides such as $\text{SiO}_2\text{-Al}_2\text{O}_3$ are well known to possess surface acidity and have great use as solid acid catalysts⁹. Many other binary metal oxides may be expected to possess enhanced surface acidity relative to the single oxides. Attempts have been made to develop a hypothesis to predict which mixtures of oxides will form solid acid catalysts. The proposals by Charles Thomas¹⁰, Tanabe¹¹ and Kung¹², are the main hypotheses. The latter two hypotheses will be discussed and they attempt to predict the nature of the acidity, either Brønsted or Lewis acid sites.

Tanabe's hypothesis discusses acidity generated in a binary oxide in relation to the excess of negative or positive charge in the model structure of a binary oxide. The model structure is pictured according to the two postulates. Firstly, the coordination number of a positive element of a metal oxide and that of a second metal oxide are maintained even when mixing. Secondly, the coordination number of a negative element (oxygen) of a major component oxide is retained for all oxygens in a binary oxide. The hypothesis examines binary oxide systems alternating the major oxide, either silica being introduced to the zirconia matrix or the other way around. An overall excess of positive charge leads to an assumption of Lewis acidity and an overall negative charge leads to the assumption of Brønsted acidity. Summarising Tanabe's hypothesis gives, the coordination number of the cation in a mixture remains constant but the anion adapts the coordination of the host oxide.

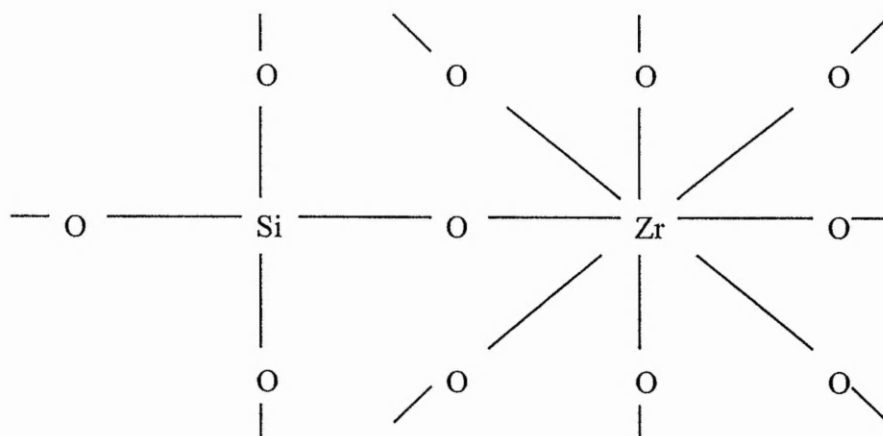
For the silica zirconia system assuming initially that zirconia was the major oxide, the following conclusions from Tanabe's hypothesis were made¹³. The silicon cation has formal charge of +4 and a coordination number of four with respect to oxygen. Whilst, the oxygen has a formal charge of -2 shared over four bond, leading to an overall charge of $4(+4/4-2/4) = +2$. The positive charge is associated with Lewis acidity.

SiO₂-ZrO₂ mixed oxide with silicon at zirconium rich site.



For a silica zirconia system assuming silica is the major oxide, the following conclusions from Tanabe's hypothesis were made. The zirconium cation has a valence of +4 shared over eight oxygen bonds. The oxygen has a valence of -2 shared over two bonds. Therefore, the overall charge is $8(+4/8 - 2/2) = -4$. The negative charge can be compensated with protons so Brønsted acidity might have been expected.

SiO₂-ZrO₂ mixed oxide with zirconium at silicon rich site



Kung's hypothesis is based on the formation of a dilute solid solution. The basis of the model employs both the electrostatic potential at the substituting cation site and the changes in the matrix necessary to balance the stoichiometry, to explain the formation and acid strength of the sites. The model involves the substitution of a metal ion A from oxide AO_y into the matrix of an oxide BO_z . The solid solution is assumed to be so dilute that adjacent A ions are far apart such that in the calculation of the electrostatic potential, the system is approximated by a single A ion in the BO_z matrix. Two outcomes are available related to the stoichiometry of the oxides. When $y = z$, there is a minimal effect on the matrix therefore, any new acidity is directly related to the electrostatic potential at the substituting ion site. When $y \neq z$, the new acidity is related to the changes in the matrix and the electrostatic potential at the substituting ion site.

The difference in the electrostatic potential ΔV , of A in the matrix BO_z and AO_y is given by

$$\Delta V = \sum_i (q_i/r_i)_{BO} - \sum_i (q_i/r_i)_{AO}$$

Where q_i equals the charge of the ion at distance r_i from the A site, in the relative matrices BO and AO. Kung continued to simplify the above equation by assuming the A site was in a three dimensional infinite solid and q_i was taken as the formal charge q_i^F , the summations were the lattice self potentials V^F at the substituting cation site. Therefore, the above was rewritten as

$$\Delta V = (V^F q_i/q_i^F)_{BO} - (V^F q_i/q_i^F)_{AO}$$

If ΔV is negative, ion A in BO_z experienced a more negative potential than in AO_y . Therefore, it will be more electrostatically stable and would more readily accept electrons. It will act as a Lewis acid site. If ΔV is positive, A will less readily accept electrons in BO_z . It will act as a Lewis base site. If q_i/q_i^F was similar in the two matrices then the sign of ΔV is determined by the lattice self potentials (V^F) for the two matrices. Therefore, it will act as a Lewis acid site if the lattice self potential of AO_y was less negative than that of BO_z .

The change in the matrix is minimal when $y = z$. However, when $y < z$, a substitution of a B ion by an A ion will result in an excess of oxygen. This excess can be balanced by the development of anion vacancies or adsorption of hydrogen at the surface or development of interstitial cation defects. The first two possibilities can occur if the sample was prepared by aqueous precipitation forming hydroxyls and upon heating the formation of anion vacancies can lead to acidity. The development of interstitial cation defects depends on the material used and is therefore, more difficult to predict.

When $y > z$. The substitution of a B ion by an A ion will result in a deficiency in oxygen. This can be removed by adsorption of negatively charged oxygen species or adsorption of OH^- or by the presence of cation vacancies. In the first two cases new acidity is not expected to develop since adsorbed oxygen and OH^- are not expected to be acidic. However, in the case of cation vacancies, Lewis acid sites could appear due to electron deficient cation vacancies.

Kung summarised his results in the following table.

6.2 Table 1 *Formation of new acid sites.*

Case	At Substituting Ion	In Matrix	
	Lewis Acid	Brønsted Acid	Lewis Acid
$y < z$	Yes	Yes	Possible
$y = z$	Yes*	No	No
$y > z$	No	No	Possible

* only if BO_z has a lower lattice self potential than AO_y .

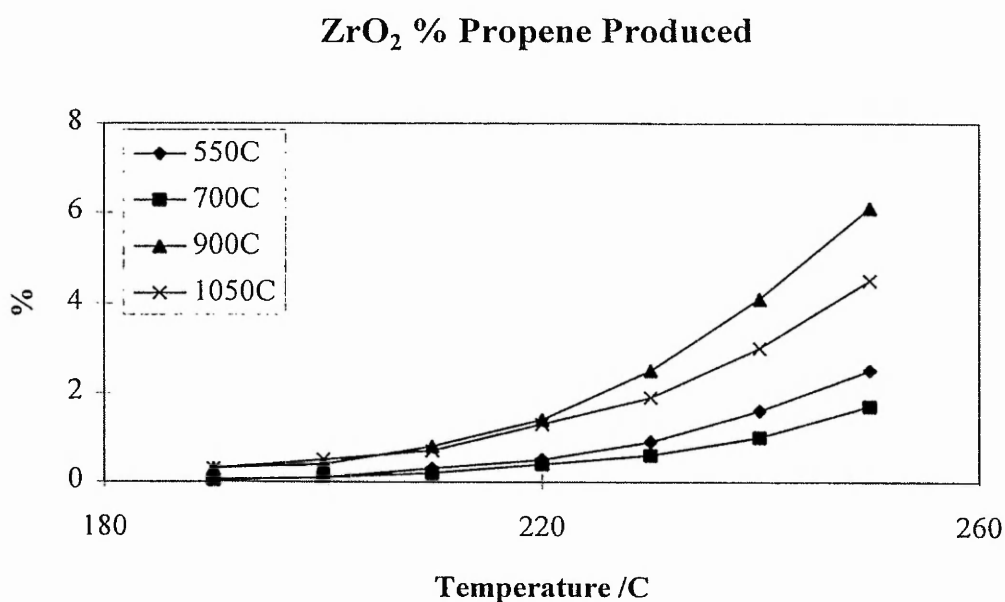
For a silica doped zirconia system, Kung's hypothesis suggests that no acidity would be generated since silica has a more negative lattice self potential than zirconia. However, it does predict that zirconia doped silica should form new acid sites. Tananbe's model suggested that silica doped zirconia should generate Lewis acid sites and Thomas' hypothesis stated that the silica zirconia system would be acidic but the greatest acidity would occur when Si/Zr ratio was 2.

6.3 Reactor Studies Results

6.3.1 Zirconia results

The decomposition of propan-2-ol over zirconia catalysts was found to yield 100% selectivity to propene. The temperature range of the decomposition was 190 to 250°C and the conversions were kept below approximately below 10% to allow the application of differential kinetics and the calculation of activation energies¹⁴ unaffected by mass transfer considerations, for the production of propene.

6.3.1 Graph 1 % conversion to propene for zirconia catalysts.



6.3.1 Table 1 Activation energies for the production of propene from propan-2-ol.

Temp. / °C	Activation Energy kJmol ⁻¹	LnA
550	122	17.6
700	123	17.5
900	107	15.0
1050	92	11.2

The activation energy decreases with increasing calcination temperature.

6.3.1 Table 2 *Normalising the conversion to propene for surface area of ZrO₂*

Temp. / °C	Normalised conversion	Normalised Conversion
	220°C	250°C
550	0.008	0.042
700	0.015	0.065
900	0.093	0.407

Upon normalising for surface area, the conversion to propene increases with calcination temperature.

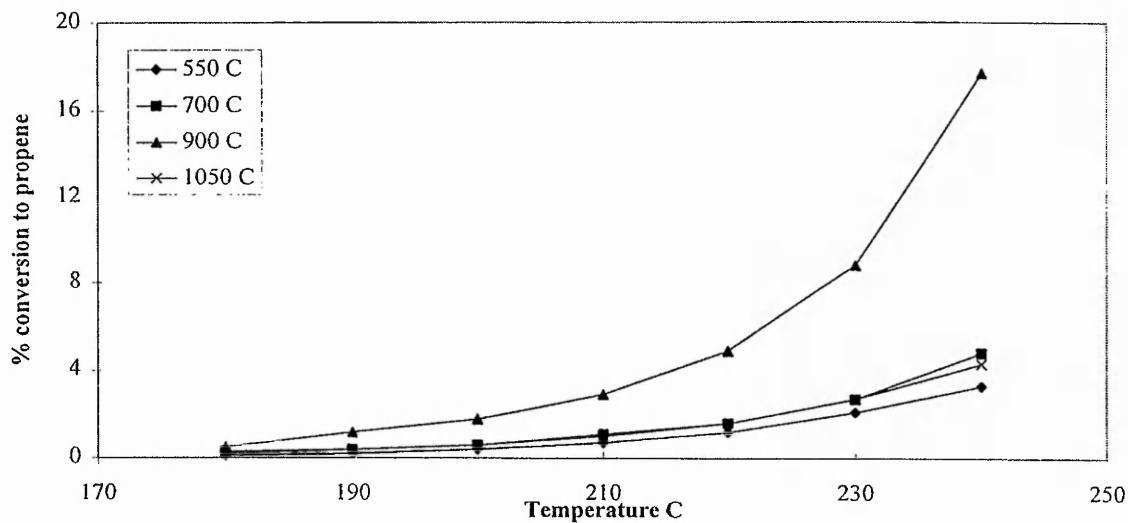
The activation energy for the production of propene from propan-2-ol for pure zirconia, decreases with increasing calcination temperature. The conversion to propene normalised for surface area increases with increasing calcination temperature, indicating more activity per unit area. Therefore, there are more active sites for the dehydration of propan-2-ol per m² as the calcination temperature is raised.

6.3.2 Silica Zirconia Coprecipitated Results

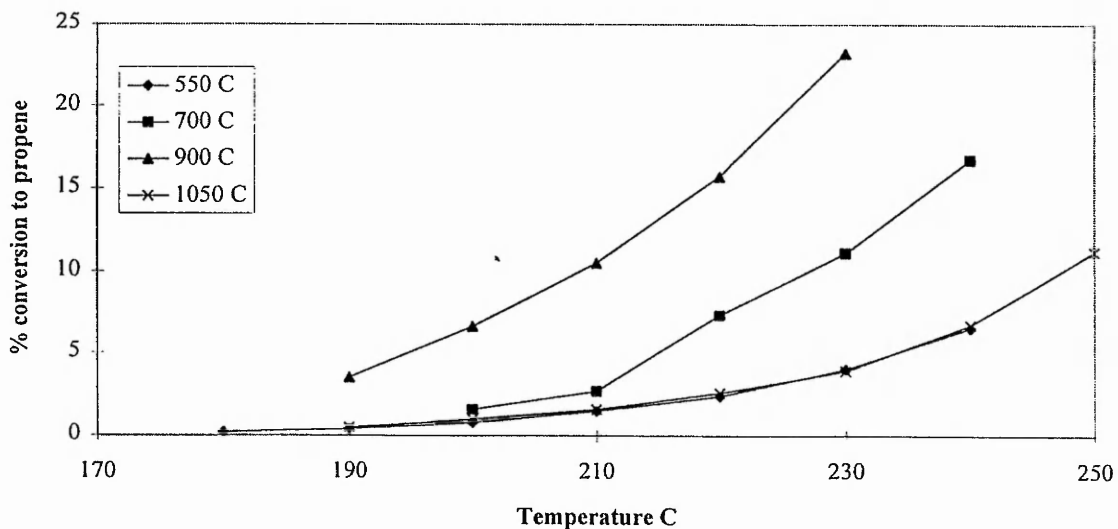
The decomposition of isopropanol over silica coprecipitated zirconia produced propene as the major product, with some acetone being produced in the samples calcined at the highest temperature.

6.3.2 Graphs 1, 2, 3 and 4 Conversion to propene for silica coprecipitated zirconia catalysts.

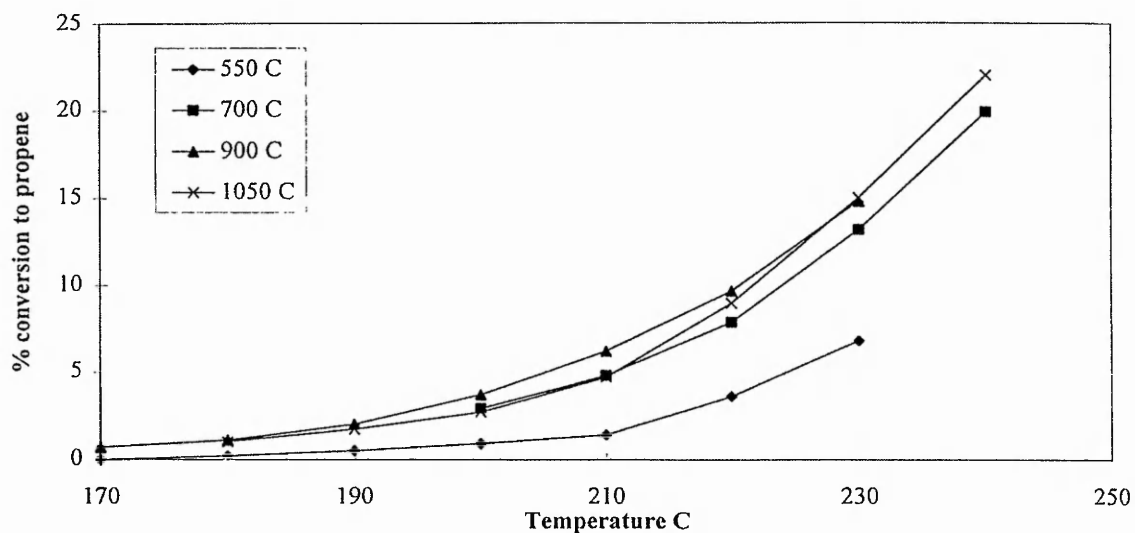
3.5wt% SiO₂/ZrO₂ pH 10 rising conversion to propene



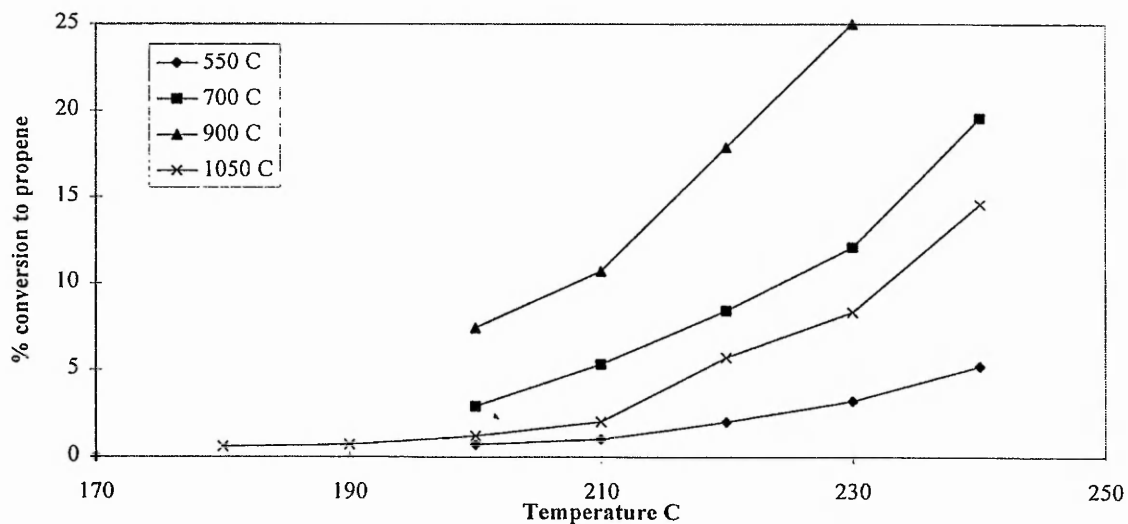
3.5wt% SiO₂/ZrO₂ pH 11 rising conversion to propene



3.5wt% SiO₂/ZrO₂ pH 11 constant conversion to propene



3.5wt% SiO₂/ZrO₂ pH 10 constant conversion to propene



In all four sets of samples, the catalysts calcined at 900°C give the greatest conversion to propene, as was also the case for pure ZrO₂.

6.3.2 Table 1 *3.5wt%SiO₂/ZrO₂ coprecipitation samples activation energies (kJ mol⁻¹) for the dehydration of propan-2-ol.*

Temperature °C	pH = 10.0 rising	pH = 11.3 rising	pH = 10.0 constant	pH = 11.3 constant
550	113	112	107	117
700	99	101	98	103
900	104	102	92	96
1050	93	96	94	91

The activation energies for the decomposition of propan-2-ol to propene generally decrease with increasing calcination temperature.

6.3.2 Table 2 *Normalisation of conversion to propene at 220°C for surface area.*

Temperature °C	pH = 10.0 rising	pH=11.3 rising	pH=10.0 constant	pH=11.3 constant
550	0.02	0.04	0.02	0.03
700	0.03	0.08	0.12	0.20
900	0.19	0.51	0.72	0.45
1050	0.17	0.54	0.94	1.00

The conversion at 220°C was divided by the BET surface area of the sample, then the results were normalised to the highest, which was for the catalyst prepared at pH 11.3 constant and calcined at 1050°C. It can be observed that the normalised activity increases with calcination temperature as in the case of pure zirconia.

As was observed in the case of pure zirconia, the activation energy for the production of propene from the dehydration of propan-2-ol, generally decreases with increasing calcination temperature for 3.5wt% SiO₂/ZrO₂ samples prepared by coprecipitation. At the highest calcination temperature, 1050°C, all the samples

including pure zirconia, have a similar activation energy. However, at the lower calcination temperatures of 550 and 700°C, pure zirconia has considerable higher activation energies than the silica-zirconia samples.

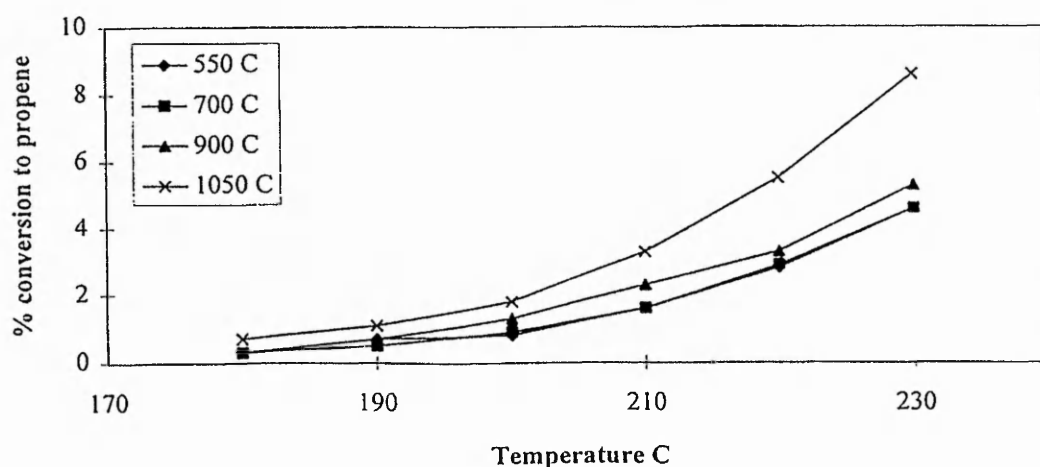
Normalising the conversions for surface area, gives an increasing conversion with sample calcination temperature. Pure zirconia calcined at 900°C, and at the reaction temperature of 240°C has a conversion to propene less than 5% whereas, all the silica zirconia samples calcined at 900°C at the same reaction temperature have a conversion greater than 15%. When these silica-zirconia samples are corrected for their greater surface area than zirconia, they still have a greater conversion to propene. Silica zirconia samples calcined at 550°C show greater conversions to propene than pure zirconia calcined at 900°C over the reaction temperature range. Therefore, the addition of silica increases the surface acidic nature of the system.

6.3.3 Silica Impregnated Results.

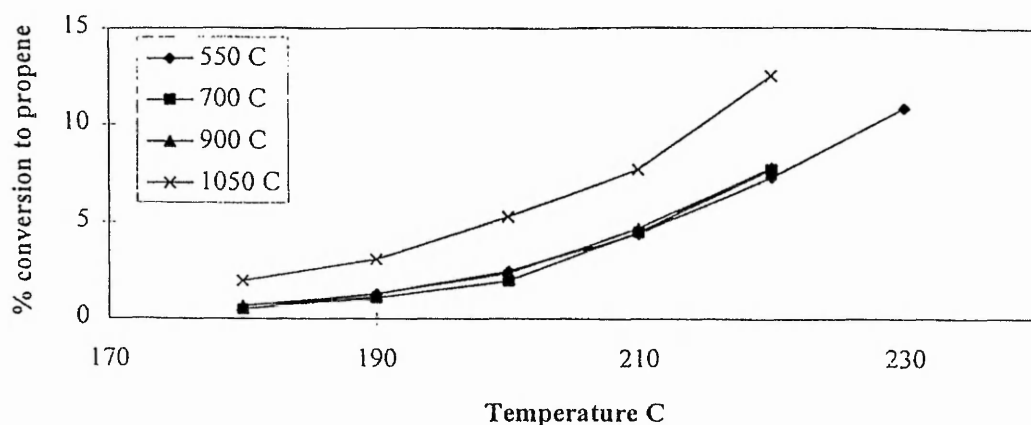
The decomposition of propan-2-ol over silica impregnated on zirconia resulted in the production of propene and trace amounts of acetone.

6.3.3 Graphs 1 and 2 Conversion to propene for silica impregnated zirconia samples.

3.5wt% SiO₂/ZrO₂ impregnated conversion to propene



5wt% SiO₂/ZrO₂ impregnated conversion to propene



In both sets of samples the conversion to propene remains approximately constant with respect to calcination temperature up to 900°C. However, at 1050°C the conversion greatly increases. The 5wt% SiO₂/ZrO₂ samples show greater conversions than the lower loading of dopants for the same calcination temperatures.

6.3.3 Table 1 *Activation Energies for production of propene for silica impregnated zirconia catalysts.*

Calcination Temperature °C	3.5 %SiO ₂ /ZrO ₂	5wt% SiO ₂ /ZrO ₂
550	136	115
700	106	121
900	107	123
1050	97	98

The activation energies generally decrease with increasing calcination temperature.

6.3.3 Table 2 *Silica impregnated zirconia normalised conversions at 220°C, after correction for surface area.*

Calcination Temperature °C	3.5 wt% SiO ₂ /ZrO ₂	5wt% SiO ₂ /ZrO ₂
550	0.037	0.097
700	0.041	0.100
900	0.057	0.113
1050	0.780	1.000

The normalised conversions are similar up to 900°C, where a great increase occurs at 1050°C.

For the silica impregnated zirconia samples, the activation energies for the production of propene from the dehydration of propan-2-ol generally decrease with increasing calcination temperature. For the relative amounts of silica doped, the samples calcined at 700 and 900°C have very similar activation energies.

The conversion to propene remains similar up to 900°C calcination temperature in both systems, but at the highest calcination temperature, 1050°C, the conversion increases greatly (see **6.3.3. graphs 1 and 2**). This can be related to the properties of silica impregnated zirconia where, up to 900°C, the surface area, phase, crystallite size and surface Si/Zr ratio remain constant (Chapter 4). However, at 1050°C, the surface area decreases, the crystallite size increases, the phase changes and the Si/Zr surface ratio increases.

Increasing the amount of dopant from 3.5 to 5wt% increases the conversion to propene. However, the conversion for impregnated silica on zirconia are lower than for coprecipitated silica zirconia but higher than for pure zirconia. At reaction temperature of 210°C, 3.5wt% impregnated SiO₂/ZrO₂ calcined at 900°C has a conversion to propene of 2.3%, pure zirconia at 900°C has a conversion of 1.4 % and 3.5wt% coprecipitated zirconia at 900°C has a conversion of 10%.

Upon normalising the conversion for surface area, the samples calcined at 1050°C are far more acidic than the rest, showing high conversions and low surface areas.

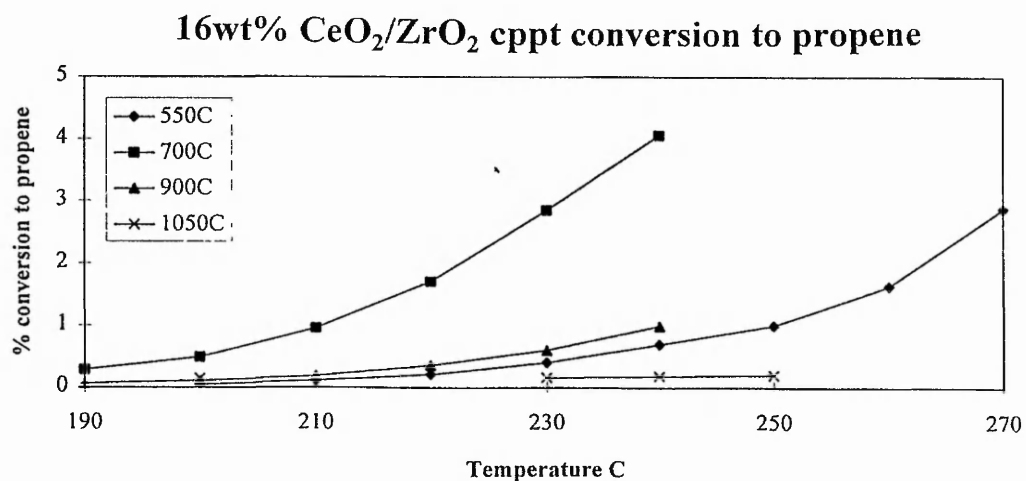
6.3.4 Ceria doped Zirconia Results

The decomposition of propan-2-ol over ceria-zirconia catalysts gave propene as the major product with trace amounts of acetone and propane being produced.

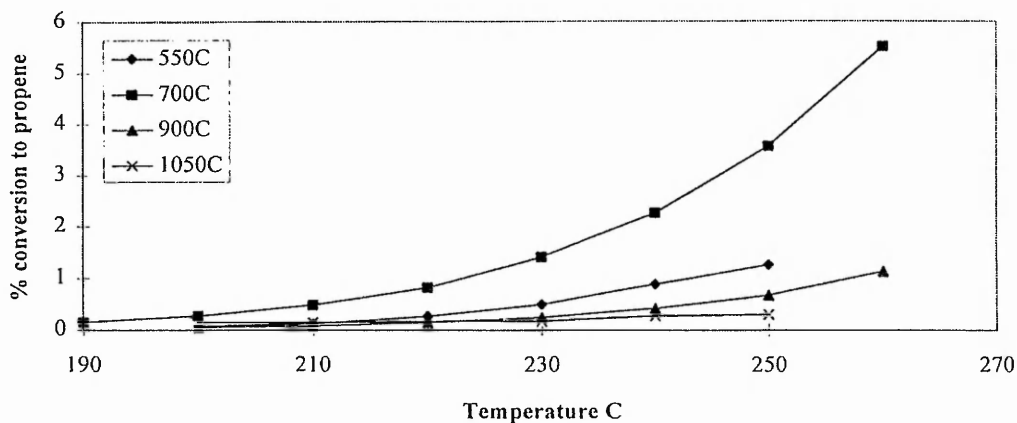
6.3.4 Table 1 Activation energies (kJ mol^{-1}) for production of propene for ceria-zirconia catalysts.

Temp./ $^{\circ}\text{C}$	16wt%	16wt% dilute	20wt%	20w% dilute	50wt%	50wt% dilute
550	121	130	125	137	87	110
700	106	98	107	108	125	125
900	113	107	112	104	113	121

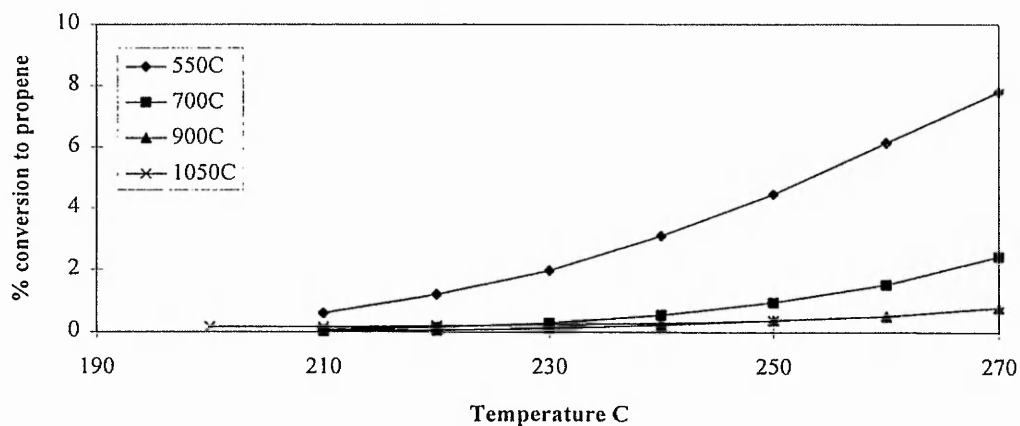
6.3.4 Graphs 1 to 6 Production of propene over varying ceria - zirconia catalysts.



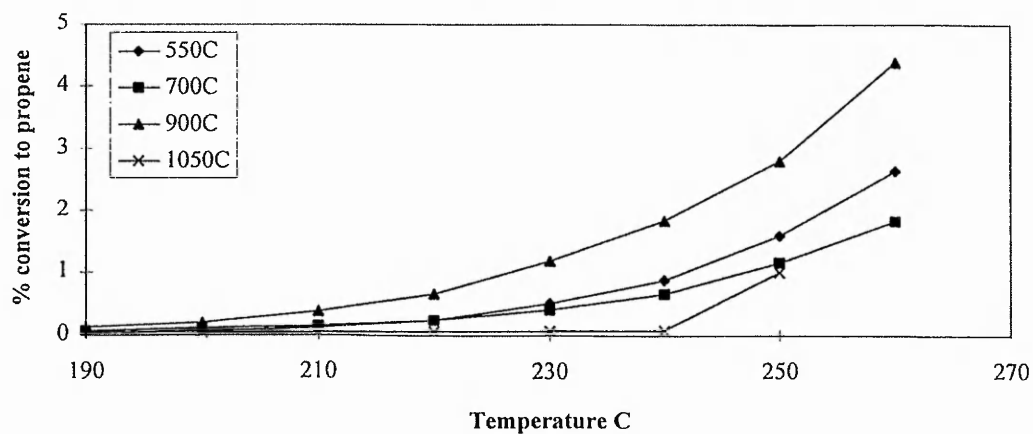
20wt% CeO₂/ZrO₂ cppt conversion to propene



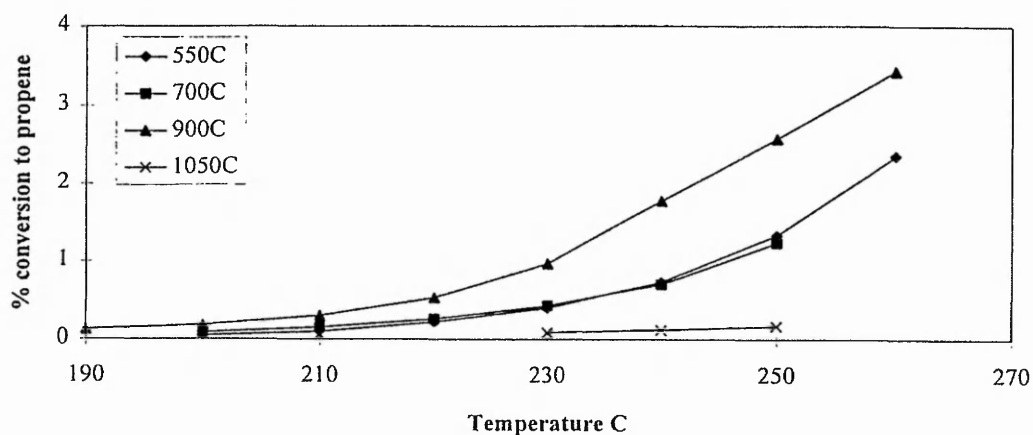
50wt% CeO₂/ZrO₂ cppt conversion to propene



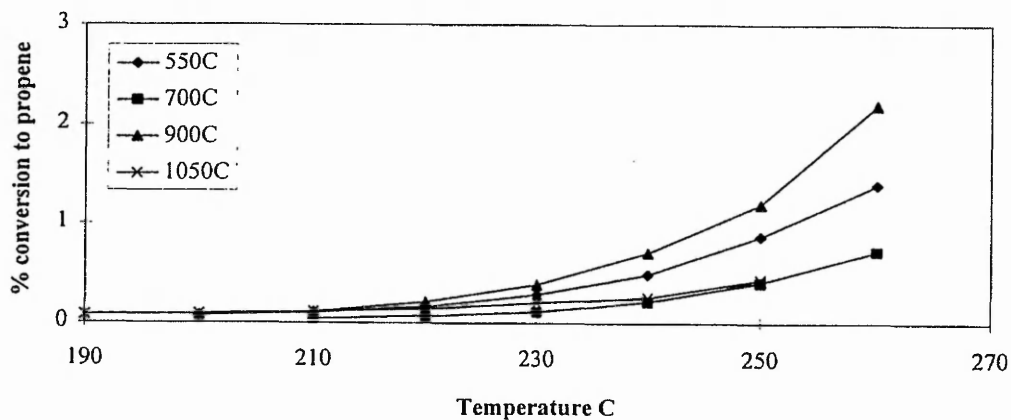
16wt% CeO₂/ZrO₂ cppt dilute conversion to propene



20wt% CeO₂/ZrO₂ cppt dilute conversion to propene



50wt% CeO₂/ZrO₂ cppt dilute conversion to propene



6.3.4 Graph 2 Conversion to propene normalised for surface area for ceria - zirconia catalysts at reaction temperature of 240°C.

Temp. °C	16wt%	16wt% dilute	20wt%	20wt% dilute	50wt%	50wt% dilute
550	0.013	0.012	0.014	0.013	0.079	0.009
700	0.203	0.018	0.066	0.024	0.037	0.007
900	0.167	0.097	0.041	0.198	0.042	0.240

For the $\text{CeO}_2/\text{ZrO}_2$ prepared from dilute systems, the samples calcined at 900°C give the greatest conversions to propene. Whereas, for $\text{CeO}_2/\text{ZrO}_2$ the samples calcined at 700°C give the greatest conversion except for 50wt% $\text{CeO}_2/\text{ZrO}_2$ at which the sample calcined at 550°C gives the greatest conversion. This sample has a low surface area similar to those calcined at 700°C . It can be noticed from all the graphs that the conversions by the highest calcination temperature samples, 1050°C , are extremely low. However, these samples have very low surface areas $<3 \text{ m}^2\text{g}^{-1}$ (see Chapter 5).

For the ceria- zirconia system, the samples with the highest conversions have the lowest activation energies for the production of propene from propan-2-ol. However, this is not the case for the ceria - zirconia dilute system. The normalised conversion for the ceria - zirconia dilute system increases with increasing calcination temperature. However, for the ceria - zirconia system it is the samples with the largest conversions which also show the largest normalised conversions.

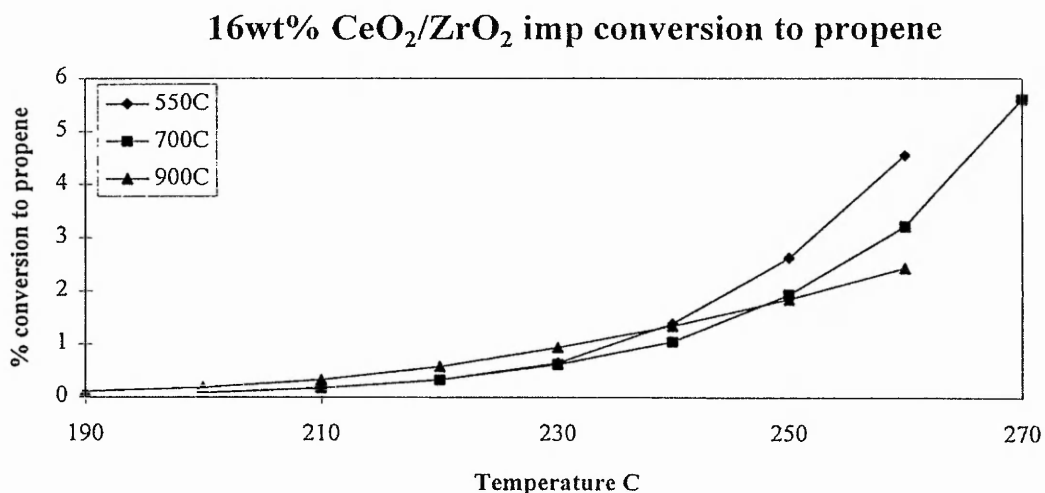
The ceria - zirconia and ceria - zirconia dilute samples are less active in the dehydration of propan-2-ol to propene than pure zirconia and silica - zirconia catalysts.

Trace amounts of propane and acetone were observed as minor products in the decomposition of propan-2-ol. The production of propane occurred in 16% and 20% $\text{CeO}_2/\text{ZrO}_2$ calcined at 700 and 900°C and 16% and 20% $\text{CeO}_2/\text{ZrO}_2$ dilute calcined at 700 and 900°C . The production of acetone releases hydrogen. The production of the hydrogen may be able to reduce the alkene to the alkane in the presence of the catalyst. Ceria is known to possess redox properties with Ce^{4+} and Ce^{3+} being stable¹⁵. Also, ceria can chemisorb hydrogen¹⁶. Therefore, the ceria - zirconia surface does possess the ability to dehydrogenate propan-2-ol to acetone, chemisorb hydrogen and possibly hydrogenate propene to propane.

6.3.5 Impregnated Ceria - Zirconia Results

The decomposition of propan-2-ol over ceria - zirconia samples prepared by impregnation produced propene only.

6.3.5 Graph 1 Production of propene over ceria impregnated zirconia catalysts.



The conversions to propene are low as in the coprecipitated samples, with the sample calcined at 550°C showing the greatest conversion.

6.3.5 Table 1 Activation energies and conversions normalised for surface area for 16% ceria impregnated zirconia samples.

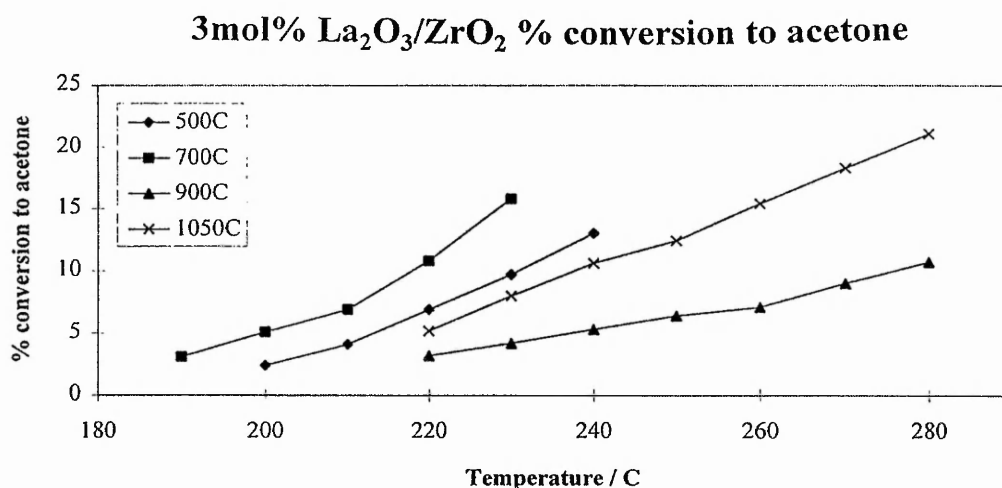
Temp./°C	Activation Energy kJmol ⁻¹	Normalised conversion at 240°C
550	145	0.19
700	132	0.36
900	94	1.00

The activation energies decrease and the normalised conversions increase with increasing calcination temperature for ceria impregnated zirconia.

6.3.6 Lanthana

The decomposition of propan-2-ol over lanthana - zirconia catalysts produced the dehydrogenation product acetone as the major product and propene as a minor product¹⁷.

6.3.6 Graph 1 Conversion to acetone for lanthana zirconia samples



The sample calcined at 700°C has the greatest conversion to acetone.

6.3.6 Table 1 Activation energies and normalised conversion for lanthana doped zirconia.

Temp./°C	Activation Energies kJmol ⁻¹	Normalised conversion at 230°C
550	88	0.18
700	83	0.39
900	44	0.19
1050	74	1.00

For lanthana doped zirconia the activation energy decreases and normalised conversion increases with increasing calcination temperature, except for the sample calcined at 900°C. The sample calcined at 900°C has a low conversion to acetone, which does not increase a great deal with temperature, hence the low activation energy.

6.4 Silica Zirconia Acidity

The addition of silica as a dopant to zirconia has increased the surface acid nature of the catalyst, as shown in the decomposition of propan-2-ol to propene. From Kung, Thomas and Tanabe's hypotheses for the prediction of acidity in mixed oxides, only one hypothesis did not predict enhanced acidity for silica doped zirconia. This was Kung's, however, he predicts enhanced acidity if zirconia is doped on silica.

From the combined infrared and pyridine adsorption experiments, only Lewis acid sites were observed on the mixed oxide surface. Brønsted acidity was not observed, indicating the lack of surface hydroxyls involved in the acidity. Tanabe's hypothesis predicted the presence of only Lewis acid sites in the silica zirconia system.

Lewis acid sites on the surface are considered to be exposed metal ions¹⁸. Cox¹⁹, defines Lewis acidity as depending on the existence of exposed metal cations at the surface, having empty orbitals and positive charges that can interact with filled orbitals and or negative charges or dipoles of donor molecules. Lewis acid strength depends upon the ion charge, the degree of coordinative unsaturation and the availability of empty orbitals. The production of Lewis acid sites is performed by dehydroxylating the surface²⁰, removal of OH groups.

The dehydration of propan-2-ol to propene can proceed via three mechanisms, E₁, E₂ and E_{1cb}. The E₁ mechanism involves Brønsted acid sites. Therefore, in the case of silica zirconia catalysts from the infrared studies, the E₁ mechanism can be

discarded. The mechanism for dehydration can proceed via E_2 and or E_{1cb} , which both involve acid base pair sites. The two mechanisms are similar with E_2 being a single step dehydration and E_{1cb} being a two step dehydration.

Concluding, the addition of silica to zirconia enhances the surface acidity compared to the single oxide of zirconia. The nature of the acidity is Lewis acid sites and the dehydration of propan-2-ol proceeds via the E_2 and or E_{1cb} mechanisms.

6.5 Conclusions

(1) Silica as a dopant increases the surface acidity relative to pure zirconia. The normalised conversions for the production of propene increased with calcination temperature. The dehydration of propan-2-ol must proceed via an E_2 or E_{1cb} mechanism.

(2) Lanthana as a dopant increases the surface basicity relative to pure zirconia. The normalised conversions for the production of acetone increased with calcination temperature

(3) Ceria as a dopant suppresses the surface reactivity and has a lower activity than pure zirconia.

References

¹ A. Ouquour, G. Coudurier and J. C. Vedrine, *J. Chem. Soc. Faraday Trans.*, 89 [16], (1993) p3151-3155.

² M. Rutherford, Ph. D. Thesis, Liverpool University, 1995.

³ S. H. Pine, *Organic Chemistry*, McGraw-Hill 5th Edition 1988.

⁴ H. Vinek, H. Noller, M. Ebel and K. Schwarz, *J. Chem. Soc., Faraday Trans. 1*, [73], (1977) p734.

⁵ H. Knozinger and A. Scheglila, *J. Catal.*, 17, (1970) p252.

-
- ⁶ F. Figueras-Roca, L. de Morgues and Y. Trambouze, *J. Catal.*, 14, (1969) p107.
- ⁷ L. Nondek and J. Sedlacek, *J. Catal.*, 40, (1975) p34.
- ⁸ K. Tomke, *Z. Phys. Chem., N. F.*, 106, (1977) p225.
- ⁹ K. Tanabe, *Solid Acids and Bases*, Academic Press, (1970).
- ¹⁰ C. L. Thomas, *Ind. Eng. Chem.*, 41, (1949) p2564.
- ¹¹ K. Tanabe, T. Sumiyoshi, K. Shibata, T. Kiyoura and J. Kitagawa, *Bull. Chem. Soc. Jpn.*, 47, (1974) p1064.
- ¹² H. H. Kung, *J. Solid State Chemistry* 52, (1984) p191.
- ¹³ H. J. M. Bosman, Ph.D. Thesis, Technische Universiteit Eindhoven, p1995.
- ¹⁴ P. W. Atkins, *Physical Chemistry*, Oxford University Press 1989.
- ¹⁵ H. Cordatos, T. Bunluesin, J. Stubenrauch, J. M. Vohs and R. J. Gorte, *J. Phys. Chem.*, 100, (1996) p785-789.
- ¹⁶ S. Bernal, J. J. Calvino, G. A. Cifredo, J. M. Gatica, J. A. Perez Omil and J. M. Pintado, *J. Chem. Soc. Faraday Trans.*, 89[18], (1993) p3499-3505.
- ¹⁷ R. Franklin and R. W. Joyner, Unpublished Results.
- ¹⁸ B. G. Gates, *Catalytic Chemistry*, Wiley 1992.
- ¹⁹ P. A. Cox, *Surface Science of Metal Oxides*, Cambridge 1994
- ²⁰ Satterfield, *Heterogeneous Catalysis in Industrial Practice*, 1987.

Appendix Activation energies and pre-exponential factors

3.5wt% SiO₂/ZrO₂ impregnated activation energies and pre-exponential factors

Temperature °C	E _a kJ mol ⁻¹	LnA
550	136	22.5
700	106	15.4
900	107	15.9
1050	97	14.0

5wt% SiO₂/ZrO₂ impregnated activation energies and pre-exponential factors

Temperature °C	E _a kJ mol ⁻¹	LnA
550	115	18.7
700	121	19.8
900	123	20.3
1050	98	14.7

3mole % La₂O₃/ZrO₂ coprecipitated activation energies and pre-exponential factors

Temperature °C	E _a kJ mol ⁻¹	LnA
550	88	11.9
700	83	10.3
900	44	5.0
1050	74	8.3

3.5wt% SiO₂/ZrO₂ pH =10.0 rising activation energies and pre-exponential factors

Temperature °C	E _a kJ mol ⁻¹	LnA
550	113	16.8
700	99	14.3
900	104	15.9
1050	93	13.5

3.5wt% SiO₂/ZrO₂ pH =10.0 constant activation energies and pre-exponential factors

Temperature °C	E _a kJ mol ⁻¹	LnA
550	107	15.7
700	98	14.5
900	92	13.4
1050	94	14.1

3.5wt% SiO₂/ZrO₂ pH =11.3 rising activation energies and pre-exponential factors

Temperature °C	E _a kJ mol ⁻¹	LnA
550	112	16.8
700	101	14.3
900	102	14.6
1050	96	13.6

3.5wt% SiO₂/ZrO₂ pH =11.3 constant activation energies and pre-exponential factors

Temperature °C	E _a kJ mol ⁻¹	LnA
550	117	18.4
700	103	15.9
900	96	13.4
1050	91	13.2

16wt% CeO₂/ZrO₂ coprecipitated activation energies and pre-exponential factors

Temperature °C	E _a kJ mol ⁻¹	LnA
550	121	16.5
700	106	14.8
900	113	15.2

20wt% CeO₂/ZrO₂ coprecipitated activation energies and pre-exponential factors

Temperature °C	E _a kJ mol ⁻¹	LnA
550	125	17.6
700	107	14.5
900	112	14.0

50wt% CeO₂/ZrO₂ coprecipitated activation energies and pre-exponential factors

Temperature °C	E _a kJ mol ⁻¹	LnA
550	87	10.0
700	125	17.2
900	113	13.4

16wt% CeO₂/ZrO₂ impregnated activation energies and pre-exponential factors

Temperature °C	E _a kJ mol ⁻¹	LnA
550	145	22.9
700	132	19.5
900	94	10.9

16wt% CeO₂/ZrO₂ dilute coprecipitated activation energies and pre-exponential factors

Temperature °C	E _a kJ mol ⁻¹	LnA
550	130	18.8
700	98	11.1
900	107	14.2

20wt% CeO₂/ZrO₂ dilute coprecipitated activation energies and pre-exponential factors

Temperature °C	E _a kJ mol ⁻¹	LnA
550	137	20.3
700	108	13.6
900	104	13.4

50wt% CeO₂/ZrO₂ dilute coprecipitated activation energies and pre-exponential factors

Temperature °C	E _a kJ mol ⁻¹	LnA
550	110, 13.6	13.6
700	125, 16.4	16.4
900	121, 16.5	16.5

Zirconia activation energies and pre-exponential factors.

Temperature °C	E_a kJmol ⁻¹	LnA
550	122	17.6
700	123	17.5
900	107	15.0
1050	92	11.2

7. Discussion of characterisation and reactor studies

The addition of dopants to zirconia is intended to stabilise the surface area of the oxide. However, upon increasing the calcination temperature the surface area still decreases as would be expected¹. For pure zirconia the surface area drops from 109 to 15 m²g⁻¹ over the temperature range 400 to 900°C, whereas the surface area of 3.5 wt% SiO₂/ZrO₂ drops from 169 to 38 m²g⁻¹ over the same temperature range. For the majority of samples prepared by coprecipitation, the XRD data shows that increasing the calcination temperature results in a highly crystalline phase. The crystallite size of 3.5 wt% SiO₂/ZrO₂ increases from 14 to 27 nm over the temperature range 550 to 1050°C. One exception is 50wt% CeO₂/ZrO₂ where the pattern looks broad and there is a possibility of phase separation in the system at higher calcination temperatures of 900 to 1050°C. For silica and lanthana, as dopants, no monoclinic phase is observed at the highest calcination temperatures, whereas at lower calcination temperatures a small amount of monoclinic phase is observed due to the incomplete stabilisation of the tetragonal phase. The ceria doped materials contain monoclinic zirconia at high temperatures, indicating that ceria is not as effective at stabilising the tetragonal phase as the other dopants used, however the amount of amorphous material does not exceed 10% at the highest calcination temperature. Generally for the coprecipitation methods, increasing the calcination temperature increases the crystallinity of the samples and the amount of tetragonal phase. The increased crystallinity is observed by the reduction in the amorphous background and increased sharp peak size, indicating long range order.

For impregnated samples, the monoclinic phase is stabilised up to 900°C when the dopant is impregnated onto zirconia, as in the case for samples prepared in the presence of silica and lanthana. Above 900°C the tetragonal phase is dominant. The monoclinic phase content for 3.5wt% impregnated SiO₂/ZrO₂ decreases from 96 to 26 % over the temperature range 550 to 1050°C. This is due to zirconia calcined at 500°C already being in the monoclinic phase and when the dopants are impregnated and recalcined the bulk structure is already formed and is monoclinic. The dopant is on the

surface as is observed from the XPS results. However, when the dopant is impregnated into zirconium hydroxide the tetragonal phase remains the major phase over the calcination range, but the monoclinic phase can be observed. This applies when ceria is used as the dopant. Zirconium hydroxide is amorphous and when calcined with the dopant, the tetragonal phase is stabilised. From the XPS results for 16wt% CeO₂/ZrO₂ prepared by impregnation and coprecipitation, the calcined results are similar, the surface ratios of Ce/Zr for the impregnated sample increase from 0.11 to 0.21 over the temperature range 550 to 1050°C, and the coprecipitated sample increases from 0.10 to 0.22 over the same temperature range. Therefore, coprecipitation and impregnation onto the hydroxide yield the tetragonal phase and have similar surface concentrations of ceria. The two preparation routes produce similar samples.

For all the doped materials produced by coprecipitation the amount of dopant observed on the surface, by XPS, increases with calcination temperature. Results for silica doped zirconia samples can be better understood by referring to the XRD results. A shift in peak position of an XRD peak is caused by a change in the cell volume. The cell volume relates to the d-spacing in the system, and from the Bragg equation the d-spacing is related to the peak position (angle)². A dopant metal ion which is not the same or of similar size to that of the zirconia host ion migrating out of the lattice to the surface region causes a change in the bulk cell volume which results in a change in the position of the peak. For an atom smaller than zirconium (i.e. silicon) the peak shift will be to lower 2θ. For pure tetragonal zirconia the measured (111) tetragonal peak is at 2θ = 30.3°, when Cu K_α radiation is used. For the silica doped samples calcined from 700 to 1050°C, the tetragonal (111) peak shifts from 30.6° to 30.4°. As the calcination temperature is increased the peak position moves closer to that of pure zirconia, being at approximately 30.3°. Therefore, the cell volume is becoming closer to that of pure zirconia, indicating the migration of dopants from the bulk to the surface of the sample, which is consistent with the increasing dopant to zirconium ratio observed by XPS as the calcination temperature increases.

The addition of dopants to zirconia increase the activity of the decomposition of propan-2-ol in the cases of silica and lanthana. However, when ceria is used as the dopant the activity is less than that of pure zirconia.

In what follows we shall concentrate on the specific rates of reactions, those which have been corrected for surface area. Relating the ceria doped zirconia reactor studies to the physical characteristics provides the following conclusions. The conversions of propan-2-ol to propene, corrected for surface area, are low compared to that of pure zirconia. The surface areas of the ceria doped zirconia samples are low compared to pure zirconia itself. Also, the specific rate of reaction of propan-2-ol over the ceria doped materials is lower than that observed with pure zirconia. The normalised conversions for the production of propene at 240°C for ZrO_2 and 16% dilute CeO_2/ZrO_2 both calcined at 900°C is 0.267 and 0.097. Thus addition of ceria both reduces the surface area, and blocks the zirconia surface which is active in propan-2-ol dehydration.

For silica coprecipitated zirconia, the specific conversions to propene increase with increasing calcination temperature, typically from 0.04 to 0.54 over the temperature range 550 to 1050°C. It is found that both the activation energies (E_a) and the pre-exponential factors (LnA) generally decrease with increasing calcination temperature³. The drop in activation energy for the reaction is the main reason for the rate increase. The pre-exponential factors also decrease, which rules out an increase in site density as the calcination temperature increases. Therefore, the sites become more active as the calcination temperature is increased. Assuming that the coprecipitated silica samples have Lewis acid sites⁴, similar to the impregnated samples, which have been described as having exposed metal ions⁵, they must have a greater turnover in the removal of water from propan-2-ol via the E_{1cb} or E_2 mechanism as the calcination temperature is increased. Dzis'ko⁶ investigated the acidity of silica zirconia materials and noticed that increasing the silica loading increased the acidity of the samples but the acidity dropped off after a certain loading of silica. This is explained by Soled⁷ where at high Si concentrations Si-Si interactions predominated and the number of acid sites decreased. The two investigations saw increased acid sites and increased acidity when loadings were increased. However, we see an increase in acidity due to an increased turnover of the acid sites with calcination temperature.

The specific conversions to acetone from propan-2-ol for lanthana doped zirconia, increase from 0.18 to 1.00 with increasing calcination temperature of 550 to 1050°C. Lanthana is the only dopant investigated to give acetone as the major decomposition

product. The production of acetone is associated with basicity indicating the addition of lanthana with its formal +3 valence compared to zirconia and the other dopants used, produces more active basic sites than acid sites. As with silica, the activation energies generally decrease, as do the pre-exponential factors³.

For most catalysts, the specific activity for the dehydration or dehydroxylation reaction increases with calcination temperature. This is also generally followed by a decrease in the activation energies and a decrease in the pre-exponential factor (Appendix Chapter 6). If the number of active sites increases as the calcination temperature of the samples increases, the activation energies would be similar and the pre-exponential factor would increase, indicating an increase in the number of active sites for a similar series of samples. Since the activation energies and pre-exponential factors decrease with calcination temperature, the number of active sites does not appear to increase but the sites become more active with increasing calcination temperature. Even though the dopant concentration increases with calcination temperature, this does not increase the number of active sites. The drop in activation energies is the contributing factor to the increase in specific conversions.

In relating the reactor studies for the impregnated silica/zirconia samples with the combined FTIR and pyridine adsorption experiments for the 5wt% SiO₂/ZrO₂ samples calcined at 700 and 900°C, the pyridine adsorption data combined with infrared spectroscopy experiments shows that the two samples have similar numbers of acid sites 0.13 and 0.11 pyridine molecules adsorbed per nm². The amount of pyridine adsorbed at 50°C is similar in both cases upon correcting for surface area. This directly relates to the test reaction decomposition of propan-2-ol results as the two catalysts have similar conversions and activation energies (121 and 123 kJmol⁻¹) and the pre-exponential factors are similar (19.8 and 20.3). This information supports the conclusion that the density of acid sites does not increase with calcination temperature. The strength of the acid sites remains similar, as can be seen from increasing the temperature in the pyridine adsorption experiments. The amount of pyridine on the surface also remains similar. Both samples contained some strong acid sites as a small amount of remained pyridine on the surface at 550°C. Infrared spectroscopy shows that with pure zirconia, pyridine is desorbed from the surface below 400°C. Together, the pyridine adsorption and combined infrared experiments show that there are strong

acid sites on doped zirconia as opposed to pure zirconia leading to an increase in acidity of the doped catalysts compared with the single oxide. This is in direct agreement with the reactor studies, where the production of propene over silica doped catalysts is greater than that on pure zirconia.

The reactor studies and the FTIR experiments complement each other. Therefore, looking at the physical characteristics of the 5wt% silica impregnated zirconia samples, it can be observed from the surface area measurements that the sample calcined at 700°C has a larger surface area than the sample calcined at 900°C (99 and 88 m²g⁻¹), however the difference is not great. The XRD patterns of the two samples are similar, with the monoclinic phase being stabilised. And from the XPS results the two samples have similar surface ratios of Si/Zr (0.16 and 0.17). Therefore, the effect of temperature over the range 700 to 900°C has little effect on the catalysts. This is in contrast to the silica /zirconia coprecipitated samples in which temperature plays an important role. The infrared investigation of silica impregnated zirconia catalysts calcined at 1050°C proved difficult since the samples could not be pressed into self supporting wafers. These results would have given valuable information since the physical characteristics, such as surface area and surface dopant to zirconium ratio, of high temperature calcined samples are different to those calcined at lower temperatures.

From infrared results, only Lewis acid sites are observed. Therefore, the production of propene on silica doped zirconia takes place through either an E₂ or an E_{1cb} mechanism, neither of which requires the presence of Brønsted acid sites. The Lewis acid sites have a greater turnover after increasing calcination temperatures. The number of sites does not increase with increasing calcination temperature.

References

¹ P. D. L. Mercera, J. G. van Ommen, E. B. M. Doesburg, A. J. Burggraaf and J. R. H. Ross, *Applied Catalysis*, 78 (1991) 79-96.

² B. D. Cullity, *Elements of X-ray Diffraction*, Addison-Wesley 1956.

³ Chapter 6

⁴ Z. Dang, B. G Anderson, Y. Amenomiya and B. A. Morrow, *J. Phys. Chem.*, 99 (1995) p14437-14443.

⁵ B. C. Gates, *Catalytic Chemistry*, Wiley 1992.

⁶ V. A. Dzis'ko, G. K. Boreskov and A.D. Makarov, *Kin i Katal.*, 2 (1961) p 84-93.

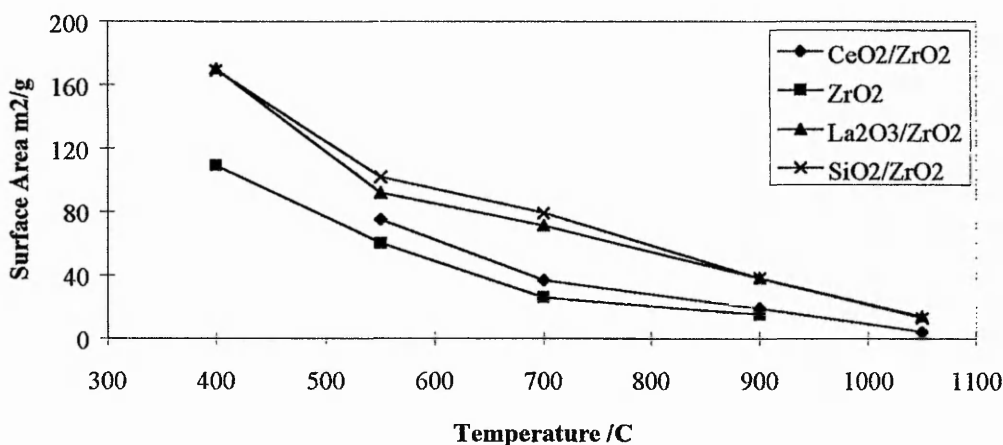
⁷ S. Soled and G. B. McVicker, *Catalysis Today*, 14 (1992) 189-194.

8 Summary

8.1 Coprecipitated doped zirconia

The surface area of pure zirconia is known to decrease dramatically upon heating (see graph below). The addition of dopants to pure zirconia has been shown, in this thesis, to stabilise the surface area of zirconia against sintering. The three dopants investigated were lanthana, silica and ceria, with ceria proving to be the least active in surface area stabilisation. The other two dopants stabilised the surface area to a similar amount from 170 to $38\text{m}^2\text{g}^{-1}$ over the temperature range 400 to 900°C , which was a 78% decrease. The surface area of pure zirconia dropped from 109 to $15\text{m}^2\text{g}^{-1}$ over the temperature range 400 to 900°C , which was an 86% decrease.

Surface Area vs. Calcination Temperature



The surface area of the samples can be related to the crystallite size and the porosity of the system. The addition of dopants retards crystallite growth and sintering. Mercera ¹ identified two processes responsible for the changes in the pore structure and surface area of pure zirconia, which were crystallite growth accompanied with a phase change and inter crystallite sintering. He proposes that these occur via a mechanism of surface diffusion. Therefore, thermal stability of zirconia by the addition of dopants is due to the inhibition of crystallite growth and inter crystallite sintering.

Powder x-ray diffraction was used to determine the phase, phase composition and crystallite size of the catalyst. The phase composition of pure zirconia at 550°C and above was 100% monoclinic. However, at 400°C a broad tetragonal pattern was observed. The addition of dopants retarded the crystallisation of the tetragonal phase of zirconia. The powder XRD pattern at 400°C for the doped samples was amorphous. However, at 550°C tetragonal zirconia was observed and remained almost 100% tetragonal up to 1050°C, with trace amounts of the monoclinic phase being observed at the highest calcination temperatures.

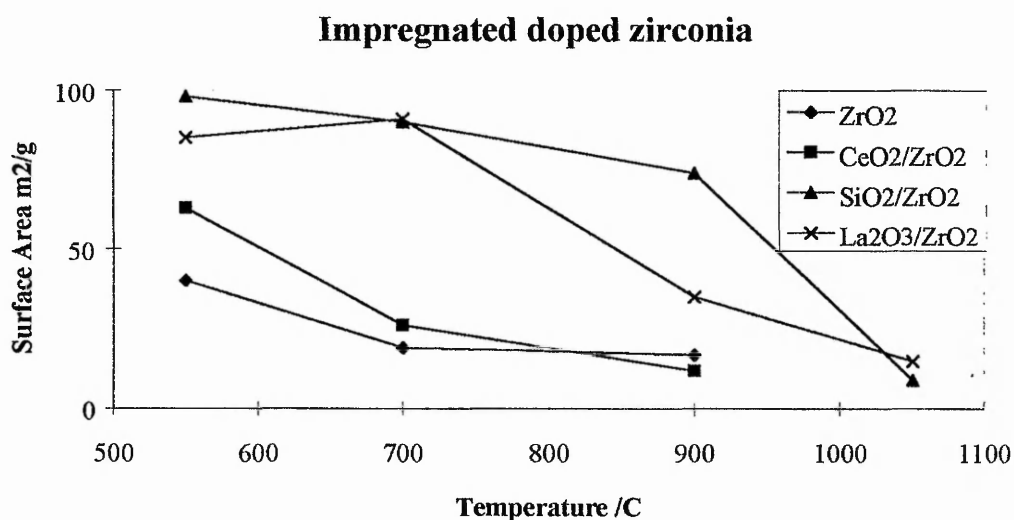
Upon increasing the calcination temperature, the crystallite size increased as was expected from the decrease in surface area. The crystallite sizes generally agreed with Garvie's theory² that above a crystallite size of 30 nm the tetragonal crystallites transform to monoclinic crystallites. Therefore, tetragonal crystallites should not exist above 30 nm.

X - ray photoelectron spectroscopy was employed to determine the surface ratio of dopant metal to zirconium. The surface ratio increased with increasing calcination temperature, indicating an enrichment of dopant at the surface or near surface region, for all the dopants studied. In the study of lanthana doped zirconia, experiments were performed to relate the surface ratio of La/Zr to the final pH of coprecipitation. It was observed that increasing the pH of preparation decreased the La/Zr surface ratio but the surface area increased. Therefore, a certain amount of dopant is required to stabilise the surface area but too much at the surface can cause a detrimental effect.

For silica and ceria doped zirconia the surface ratios of Si/Zr and Ce/Zr were determined for the precursor to the mixed oxide, $\text{Si(OH)}_4 / \text{Zr(OH)}_4$ and $\text{Ce(OH)}_4 / \text{Zr(OH)}_4$. It was found that the surface ratio was approximately equivalent to the theoretical bulk value for both systems. Therefore, the coprecipitation preparation method produced a homogeneous mix of the dopant hydroxide and zirconium hydroxide. However, upon calcination the surface Si/Zr and Ce/Zr ratios increased due to the migration of the dopant to the surface.

8.2 Impregnated, doped zirconia

Impregnation using lanthana and silica as the dopants stabilised the surface area of zirconia. The addition of ceria did not enhance the surface area, which remained similar to that of pure zirconia. Silica stabilised the surface area to the greatest extent with a decrease from 96 to 16 m²g⁻¹ over the calcination temperature range 550 to 1050°C, an 83% drop.



The surface areas at the highest calcination temperature of 1050°C are similar to those of samples prepared by coprecipitation. The highest surface area obtained at 1050°C for all samples and preparations, was for 3 mole% La₂O₃/ZrO₂ impregnated and was 16 m²g⁻¹.

Samples prepared by an impregnation technique showed stabilisation of the monoclinic phase up to 900°C, if the pure zirconia had been precalcined to 500°C, but above this calcination temperature mixed phases were observed. However, if the dopant was impregnated onto zirconium hydroxide, the tetragonal phase was stabilised to 1050°C. *Therefore, a high surface area zirconia can be produced in either the monoclinic or tetragonal phase depending on the method of*

preparation. The tetragonal phase can be stabilised up to 1050°C using the coprecipitation technique.

From XPS experiments, the dopant to zirconium ratio was greater for the impregnated samples than for the coprecipitated samples, as is expected from the nature of the preparation. The surface ratio of dopant to zirconium remained essentially constant up to 900°C, but increased when the temperature was raised to 1050°C, as an effect of increasing crystallite size.

8.3 Catalytic Studies

The addition of dopants to pure zirconia altered the catalytic properties of the system in the test reaction of the decomposition of propan-2-ol. The decomposition can produce two main products, acetone or propene, where the production of acetone is associated with basic activity and the production of propene associated with acidic activity. The test reaction is a measure of the acidic or basic properties of the oxides. Pure zirconia produced propene only, with the conversion normalised for surface area increasing with increasing calcination temperature. The sample calcined at the highest temperature, 1050°C, is more active to the production of propene per unit area than the samples calcined at lower temperatures.

The addition of lanthana to zirconia brought about the dehydrogenation reaction ³, as the major reaction, to produce acetone from propan-2-ol, with propene being formed in trace amounts. As in the case of pure zirconia, the normalised conversion for surface area increased with increasing calcination temperature. The production of acetone was more prevalent, per unit area, in the sample calcined at 1050°C.

Tanabe's prediction ⁴ that silica doped zirconia should possess enhanced acidity relative to the single oxides, is shown to be correct. This hypothesis also predicts the appearance of Lewis acid sites as opposed to Brønsted acid sites, which was confirmed experimentally using combined FTIR and pyridine adsorption.

The addition of silica to zirconia produced propene as the major product in the decomposition of propan-2-ol with, trace amounts of acetone being produced only in the samples calcined at high temperatures. The normalised conversion for surface area increased with increasing calcination temperature.

Upon doping zirconia with ceria, the catalytic activity of the system decreased, with low activities to the production of propene.

8.4 Conclusions

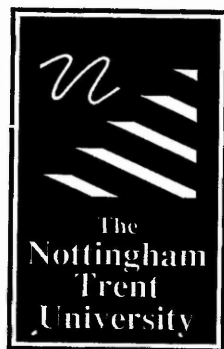
Stabilised high surface area zirconia can be prepared by the addition of dopants. The nature of the dopant and the preparation method of the mixed oxides greatly effect the degree of stabilisation. A zirconia catalyst can be designed with a desired phase of monoclinic, tetragonal or of a mixed phase of the two, by altering the preparation method. The surface area can be tailored by the dopant used and the calcination temperature.

The catalytic properties of the sample can be altered by using various dopants. Enhanced acidity and basicity, with respect to the pure zirconia, can be achieved by the addition of silica and lanthana respectively.

References

-
- ¹ P. D.L. Mercera, J. G. Van Ommen, E. B. M. Doesburg, A. J. Burgraaf and J. H. Ross, *Applied Catalysis*, 78 (1991) p79-96 and P. D.L. Mercera, J. G. Van Ommen, E. B. M. Doesburg, A. J. Burgraaf and J. H. Ross, *Applied Catalysis*, 71 (1991) p363-391.
 - ² R. C. Garvie, *J. Phys. Chem.*, 65 (1969) p1238.
 - ³ R. Franklin, P. Goulding, J. Haviland, R. W. Joyner, I. McAlpine, P. Moles, C. Norman, T. Nowell, *Catalysis Today* 10 (1991) p405.

⁴ K. Tanabe, T. Sumiyoshi, K. Shibata, T. Kiyoura and J. Kiagawa, Bull. Chem. Soc. Jpn., 47, (1974), p1064



Libraries & Learning Resources

The Boots Library: 0115 848 6343
Clifton Campus Library: 0115 848 6612
Brackenhurst Library: 01636 817049

DIG
11.5.09.

FOR REFERENCE ONLY

41 0565879 2

